

**ON HYPERBOLIC SURFACE TESSELLATIONS AND  
EQUIVARIANT SPACELIKE CONVEX POLYHEDRAL  
SURFACES IN MINKOWSKI SPACE**

DISSERTATION

Presented in Partial Fulfillment of the Requirements for  
the Degree Doctor of Philosophy in the Graduate  
School of the Ohio State University

By

Igor Iskhakov

\* \* \* \* \*

The Ohio State University  
2000

**Dissertation Committee:**

Mike Davis, Advisor

Ruth Charney

Fangyang Zheng

**Approved by**



Advisor

Department Of Mathematics

© Copyright by

Igor Iskhakov

August 27, 2000

## ABSTRACT

We are interested in generalizing the classical Cauchy Rigidity Theorem and the Aleksandrov's Existence Theorem for convex polyhedra and the sphere to the closed surfaces of constant negative curvature. We prove that tessellations of the surfaces with hyperbolic metric cannot be infinitesimally perturbed so as to preserve their face angles. This is an analog of the Cauchy Rigidity for "polyhedra" on the hyperbolic surfaces. We also show an analog of the Cauchy Rigidity Theorem for tessellations in the same isotopy class of the tessellations. For existence we show that in a certain "convex hull" construction any set of cone angles can be realized which provides a first step in the suggested proof of the analog of the Aleksandrov's Theorem.

To my grandmother Polya, who dreamed of this dissertation for so long, to my mother, who was my first mathematics teacher and whose unparalleled effort did not let me miss this career, and to my father, who predicted this when I was seven.

In memory of my grandfather Solomon who first showed me the beauty and subtleties of geometry by disproving the Pythagorean Theorem.

## ACKNOWLEDGMENTS

I would like to express my deep gratitude to my advisor professor Mike Davis for his infinite patience and gentle guiding. I also would like to thank professor A.T.Fomenko for suggesting the problem of minimal networks on the surfaces. My very special thanks go to professors A.Tuzhilin and A.Ivanov who introduced me to the beautiful world of geometry and topology and studying and conducting research with whom greatly impacted my development as a mathematician.

## VITA

- 1972 ..... Born in Moscow, Russia
- 1989 ..... Entered Mechanical-Mathematical Department of Moscow State University
- 1993 ..... Entered Graduate School of The Ohio State University, Mathematics Department

## PUBLICATIONS

1993, *Minimal networks spanning regular  $n$ -gons: linear tilings realization*, (in Russian), Vestnik Moskov.Univers.Ser.1,Mat.-Mech.,6,1993, joined with A.Ivanov and A.Tuzhilin

## FIELDS OF STUDY

Major field: Mathematics

Specialization: Hyperbolic geometry and low-dimensional topology

Studies in	Hyperbolic Geometry	Prof. M.Davis
	Algebraic Topology	Prof. M.Davis
	Minimal Networks	Prof. A.Ivanov, Prof. A.Tuzhilin

## TABLE OF CONTENTS

	Abstract . . . . .	ii
	Dedication . . . . .	iii
	Acknowledgments . . . . .	iv
	Vita . . . . .	v
	List of Figures . . . . .	ix
CHAPTER <span style="float: right;">PAGE</span>		
1	Introduction . . . . .	1
2	Preliminaries on Minkowsky space, hyperbolic plane and surface groups	14
3	Tessellations . . . . .	20
	3.1    Definitions and reduction to the one-cell tessellation case	20
	3.2    Representation of the tessellation in the same isotopy class	23
4	Local rigidity of hyperbolic surface tessellations with constant angles .	25
	4.1    The Main Theorem and an outline of the proof . . . . .	25
	4.2    System of Side Pairing Equations . . . . .	28
	4.3    Equations for the coefficients . . . . .	31
	4.4    "Four-legged" pictures . . . . .	34
	4.5    Relations for $b$ -coefficients in the star of a vertex . . . . .	37
	4.6    Solving for the coefficients . . . . .	39
	4.7    The Local Vertex Equations . . . . .	42
	4.8    Structural equations for the group $G$ and the Global Vertex Equations . . . . .	43
	4.9    Augmented system of Tessellation Equations . . . . .	46
	4.10   Equations for $c$ -coefficients . . . . .	49

	4.11	A special case - one cycle . . . . .	56
	4.12	General case - $V$ cycles . . . . .	57
5		On global rigidity . . . . .	58
	5.1	Global Rigidity in a fixed isotopy class . . . . .	58
	5.2	Rigidity and unboundness of the edge lengths . . . . .	59
	5.3	Example of a potential counterexample . . . . .	62
6		Equivariant spacelike convex polyhedra in Minkowsky space and the Local Rigidity Theorem . . . . .	69
	6.1	Spacelike convex cones . . . . .	69
	6.2	Equivariant spacelike convex polyhedra . . . . .	73
	6.3	The Gauss Map in Minkowsky space and the dual tessellation . . . . .	74
	6.4	The Local Rigidity Theorem . . . . .	75
7		The Convex hull construction in Minkowsky Space and the realization of singular Euclidean structures of non-positive curvature on closed Riemann surfaces by convex polyhedra . . . . .	78
	7.1	The Basic Construction and the Main Theorem . . . . .	78
	7.2	Pseudo-Dirichlet regions . . . . .	80
	7.3	Map $\theta$ and its properties . . . . .	85
	7.4	The region $\mathcal{R}$ and its topology . . . . .	88
	7.5	Proof of the Main Theorem . . . . .	100
	7.6	Barycentric representation of the function $\alpha$ . . . . .	102
	7.7	Proof of transversality in proposition 7.4.7 . . . . .	104
APPENDICES			
A		One simple lemma of Euclidean planimetry . . . . .	106
B		One simple lemma of linear algebra . . . . .	110
C		Differentiation of a distance function in barycentric representation in normed affine spaces . . . . .	111
D		Convexity of the inverse distance function on a spacelike affine plane . . . . .	117
E		Closed minimal networks and Fomenko's conjecture . . . . .	120



Bibliography . . . . . 131

## LIST OF FIGURES

FIGURE	PAGE
4.1	Hyperbolic polygon with identifications . . . . . 26
4.2	$2E$ -gon with side normals and identifications . . . . . 29
4.3	Four-legged picture . . . . . 35
4.4	Right-angle triangle . . . . . 37
4.5	Vertex star of $v_{i-1i} \in V_j$ . . . . . 38
4.6	Intersecting planes . . . . . 39
4.7	Picture in the plane $v_{i-1i}^\perp$ . . . . . 40
4.8	Structural Equations for the group $G$ and involution $\psi$ . . . . . 44
4.9	Functions $\omega$ and $\eta$ . . . . . 47
4.10	Polygon chasing 1 . . . . . 53
4.11	Polygon chasing 2 . . . . . 54
5.1	Loop . . . . . 60
5.2	Two loops . . . . . 61
5.3	Octagon producing $S_2$ by identifying opposite sides . . . . . 63
5.4	Octagon with a pair of long sides . . . . . 64
5.5	Accumulation polygons . . . . . 65
5.6	Side shift . . . . . 66

5.7	Possible tessellation . . . . .	67
5.8	Limit of a sequence of tessellations . . . . .	68
6.1	Sliding vertices . . . . .	71
6.2	Cell area evolving . . . . .	73
7.1	Degeneration of an edge of a Pseudo-Dirichlet tessellation . . . . .	84
7.2	Degeneration of a cell of a Pseudo-Dirichlet tessellation . . . . .	84
7.3	To the proof of Proposition 7.4.2 . . . . .	90
7.4	Impossible configuration . . . . .	93
7.5	Case $p = 2$ . . . . .	94
7.6	Hypersurfaces $\Sigma$ and $\tilde{\Sigma}$ . . . . .	98
7.7	Impossible shape . . . . .	101
A.1	Unit star . . . . .	106
A.2	Unit star of degree 3 . . . . .	108
C.1	Differentiating the distance function . . . . .	113
D.1	Graph of function $f(x)$ . . . . .	118
E.1	Variation splitting the vertex and reducing total length . . . . .	122
E.2	Variation of a curve . . . . .	123
E.3	Edge velocity vectors coming into the vertex . . . . .	124
E.4	Steiner-Torricelli point . . . . .	126
E.5	Variation splitting the vertex and reducing total length . . . . .	127

# CHAPTER 1

## INTRODUCTION

The celebrated *Cauchy Rigidity Theorem* states that convex polyhedron in the Euclidean space with prescribed face angles is rigid, that is to say the dihedral angles are uniquely determined by the face angles (see [21], ch.20,sec.8).

*Remark 1.* Convexity here is essential as according to R.Connelly this assertion is false without its assumption.

When discovered, the result looked (and still looks) strikingly surprising for it means that a wire frame in the form of any convex polyhedron with faces attached along the edges by hinges can not be deformed in any way. Nevertheless, its proof is rather elementary. By passing to the dual tessellation of the sphere by means of the *Generalized Gauss Map*, this statement is equivalent to the rigidity of the tessellations of the round sphere by convex polygons with prescribed polygonal angles. Equivalently, this means that the edge lengths of these polygons are uniquely determined by the angles and that such a tessellation is unique up to the action of  $SO(3)$  on the round sphere by isometries. The theorem then follows from two simple observations known as *Cauchy Lemmas* (see [23]).

The first of them has to do with the geometry of the convex spherical polygons.

An equivalent version of it may be stated and proved in terms of polyhedral cones.

The two dual formulations are:

**Proposition (Cauchy's Geometric Lemma).** *Let  $C_1$  and  $C_2$  be two convex polyhedral cones in  $\mathbb{R}^3$  with equal number of edges and equal corresponding face angles. Let now assign  $+$  ( $-,0$ ) to each edge of  $C_1$  if its dihedral angle is bigger (smaller, equal) than the corresponding dihedral angle of  $C_2$ . Then moving around the apex of  $C_1$  in either direction there will be either at least four changes of signs or none (in which case all signs are 0 and cones are congruent).*

**Proposition (Cauchy's Geometric Lemma - dual form).** *Let  $P_1$  and  $P_2$  be two convex spherical polygons with equal number of sides and equal corresponding angles. Let now assign  $+$  ( $-,0$ ) to each side of  $P_1$  if it is longer (shorter, equal) than the corresponding side of  $P_2$ . Then moving around  $P_1$  in either direction there will be either at least four changes of signs or none (in which case all signs are 0 and polygons are congruent).*

*Remark 2.* The dual version of the Cauchy's Geometric Lemma holds in the hyperbolic plane  $\mathbb{H}^2$  as well. See [23].

The second observation, combinatorial and topological in nature, heavily depends on the fact that the Euler characteristic of the two-sphere is 2.

**Proposition (Cauchy's Topological Lemma for the Sphere).** *Let  $\Gamma$  be the 1-skeleton of a cellulation of the 2-sphere. Assume that each edge of  $\Gamma$  is labeled with one of the three symbols  $+, -$  or  $0$ , so that at each vertex the number of strict sign*

*changes, as one goes around the edges incident to the vertex, is always  $\geq 4$  or is 0. Then all the edges actually have the same sign (0) assigned to them.*

Its dual form is then immediately obtained by duality.

**Proposition (Cauchy's Topological Lemma for the Sphere - dual form).** *Let  $\Gamma$  be the 1-skeleton of a cellulation of the 2-sphere. Assume that each edge of  $\Gamma$  is labeled with one of the three symbols  $+$ ,  $-$  or  $0$ , so that at each face the number of strict sign changes, as one goes around the edges of the face, is always  $\geq 4$  or is 0. Then all the edges actually have the same sign (0) assigned to them.*

Separated by a century from the uniqueness statement of this famous Cauchy Rigidity Theorem for Convex Polyhedra, its existence counterpart, a very deep result of A.D.Aleksandrov, states that any given polyhedral metric of non-negative curvature on a 2-dimensional manifold homeomorphic to a sphere is realized by a (unique) convex polyhedron in the three-dimensional Euclidean space. In fact, it says even more, namely:

**Theorem (A.D.Aleksandrov).** *Given a set of flat convex polygons with pairing of the sides such that upon side identifications the resulting space is homeomorphic to  $S^2$ . the side lengths in pairs are equal and the sum of the face angles around each vertex is not greater than  $2\pi$ , there exists a (unique) convex polyhedron in  $\mathbb{R}^3$  with these polygons as faces.*

Its proof is heavily based on the use of the *Cauchy Rigidity Theorem*. The local rigidity implied by the former then guarantees that a certain map has a non-degenerate differential, i.e. the determinant of a certain system of linear equations is

not zero. The local injectivity of this map along with other differential-topological considerations show its surjectivity (see [20],ch.1,sec.6).

It seems reasonable and very tempting to expect something analogous in case of the other closed surfaces.

In case of a torus and Klein bottle with flat metric the rigidity assertion is obviously false due to the presence of similarities. As for the analog of Aleksandrov's Theorem, any polyhedral metric on the torus or Klein bottle with non-positive curvature is necessarily nonsingular and hence is realized as the quotient of the Euclidean plane  $\mathbb{R}^2$  by the action of the corresponding discrete group of euclidean translations (and reflections in the non-orientable case).

We therefore will concentrate on the closed surfaces of genus  $g > 1$  with metric of constant negative curvature, otherwise known as hyperbolic Riemann surfaces. Let's notice first of all that generalizations of both results, once proved and properly interpreted for orientable surfaces will automatically hold for non-orientable as well by passing to the two-sheeted cover. Scaling of the curvature will not affect the results either. Hence we will restrict our attention to the orientable closed surfaces of genus  $g > 1$  with the metric of constant curvature  $-1$ .

In this thesis we will attempt to find reasonable interpretations and generalizations of the aforementioned results.

After generalizing the notion of the convex polyhedron to closed surfaces of constant negative curvature, the desired *Rigidity Theorem for polyhedra* will just as well be reduced to that for hyperbolic surface tessellations. The topological argument proving the Cauchy Theorem for the sphere is no longer valid for quite an obvious

reason. While there exists only one isometry class of the sphere of a given positive constant curvature, this is not true for the negatively curved surfaces. If we fix the constant curvature to be 1 for the sphere and  $-1$  for the negatively curved surfaces, then the isometry classes are in one to one correspondence with the conformal classes of the metrics on these surfaces. As is well known, the space of conformal classes of marked surfaces of genus  $g$  greater than 1, called the *Teichmüller space*  $T_g$ , is a  $6g - 6$  dimensional open ball, while for the sphere it is just a point.

The next problem of a generalization is presented by rather large fundamental groups of surfaces of high genus. Therefore, we will distinguish between two different directions of such a generalization dealing with two different versions of *Cauchy Rigidity Theorem*. The first version is the so-called *Local Cauchy Rigidity Theorem*, which is exactly the one used in the proof of the Aleksandrov's Theorem. It states that convex polyhedron with fixed face angles cannot be infinitesimally perturbed, i.e. the dihedral angles are locally determined. In terms of tessellations that means that a tessellation on the round sphere with fixed face angles cannot be infinitesimally perturbed, of course up to the action of  $SO(3)$ , i.e. edge lengths are locally determined. It is this version of *Cauchy Rigidity Theorem* which generalizes without any change.

**Theorem A (Local Rigidity).** *A tessellation with prescribed angles of a closed surface of genus  $g > 1$  with hyperbolic metric on it cannot be infinitesimally perturbed, i.e. its edge lengths are locally determined by the face angles.*

In fact, we prove even more. We do not necessarily require that the faces of such



tessellation are convex polygons. This probably should be true for the round sphere as well, but the author is unaware of results in this direction.

As in the Euclidean case an immediate corollary of this theorem is its polyhedral version. Before we can state it we need to give few definitions.

First of all, much like the round sphere and Euclidean convex polytopes "live" in the 3-dimensional Euclidean space  $\mathbb{R}^3$ , the polyhedra that we want to talk about, just as well as their smooth counterparts, the hyperbolic surfaces, "live" in the Minkowski space  $\mathbb{R}^{2,1}$ , which is a 3-dimensional linear space endowed with the (indefinite) Minkowski inner product:

$$\langle v, u \rangle = -v^0 u^0 + v^1 u^1 + v^2 u^2$$

**Definition.** A connected surface in  $\mathbb{R}^{2,1}$  will be called *an equivariant spacelike convex polyhedron* if it is the boundary of a convex body lying entirely inside the light cone and possessing a defining it locally finite collection of supporting planes all of which are spacelike and is equivariant under the action of a Fuschian group  $\Gamma \in SO^+(2, 1)$ .

An equivariant convex polyhedron is homeomorphic to  $\mathbb{H}^2$  and its quotient under the action of  $\Gamma$  is homeomorphic to the Riemann surface obtained as the quotient  $\mathbb{H}^2 / \Gamma$ . It is this quotient which we will call the *convex polyhedron on the surface  $S_g$* .

Now we can present the desired polyhedral version of the Local Rigidity.

**Theorem B (Local Rigidity Theorem for convex polyhedra on surfaces of genus  $g > 1$ ).** *A convex polyhedron on a surface  $S_g$  with fixed metric of constant curvature  $-1$  can not be infinitesimally perturbed as to preserve the face angles. Equivalently, the dihedral angles are locally determined by the face angles.*

Of course it can be reformulated in terms of the equivariant spacelike convex polyhedra, but this form seems more compact and closer to the classical statement.

Next we may attempt to generalize the "global" *Cauchy Rigidity Theorem*, saying that (convex) tessellation with fixed angles is unique up to isometry of the sphere. The generalization obtained by the author is semi-local, semi-global. Namely:

**Theorem C (Global Rigidity in a fixed isotopy class).** *Given an isometry class of a marked hyperbolic surface, there exist at most finitely many tessellations with the same combinatorial structure, face angles and isotopy class.*

The author also conjectures that this can actually be improved to match the classic case.

**Conjecture 1 (Uniqueness in a fixed isotopy class).** *Given an isometry class of a marked hyperbolic surface, there exists at most one tessellation with prescribed angles in its isotopy class.*

Evidence for this conjecture is provided by the fact that the conjecture is true in the special case of "minimal networks". These are the tessellations with all angles equal to  $2\pi/3$  (and therefore all vertices of order 3). The sketch of the proof of the local rigidity by actually showing uniqueness in a fixed homotopy class in this particular case was obtained by the author under the direction of A.A.Tuzhilin and A.O.Ivanov and is based on the minimizing properties of such tessellations. An account of this special case is presented in Appendix E.

Finally one might hope to generalize the "global" version. At the moment, this

seems doubtful as the author has a procedure for constructing a potential counterexample. On the other hand, triangulations of the surface conform to the global rigidity statement, since a hyperbolic triangle is uniquely determined by its angles. This provides the primary evidence that it could be true. Thus there still remains an open

**Question 1 (Global Rigidity).** *Given an isometry class of a marked hyperbolic surface, there exists at most one tessellation of this surface with prescribed combinatorial structure and angles up to the action of the isometry group.*

This is then better stated if we consider surfaces as elements of the moduli space instead of the Teichmüller space. We then have the following

**Question 2 (Global Rigidity - moduli form).** *Given an isometry class of a non-marked hyperbolic surface, there exists at most one tessellation of this surface with prescribed combinatorial structure and angles, or equivalently, a set of edge lengths producing given surface, if it exists, is unique.*

Since the isometry group of a closed surfaces of constant negative curvature is finite (Swartz-Hurwitz Theorem, see theorem 9.19 in [26]), we could ask instead a slightly weaker

**Question 3 (Weak Generalized Global Rigidity).** *Given an isometry class of a marked hyperbolic surface, there exist at most finitely many tessellations of this surface with prescribed combinatorial structure and angles.*

This is equivalent to saying that there exist finitely many sets of edge lengths for a given tessellation with prescribed angles producing given surface. Indeed, it is clear

that this follows from Question 3. On the other hand, the positive answer to this question follows from this statement since each such set of edge lengths can only give rise to finitely many different tessellations since all of them will produce isometric surfaces and the isometry group of a hyperbolic surface is finite.

A special case of this question is known as *Fomenko's conjecture* for the "minimal networks" and provided another motivation for this work.

It is a good place to mention that, perhaps of their beauty, tessellations have always attracted attention of many mathematicians and artists. Starting with Platon and his famous five Platonic solids, the list of names includes Euler, Cauchy, Poincare, Weyl, Steiner, Pogorelov, Thurston to just name a few. As for hyperbolic tessellations, two good sources of inspiration are [16] and [17]. Existence of symmetric "Platonic" solids on the surfaces of higher genus is shown in [10], and some examples of minimal networks can be found in [13].

Let's now move on to the Aleksandrov's theorem and its possible generalizations.

M.Davis conjectured that an analogue of the Aleksandrov's theorem may hold for the closed surfaces of higher genus. Namely:

**Conjecture 2 (M.Davis).** *Any singular Euclidean metric of non-positive curvature on a closed surface is realized by a unique equivariant convex spacelike polyhedron in the three dimensional Minkowski space.*

To produce such a polyhedron M.Davis suggested using the following convex hull construction in Minkowski space.

Choose a hyperbolic plane  $\mathbb{H}^2$  (a sheet of a two-sheeted hyperboloid which is

a locus of points of the same imaginary "length" in Minkowski space), fix a group of isometries of  $\mathbb{R}^{2,1}$ , which restricts to the group of isometries of  $\mathbb{H}^2$ , pick finitely many points inside of the fundamental region of this group on  $\mathbb{H}^2$  corresponding to the vertices of the polyhedron and translate them over entire  $\mathbb{H}^2$  by means of the group action. Then perturb the points (to be precise, orbits of points) in an invariant manner along the central rays corresponding to them so that after taking the convex hull of all these points they really are the vertices and all the faces are spacelike. The quotient under the group action of the convex hull boundary is the desired convex polyhedron (see also [8] and [18]). The boundary itself is an equivariant convex polyhedron and to be precise it is this object which should be called the polyhedron in the Minkowski space. Nevertheless by abuse of notation we will stick with the above definition. If the group is the fundamental group of the Riemann surface, then the constructed polyhedron is homeomorphic to the surface and has a piecewise Euclidean metric of non-positive curvature on it.

M.Davis therefore conjectured that any piecewise Euclidean metric of non-positive curvature on the surface comes as a metric of a polyhedron obtained from this convex hull construction.

One of the possible approaches to showing this is based on the result of M.Troyanov. In [30] he showed that given any conformal structure on a closed surface (of any genus  $g \geq 0$ ), any set of  $p$  points  $v = \{v_i\}$  on the surface and any  $p$ -tuple  $(\theta_1, \dots, \theta_p)$  of positive real numbers satisfying only Gauss-Bonnet condition

$$\sum_{i=1}^p \theta_i = \sum_{i=1}^p (2\pi - k_i) = 2\pi p - \sum_{i=1}^p k_i = 2\pi(p - \chi)$$

where  $\chi$  is the Euler characteristic of the surface and  $k_i = 2\pi - \theta_i$  is the curvature, there exists a singular Euclidean metric on the surface with the given cone angles  $\theta_i$  at the given points  $v_i$  in the given conformal class. In other words

$$SE_g \cong T_g^p \times \Delta_\theta^{p-1}$$

where  $SE_g$  denotes the space of all singular Euclidean structures on  $S_g$ ,  $T_g^p$  is the Teichmuller space of  $S_g$  with  $p$  marked points and  $\Delta_\theta^{p-1}$  is a  $(p - 1)$ -dimensional simplex.

Let  $Pol_g$  be the set of all spacelike equivariant convex polyhedra homeomorphic to  $S_g$  up to isometries of Minkowski space  $\mathbb{R}^{2,1}$ .

Let us fix the conformal structure  $\zeta$  and the cone points  $v = \{v_i\}_{i=1}^p$  on the surface. Then the space of all possible polyhedra  $Pol(\zeta, v)$  is parametrized by the positions of the vertices on the rays, e.g., by the lengths of  $p$  vectors, modulo scaling since all singular Euclidean metrics are considered up to similarity. Therefore this space is  $p - 1$  dimensional and is a subset of the  $(p - 1)$ -simplex. There is an obvious map

$$\Theta : Pol(\zeta, v) \rightarrow \Delta_\theta^{p-1}$$

corresponding to each polyhedron its set of cone angles. We prove following

**Theorem D.** *The map  $\Theta : Pol(\zeta, v) \rightarrow \Delta_\theta^{p-1}$  is a homeomorphism.*

This in particular means that convex hull construction gives rise to a map

$$T_g^p \times \Delta_\theta^{p-1} \rightarrow \cup Pol(\zeta, v)$$

Since  $\cup Pol(\zeta, v) \subset Pol_g$  we obtain a map

$$\phi : T_g^p \times \Delta_\theta^{p-1} \rightarrow Pol_g \subset SE_g \cong T_g^p \times \Delta_\theta^{p-1}$$

where the last equivalence is the Troynov's isomorphism. This map factors through the identity map on the second factor and a map

$$\phi_\theta : T_g^p \rightarrow T_g^p$$

which explicitly could be described as follows.

Given a pair  $(\zeta, v) \in T_g^p$  and an angle assignment  $\theta \in \Delta_\theta^{p-1}$  one uses the convex hull construction to get a  $\Gamma_\zeta$ -equivariant convex surface  $\Sigma(\zeta, v)$  in Minkowski space with vertex angles given by  $\theta$  (where  $\Gamma_\zeta$  denotes the subgroup of  $SO^+(2, 1)$  corresponding to  $\zeta$ ). By the Riemann Uniformization Theorem,  $\Sigma(\zeta, v)$  is conformally equivalent to the hyperbolic plane  $\mathbb{H}^2$ . Transporting the structure on  $\Sigma(\zeta, v)$  to  $\mathbb{H}^2$ , we get a new subgroup  $\Gamma'_\zeta$  and a new element  $(\zeta', v') \in T_g^p$ . By definition

$$\phi_\theta(\zeta, v) = (\zeta', v')$$

To prove the conjecture of M.Davis one now needs to show that this map is onto. In fact it is expected to be a homeomorphism.

*Remark 3.* It is not difficult to see that this map is continuous. If one shows that it is closed and injective, than by invariance of domain principle it is open and therefore is onto since  $T_g^p$  is connected (in fact a finitely dimensional ball). To show it is closed one could show that it is proper. Showing injectivity is a kind of isometric embedding statement. Indeed, one needs to show that if two polyhedra are isometric, then they are actually congruent in Minkowski space, thus showing they come from the same conformal structure and choice of points in convex hull construction.

*Remark 4.* It is very unlikely however that this map is identity, i.e. that the conformal class of the polyhedron is the same as that of the conformal structure we start with

in the convex hull construction. To say the least, the central projection, being the most natural candidate, is not conformal. The two classes are, though, probably not too distant from each other in the Teichmüller space (i.e. there is a quasi-isometry of one onto another with bounded factor).



## CHAPTER 2

### PRELIMINARIES ON MINKOWSKY SPACE, HYPERBOLIC PLANE AND SURFACE GROUPS

We will denote by  $S_g$  an orientable closed surface of genus  $g$ . As is well known, such surfaces are topologically classified by this non-negative integer parameter. Once the surfaces are given complex structures, making them into Riemann surfaces, there appears a question of their conformal classification which is much more subtle. As a result of existence of isothermal coordinates on two-dimensional Riemannian manifolds such a classification is equivalent to the conformal classification of Riemannian metrics on the surfaces. Due to the Riemann Mapping Theorem, the universal cover of a surface is conformally either a (Riemann) sphere, a Euclidean plane or an open unit disk. The sphere, which is  $S_0$ , is, of course, covered by itself and therefore possesses a unique conformal structure. The torus ( $S_1$ ) is covered by the plane and the conformal classification is that of discrete subgroups of Euclidean translations isomorphic to its fundamental group, i.e.  $\mathbb{Z}^2$ , up to conjugation by  $Isom(\mathbb{R}^2)$ . It turns out that the moduli space of such subgroups can be identified with  $\mathbb{H}^2 / PSL_2(\mathbb{Z})$ , where  $PSL_2(\mathbb{Z})$  acts on the hyperbolic plane by the hyperbolic isometries. The moduli space thus is represented by the fundamental domain of this action, called *modular figure*, factored by the identifications of the boundary components (for a beautiful treatment see [19])

or [27]). The upper half plane itself is called Teichmuller space of such structures and takes account of how the conformal structure is worn by the surface, making it marked. Similarly, surfaces of higher genus  $g$  are covered by the unit disk. If this disk is endowed with constant metric of negative curvature, which will be chosen to be  $-1$ , than conformal classification is that of discrete groups of isometries of this metric isomorphic to the fundamental group  $\pi_1(S_g)$ . That in particular shows that it is equivalent to the classification of isometry classes of metrics of constant negative curvature (i.e.  $-1$ ) on such surfaces. The metric of curvature  $-1$  on the open unit disk is unique and is given by

$$ds^2 = \frac{4|dz|^2}{(1 - |z|^2)^2} \quad (2.1)$$

where  $z = x + iy$ . With this metric unit disk becomes a well known Poincaré model of the hyperbolic (Lobachevskian) plane. Thus, isometry classes of the "marked" two-dimensional surfaces of genus  $g > 1$  are parametrized by the conjugacy classes of faithful representations of  $\pi_1(S_g)$  into the group of orientation-preserving hyperbolic isometries. Their totality is called the Teichmuller space  $T_g$ . As before, considering the "non-marked" surfaces, the moduli spaces  $M_g$  are the quotients of these bigger spaces by the action of the mapping class group, which is discrete in Teichmuller metric. In fact, following relation is true (see [27]):

$$M_g \equiv T_g / \text{Out}(\pi_1(S_g))$$

Passing from non-marked surface to the marked one is therefore a choice of the generators for the fundanemental group representation. Going the other way is simply forgetting the generator set and remembering only the image of this representation.

It is a classical result that the Teichmüller space  $T_g$  is homeomorphic to  $\mathbb{R}^{6g-6}$ . We will also remark that the space of conformal structures on surfaces with marked  $p$  points is homeomorphic to the space  $T_g^p$  of conformal structures on  $p$  times punctured surfaces, which is again an open ball of dimension  $6g - 6 + 2p$  (see [15]).

The topological classification of surfaces is based on the fact that a surface can be obtained by gluing the corresponding sides of a (topological) polygon. When such a polygon is given metric of curvature  $-1$  for genus higher than 1 by embedding it into the hyperbolic plane so that it satisfies the conditions of the Poincaré theorem (cf. [3], Theorem 9.8.4), it becomes a fundamental polygon for the action of the corresponding discrete group. The aforementioned conditions are necessary and sufficient and require that sides identified in pairs are of equal length and polygon angles meeting at the same vertex on the surface (identified by the group action) add up to  $2\pi$ . Such a polygon then also defines (up to conjugation) the generators of the group, i.e. it is marked, and thus contains enough information to define an element of the Teichmüller space. If the generators are forgotten and only metric of the resulting surface is remembered, we obtain an element of the moduli space.

We will need to make use of another model of the hyperbolic plane - the hyperboloid model (see [27] for more detail). There are two reasons. Firstly, it will be very convenient for our calculations allowing us to use powerful machinery of linear algebra as opposed to dealing with cumbersome formulas of hyperbolic trigonometry. Secondly, as we will attempt (as we have done in the Introduction) to define "convex" polyhedra for the surfaces in analogy to the case of the sphere, we will need to look at the ambient affine space where surfaces of higher genus "live". This is readily

provided by the hyperboloid model in Minkowski space and seems to be a natural way of generalizing the concept of polyhedra.

Therefore, let us consider Minkowski space  $\mathbb{R}^{2,1}$  which is a linear space  $\mathbb{R}^3$  with the (indefinite) Minkowski inner product:

$$\langle v, u \rangle = -v^0 u^0 + v^1 u^1 + v^2 u^2$$

This is of course the Lorentz space of the special relativity, except for that there the sign of the inner product is customarily reversed and the dimension is 4 instead of 3.

A vector in  $\mathbb{R}^{2,1}$  is spacelike, lightlike or timelike if its length is correspondingly  $>$ ,  $=$  or  $<$  0. A two-dimensional plane is called spacelike if its orthogonal complement is timelike. Such a plane becomes Euclidean with its inherited metric.

Let us then define

$$\mathbb{H}^2 = \{v \in \mathbb{R}^{2,1} : \langle v, v \rangle = -1, v^0 > 0\}$$

which is the upper sheet of a two-sheeted hyperboloid. It turns out that with the metric inherited from its embedding into  $\mathbb{R}^{2,1}$  it is a Riemannian manifold of constant curvature  $-1$ . Being simply-connected, it is, therefore, isometric to the hyperbolic plane. Indeed, all tangent planes to  $\mathbb{H}^2$  are spacelike. In fact they are orthogonal to the point of tangency in total analogy to the sphere. Thus,  $\mathbb{H}^2$  could be considered a "sphere of radius  $\sqrt{-1}$ " in Minkowski space.

The straight lines in this model of the hyperbolic plane are represented by the sections of the hyperboloid by the central planes. The set of all (oriented) straight lines in  $\mathbb{H}^2$  is therefore parametrized by the *de Sitter Sphere* :

$$\mathbb{S}_1^1 = \{v \in \mathbb{R}^{2,1} : \langle v, v \rangle = 1\}$$

In Poincaré disk model the straight lines are, as well known, the arcs of the Euclidean circles (segments of straight Euclidean lines) inside the disk and orthogonal to its boundary, called the "circle at infinity" and denoted  $\partial\mathbb{H}^2$ . By abuse of notation, we will denote both models of the hyperbolic plane along with itself by  $\mathbb{H}^2$ . It will always be clear from the context which model  $\mathbb{H}^2$  really stands for.

The transition from one model to another is provided by the spherical projection from point  $(-1, 0, 0)$  in  $\mathbb{R}^{2,1}$  where open unit disk is embedded into the plane  $x^0 = 0$  as a unit disk about the center. This projection is checked to be an isometry of the hyperboloid with its inherited metric and the disk with the hyperbolic metric 2.1 on it.

The remarkable fact is that as in the Euclidean case, the isometry group of  $\mathbb{R}^{2,1}$  is closely related to that of  $\mathbb{H}^2$ . The situation is just slightly more complicated since isometries of  $\mathbb{R}^{2,1}$  can exchange the sheets of the hyperboloid. It turns out that the full group of isometries of  $\mathbb{H}^2$ , denoted  $O^+(2, 1)$  is of index 2 in the full group of isometries of  $\mathbb{R}^{2,1}$ , denoted  $O(2, 1)$ . Similarly,  $SO^+(2, 1)$  is the group of orientation-preserving isometries of  $\mathbb{H}^2$  and is of index 2 in  $SO(2, 1)$  and index 4 in  $O(2, 1)$ .

Thus, fixing a hyperbolic metric (of constant curvature  $-1$ ) on a surface of genus  $g$ , or equivalently, its conformal class, is equivalent to choosing a faithful representation

$$G : \pi_1(S_g) \rightarrow SO^+(2, 1)$$

up to conjugation. That yields the action of  $\pi_1(S_g)$  on  $\mathbb{H}^2$  by covering transformations.

We will now present two well-known formulas showing the connection of hyperbolic geometry on  $\mathbb{H}^2$  with the geometry of  $\mathbb{R}^{2,1}$ . These are absolutely analogous to the case of the sphere in  $\mathbb{R}^3$  and may either be considered as definitions or obtained by simple calculation using spherical projection of the hyperboloid onto the open unit disk. We have:

$$\cosh \operatorname{dist}(v_1, v_2) = -\langle v_1, v_2 \rangle \quad (2.2)$$

$$\sinh \operatorname{dist}(v, l^\perp) = \langle v, l \rangle \quad (2.3)$$

Here  $\operatorname{dist}$  is the distance function on  $\mathbb{H}^2$ ,  $v_1, v_2, v$  are the points on the hyperboloid and, therefore, vectors of imaginary unit length in  $\mathbb{R}^{2,1}$ ,  $l$  is a point in  $\mathbb{S}_1^1$  representing straight line  $l^\perp$  in  $\mathbb{H}^2$ .

For the background information on the geometry of discrete hyperbolic groups and Teichmüller space see, for example, [3], [24], [27], [1], [29], [6], [9], [31].

## CHAPTER 3

### TESSELLATIONS

#### 3.1 Definitions and reduction to the one-cell tessellation case

**Definition 3.1.1.** A *tessellation*  $T$  on a surface  $S$  is an embedding  $T : C \rightarrow S$ , where  $C$  is a finite, connected one-dimensional cell complex with all vertices of valence at least three, such that the complement of  $T(C)$  is a union of open two-dimensional cells.

Given a tessellation we have well defined vertices, edges and faces (the images of zero-, one- and two-dimensional cells, respectively).

**Definition 3.1.2.** A *geometric tessellation* is a tessellation on a surface with hyperbolic metric of constant curvature  $-1$  such that all edges are segments of geodesics.

When it is clear that the metric on the surface is fixed and we are dealing with the geometric tessellations, we will omit the word "geometric" and simply use the word tessellation.

The rigidity statements can be treated in a different way. A tessellation of a surface is obtained from gluing together hyperbolic polygons with prescribed angles by identifying the edges in pairs according to the given pattern. Starting with one of these polygons and adding other polygons one at a time by attaching them to

the previously glued polygons along one of the edges we will eventually arrive at the "total" polygon of the surface which consists of all polygons in the tessellation. The tessellation is now obtained by identifying edges of this "total" polygon in pairs. The "total" polygon is not uniquely determined, but possesses two important properties.

1. *It inherits the angle prescription from the tessellation and therefore provides a one-cell tessellation of the surface with prescribed angles.*
2. *There exists at least one "total" polygon with any given edge of the tessellation in its boundary.*

While problem of one-cell tessellations is a special case of the general problem of the tessellations, these two properties of "total" polygons, in fact, show that the general case follows from this special one. Indeed, the discussion in the introduction shows that it is enough to prove that there are only finitely many sets of edge lengths which produce a given surface. Assuming that the special case is true, applying it to different "total" polygon one-cell tessellations, we show that each edge has finitely many possible different lengths, which implies rigidity. Therefore, we will now restrict ourselves to the one-cell tessellation case.

For a surface to have a one cell-tessellation simply means that the surface can be glued from the polygon by identifying corresponding sides in pairs. The rigidity statements therefore can be modified as follows:



**Theorem A' (Local Rigidity).** *A hyperbolic polygon with prescribed angles producing a closed surface of genus  $g > 1$  with hyperbolic metric on it cannot be infinitesimally perturbed and still give rise to the same metric on the surface, i.e. its edge lengths are locally well defined.*

**Theorem C' (Global Rigidity in a fixed isotopy class).** *Given an isotopy class of a marked hyperbolic surface, there exist at most finitely many hyperbolic polygons producing this surface with the same combinatorial structure, angles and the isotopy class of the embedding  $T : C \rightarrow S$  of the corresponding one-cell tessellation.*

We will remark that we no longer have to say "up to isometry of the surface" as in the spherical case since the isometry group of a closed hyperbolic surface is finite. It is clear then that there are at least as many such tessellations as there are isometries of the surface, if at least one such tessellation exists. In particular, if the polygon possesses a non-trivial symmetry group, its symmetries will give rise to the isometries of the surface, thus making the symmetry group of the polygon a subgroup of the isometry group of the surface.

On the other hand it would be tempting to claim that in fact this is the only way to obtain more than one such tessellation, that is to say that all hyperbolic polygons of the same combinatorial type with same prescribed angles producing the same surface must, in fact, be congruent. Then the statement of the theorem would be that of the classical one : "unique up to isometry". This still remains a conjecture, but is now more doubtful in view of the potential counterexample.

### 3.2 Representation of the tessellation in the same isotopy class

Given a marked closed surface  $S_g$  of genus  $g > 1$  with fixed hyperbolic metric (conformal class), we obtain a well defined (up to conjugation by an element of  $SO^+(2, 1)$ ) faithful representation  $G : \pi_1(S_g) \rightarrow SO^+(2, 1)$  yielding an action of  $\pi_1(S_g)$  on  $H^2$  by covering transformations. We fix one such representation and by abuse of notation also call its image  $G$ .

Giving a one-cell geometric tessellation  $T$  on  $S_g$  with  $E$  edges is equivalent to specifying a hyperbolic  $2E$ -gon together with an edge pairing  $\psi$  so that the  $2E$ -gon is a fundamental domain for the group action (by cutting the tessellation along edges). This defines a map

$$Gen : \text{Edges} \rightarrow G$$

which sends each edge  $E_i$  of the polygon to an element  $G_i$  of  $G$  such that  $G_i(E_{\psi(i)}) = E_i$ . A theorem of Poincaré ([3], Theorem 9.8.4) now guarantees that  $\text{Im}(Gen)$  generates  $G$ .

Assume now, that we have an isotopy

$$\tilde{T} : C \times [0, 1] \rightarrow S_g$$

of geometric tessellations on  $S_g$ . This gives rise to a map

$$\tilde{Gen} : \text{Edges} \times [0, 1] \rightarrow G$$

which is continuous in the second parameter. Since  $G$  is discrete, this map is constant.

Since that same argument can be applied to tessellations, which are not necessarily geometric, we obtain the following

**Proposition 3.2.1.** *Isotopic tessellations produce the same set of the side-pairing generators of  $G$ .*

CHAPTER 4  
LOCAL RIGIDITY OF HYPERBOLIC SURFACE  
TESSELLATIONS WITH CONSTANT ANGLES

"In the end all problems of mathematics are solved  
by calculating determinants of some matrices."

*I.M. Gelfand*

#### 4.1 The Main Theorem and an outline of the proof

In this chapter we are going to prove local rigidity for the one-cell tessellations.

**Theorem 4.1.1 (Local Rigidity for one cell tessellations).** *A one-cell tessellation with prescribed angles on a closed surface of genus  $g > 1$  with a fixed hyperbolic metric cannot be infinitesimally perturbed, i.e. its edge lengths are locally well defined.*

This is a reformulation of the Theorem A'. Taken together with our discussion on the reduction to the one-cell tessellation case, it implies Theorem A.

Proving this theorem amounts to showing that a  $2E$ -gon  $P$ , which produces the given closed hyperbolic surface  $S_g$  after applying the identifications  $\psi$  of its edges, cannot be infinitesimally perturbed so that angles are preserved and so that it still gives rise to the same surface. According to the results of the previous section,

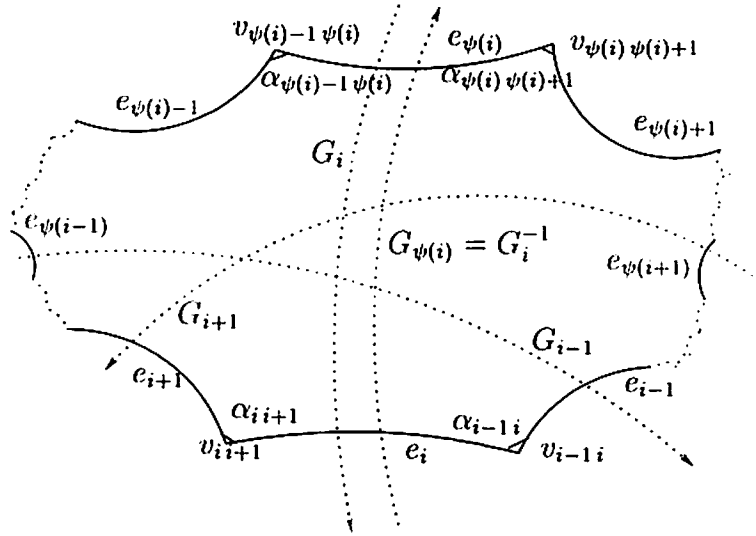


Figure 4.1: Hyperbolic polygon with identifications

perturbation within the same isotopy class means that the generators inducing the edge pairing  $\psi$  are the same for the entire deformation.

It will be convenient for us to work with the hyperboloid model of the hyperbolic plane. Thus, the universal cover of the surface will be identified with the upper sheet of the hyperboloid and  $G$  will be considered as a subgroup of  $SO^+(2, 1)$  acting as group of orientation and hyperboloid sheet preserving isometries of Minkowsky space  $\mathbb{R}^{2,1}$ .  $SO^+(2, 1)$  is also the group of orientation preserving isometries of the upper-sheet hyperboloid model of the hyperbolic plane. The one-polygon tessellation of the surface then lifts to a tessellation of the upper sheet of the hyperboloid (which we will from now on call the hyperboloid) by polygons congruent to the given one. Choose one and identify it with  $P$ . This polygon is determined by the outward pointing unit

normals to the central planes defining the polygon edges as their intersections with the hyperboloid. These vectors belong to the *de Sitter sphere* which is the one-sheeted hyperboloid in Minkowsky space defined by the equation  $-x_0^2 + x_1^2 + x_2^2 = 1$ .

Before we start calculations, let us discuss our strategy of proving local rigidity by doing some crude dimension count.

The polygon  $P$ , which produces the surface  $S$  upon side identifications, has  $2E$  sides and therefore, is defined by  $2E$  vectors in the de Sitter sphere. This gives  $4E$  degrees of freedom. Since the group is fixed, unit normals for each pair of sides are obtained from one another by applying the corresponding side-pairing generator and taking opposite sign (to get outward-pointing vector). So we have only  $E$  normal units left (independent), hence  $2E$  degrees of freedom. Now, since the group  $G$  is a surface group, it has certain "cycle" relations imposed on the side-pairing generators. These relations are obtained by taking product of all the generators corresponding to the sides incident to some cycle of vertices in the polygon in the order they are met in moving around a vertex representing cycle in some direction. This then shows that each cycle relation allows us to express one of the normal units incident to this cycle in terms of others. If  $V$  denotes the number of cycles, i.e. the number of vertices on the surface, then we are left with  $E - V$  unknown unit normals and, therefore,  $2E - 2V$  degrees of freedom.

Next we impose the angle condition by requiring angles of the polygon to be constant. There are  $2E$  angles but they are not independent. There are  $V$  obvious linear relations between them, namely, angles incident to the same cycle add up to  $2\pi$ . That means that we get  $2E - V$  relations. Comparing this with number of degrees

of freedom we see that we only need to show that at least  $2E - 2V$  of these relations are independent.

Although this dimension count is somewhat trivial, carrying it out in calculation will be quite cumbersome because we assumed normal vectors to be in the de Sitter Sphere, which is non-linear. Therefore we will prefer working with vectors in  $\mathbb{R}^{2,1}$  which must satisfy the quadratic relation defining the de Sitter Sphere.

Also, for the sake of clarity and natural progression we will first introduce the angle restrictions, which in the above count would correspond to reducing  $2E$  degrees of freedom by  $2E - V$  relations. Obviously this is not sufficient for rigidity (which is 0 degrees of freedom). But we will also show that these  $2E - V$  relations are indeed independent. Only then will we add the relations provided by the cycle conditions and find among them another  $V$  relations independent from the ones we already have. This will come down to showing that certain matrix is not degenerate.

## 4.2 System of Side Pairing Equations

Let  $\{e_i\}_{i=1}^{2E}$  be the set of these unit normals numbered as we move along the polygon clockwise looking from the interior of the upper sheet of the hyperboloid (Fig. 4.2). According to [7] these normal units form a piecewise spherical (circular) polygon in the de Sitter Sphere.

Let  $\{G_i\}_{i=1}^{2E}$  be the set of the generators of  $G$  corresponding to the pairing of the sides according to involution  $\psi$ . In other words, we have

$$G_i e_{\psi(i)} = -e_i \tag{4.2.1}$$

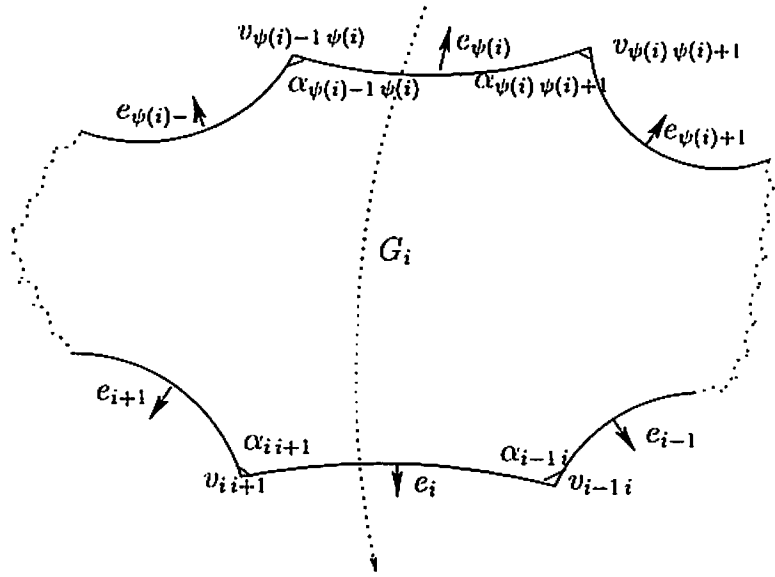


Figure 4.2:  $2E$ -gon with side normals and identifications

where minus sign is caused by the fact that all unit normals are outward-pointing and the map  $G_i$ , which is an orientation-preserving isometry, takes an outward-pointing normal to an inward-pointing one.

We also have

$$\langle e_i, e_{i+1} \rangle = -\cos \alpha_{i+1} \quad (4.2.2)$$

where  $\{\alpha_{i+1}\}_{i=1}^n$  are the prescribed angles, and

$$\langle e_i, e_i \rangle = 1 \quad (4.2.3)$$

since  $\{e_i\}$  is a set of unit normals.

Now, assume that there is a continuous (smooth) deformation  $P(t)$  of our polygon  $P = P(0)$  so that the angles do not change and all polygons  $P(t)$  give the same metric



on the surface. As we know from section 3.2 the set of generators  $\{G_i\}$  does not change up to conjugation by an element of  $SO^+(2,1)$ . Therefore, conjugating, if necessary, by an element  $g(t)$  and noticing that  $g(t)$  depends continuously on  $t$ , we may write equations 4.2.1, 4.2.2 and 4.2.3 as  $t$ -dependent:

$$\begin{cases} G_i e_{\psi(i)}(t) & = -e_i(t) \\ \langle e_i(t), e_{i+1}(t) \rangle & = -\cos \alpha_{i+1} \\ \langle e_i(t), e_i(t) \rangle & = 1 \end{cases}$$

Now, differentiating these equations with respect to  $t$  and evaluating at  $t = 0$  (or, if one prefers, taking the differential of this system of equations) we obtain

$$\begin{cases} G_i e'_{\psi(i)} + e'_i & = 0 \\ \langle e'_i, e_{i+1} \rangle + \langle e_i, e'_{i+1} \rangle & = 0 \\ \langle e'_i, e_i \rangle & = 0 \end{cases} \quad (S)$$

This is a system of homogeneous linear equations for the components  $\{e_i^{\prime 1}, e_i^{\prime 2}, e_i^{\prime 3}\}$  of vectors  $\{e'_i\}$ . The naive goal would be to show that this system has only zero solution. But as we know from our dimension count this is not the case and more analysis will be required.

First of all let us take a look at its matrix  $M$ :

$$\begin{array}{cccccccccccccccccccc}
e_i^{\prime 1} & e_i^{\prime 2} & e_i^{\prime 3} & e_i^{\prime 1} & e_i^{\prime 2} & e_i^{\prime 3} & e_{i+1}^{\prime 1} & e_{i+1}^{\prime 2} & e_{i+1}^{\prime 3} & \dots & e_{\psi(i)-1}^{\prime 1} & e_{\psi(i)-1}^{\prime 2} & e_{\psi(i)-1}^{\prime 3} & e_{\psi(i)}^{\prime 1} & e_{\psi(i)}^{\prime 2} & e_{\psi(i)}^{\prime 3} & e_{\psi(i)+1}^{\prime 1} & e_{\psi(i)+1}^{\prime 2} & e_{\psi(i)+1}^{\prime 3} \\
0 & 0 & 0 & 1 & 0 & 0 & 0 & 0 & 0 & \dots & 0 & 0 & 0 & G_{11}^i & G_{12}^i & G_{13}^i & 0 & 0 & 0 \\
0 & 0 & 0 & 0 & 1 & 0 & 0 & 0 & 0 & \dots & 0 & 0 & 0 & G_{21}^i & G_{22}^i & G_{23}^i & 0 & 0 & 0 \\
0 & 0 & 0 & 0 & 0 & 1 & 0 & 0 & 0 & \dots & 0 & 0 & 0 & G_{31}^i & G_{32}^i & G_{33}^i & 0 & 0 & 0 \\
0 & 0 & 0 & G_{11}^{\psi(i)} & G_{12}^{\psi(i)} & G_{13}^{\psi(i)} & 0 & 0 & 0 & \dots & 0 & 0 & 0 & 1 & 0 & 0 & 0 & 0 & 0 \\
0 & 0 & 0 & G_{21}^{\psi(i)} & G_{22}^{\psi(i)} & G_{23}^{\psi(i)} & 0 & 0 & 0 & \dots & 0 & 0 & 0 & 0 & 1 & 0 & 0 & 0 & 0 \\
0 & 0 & 0 & G_{31}^{\psi(i)} & G_{32}^{\psi(i)} & G_{33}^{\psi(i)} & 0 & 0 & 0 & \dots & 0 & 0 & 0 & 0 & 0 & 1 & 0 & 0 & 0 \\
-e_i^{\prime 1} & e_i^{\prime 2} & e_i^{\prime 3} & -e_{i-1}^{\prime 1} & e_{i-1}^{\prime 2} & e_{i-1}^{\prime 3} & 0 & 0 & 0 & \dots & 0 & 0 & 0 & 0 & 0 & 0 & 0 & 0 & 0 \\
0 & 0 & 0 & -e_{i+1}^{\prime 1} & e_{i+1}^{\prime 2} & e_{i+1}^{\prime 3} & -e_i^{\prime 1} & e_i^{\prime 2} & e_i^{\prime 3} & \dots & 0 & 0 & 0 & 0 & 0 & 0 & 0 & 0 & 0 \\
0 & 0 & 0 & 0 & 0 & 0 & 0 & 0 & 0 & \dots & -e_{\psi(i)}^{\prime 1} & e_{\psi(i)}^{\prime 2} & e_{\psi(i)}^{\prime 3} & -e_{\psi(i)-1}^{\prime 1} & e_{\psi(i)-1}^{\prime 2} & e_{\psi(i)-1}^{\prime 3} & 0 & 0 & 0 \\
0 & 0 & 0 & 0 & 0 & 0 & 0 & 0 & 0 & \dots & 0 & 0 & 0 & -e_{\psi(i)+1}^{\prime 1} & e_{\psi(i)+1}^{\prime 2} & e_{\psi(i)+1}^{\prime 3} & -e_{\psi(i)}^{\prime 1} & e_{\psi(i)}^{\prime 2} & e_{\psi(i)}^{\prime 3} \\
0 & 0 & 0 & -e_i^{\prime 1} & e_i^{\prime 2} & e_i^{\prime 3} & 0 & 0 & 0 & \dots & 0 & 0 & 0 & 0 & 0 & 0 & 0 & 0 & 0 \\
0 & 0 & 0 & 0 & 0 & 0 & 0 & 0 & 0 & \dots & 0 & 0 & 0 & -e_{\psi(i)}^{\prime 1} & e_{\psi(i)}^{\prime 2} & e_{\psi(i)}^{\prime 3} & 0 & 0 & 0
\end{array}$$

where

$$\begin{pmatrix} G_{11}^i & G_{12}^i & G_{13}^i \\ G_{21}^i & G_{22}^i & G_{23}^i \\ G_{31}^i & G_{32}^i & G_{33}^i \end{pmatrix}$$

is the matrix of  $G_i$ .

This is a system of  $6E + 2E + 2E = 10E$  homogeneous linear equations for  $6E$  unknowns  $\{e_i^{\prime 1}, e_i^{\prime 2}, e_i^{\prime 3}\}_{i=1}^{2E}$ . It would be desirable to show that the rank of this system is precisely  $6E$ , i.e. this system has only trivial solution, which is equivalent to the local rigidity statement. Unfortunately this is not the case and we will calculate the rank of this matrix to find the dimension of the space of the solutions of this system.

### 4.3 Equations for the coefficients

To calculate the rank of matrix  $M$  we pick one side  $e_i$  in each pair, look at the columns corresponding to  $e_i$  and consider the linear combination of the rows having non-zero entries in these three columns. These rows are explicitly written out in

the matrix above. First, notice that the three rows corresponding to the equation  $e'_{\psi(i)} + G_{\psi(i)}e'_i = 0$  are linear combinations of the three rows corresponding to the equation  $G_i e'_{\psi(i)} + e'_i = 0$  because these two equations are equivalent. The first is obtained from the second by applying  $G_{\psi(i)}$  to both sides of the equation since  $G_{\psi(i)} = G_i^{-1}$  by the definition of the pairing action of  $G$  on the set of sides of the polygon  $P$ . Similarly, the equation  $\langle e'_{\psi(i)}, e_{\psi(i)} \rangle = 0$  is equivalent to the equation  $\langle e'_i, e_i \rangle = 0$  since  $G_i$  is an isometry. Therefore, the corresponding row of the former is a linear combination of the row corresponding to the second and rows corresponding to the equations  $G_i e'_{\psi(i)} + e'_i = 0$ , and hence, can be eliminated.

Therefore, we only have  $6E$  equations left for  $6E$  unknowns.

Assume now that some nontrivial linear combination of the remaining  $6E$  rows is zero and that the coefficients in this linear combination are specified in the following table:

$$\begin{array}{rcccccccc}
\text{Coef} & \vdots & e_i^{\prime 1} & e_i^{\prime 2} & e_i^{\prime 3} & \dots & e_{\psi(i)}^{\prime 1} & e_{\psi(i)}^{\prime 2} & e_{\psi(i)}^{\prime 3} \\
\Lambda_{i1} & \vdots & 1 & 0 & 0 & \dots & G_{11}^i & G_{12}^i & G_{13}^i \\
\Lambda_{i2} & \vdots & 0 & 1 & 0 & \dots & G_{21}^i & G_{22}^i & G_{23}^i \\
\Lambda_{i3} & \vdots & 0 & 0 & 1 & \dots & G_{31}^i & G_{32}^i & G_{33}^i \\
b_{i-1i} & \vdots & -e_{i-1}^1 & e_{i-1}^2 & e_{i-1}^3 & \dots & 0 & 0 & 0 \\
b_{ii+1} & \vdots & -e_{i+1}^1 & e_{i+1}^2 & e_{i+1}^3 & \dots & 0 & 0 & 0 \\
b_{\psi(i)-1\psi(i)} & \vdots & 0 & 0 & 0 & \dots & -e_{\psi(i)-1}^1 & e_{\psi(i)-1}^2 & e_{\psi(i)-1}^3 \\
b_{\psi(i)\psi(i)+1} & \vdots & 0 & 0 & 0 & \dots & -e_{\psi(i)+1}^1 & e_{\psi(i)+1}^2 & e_{\psi(i)+1}^3 \\
a_i & \vdots & -e_i^1 & e_i^2 & e_i^3 & \dots & 0 & 0 & 0
\end{array}$$

For this linear combination to be zero the sum of entries with corresponding coefficients in each of these six columns must be zero. This can be written as two vector equations, where vector  $\Lambda_i = (\Lambda_{i1}, \Lambda_{i2}, \Lambda_{i3})$  and all vectors are treated as rows:

$$\begin{cases} \Lambda_i + b_{i-1i}e_{i-1}^* + b_{ii+1}e_{i+1}^* + a_i e_i^* = 0 \\ \Lambda_i G_i + b_{\psi(i)-1\psi(i)}e_{\psi(i)-1}^* + b_{\psi(i)\psi(i)+1}e_{\psi(i)+1}^* = 0 \end{cases} \quad (I)$$

Here  $e^*$  is the conjugate of vector  $e$ , i.e.  $(e_1, e_2, e_3)^* = (-e_1, e_2, e_3)$ .

This is now a system of homogeneous linear equations for the coefficients. We would like to find the fundamental solution of this last system to find the dimension of the space of solutions of the original one. To this end we first get rid of  $\Lambda_i$ . Namely, we take transpose of both equations considering all vectors as columns, multiply the

first equation by  $J$  and the second by  $G_i J$ , where  $J = \begin{pmatrix} -1 & 0 & 0 \\ 0 & 1 & 0 \\ 0 & 0 & 1 \end{pmatrix}$  is the matrix of the Minkowsky metric, and subtract the second equation from the first:

$$- \begin{cases} J \left\{ \Lambda_i + b_{i-1} e_{i-1}^* + b_{i+1} e_{i+1}^* + a_i e_i^* = 0 \right. \\ \left. G_i J \left\{ G_i^T \Lambda_i + b_{\psi(i)-1} e_{\psi(i)-1}^* + b_{\psi(i)+1} e_{\psi(i)+1}^* = 0 \right. \right. \end{cases}$$

Since  $G_i$  is an isometry for the Minkowsky metric  $G_i J G_i^T = J$ , and  $J e^* = e$ , we get

$$a_i e_i + b_{i-1} e_{i-1} + b_{i+1} e_{i+1} - b_{\psi(i)-1} G_i e_{\psi(i)-1} - b_{\psi(i)+1} G_i e_{\psi(i)+1} = 0 \quad (i)$$

It is here where one would hope to show all these coefficients must be zero, but it will not be the case as the original equations will turn out to be linearly dependent.

We can think of the coefficients  $a_i$  to be assigned to the corresponding sides of the polygon  $P$  (or even the pair of sides) and coefficients  $b_{i+1}$  to be assigned to the corresponding angles.

#### 4.4 "Four-legged" pictures

We will solve the equation (i) by a geometric argument which is based on examining the so-called "four-legged" picture (Fig. 4.3 ) Notice that such "four-legged" picture with the corresponding equation (i) exists for each edge, but for two edges in the same pair the equations (and pictures) are equivalent as one can be obtained from the other by applying correspondingly  $G_i$  or  $G_{\psi(i)}$  to both sides of the equation and

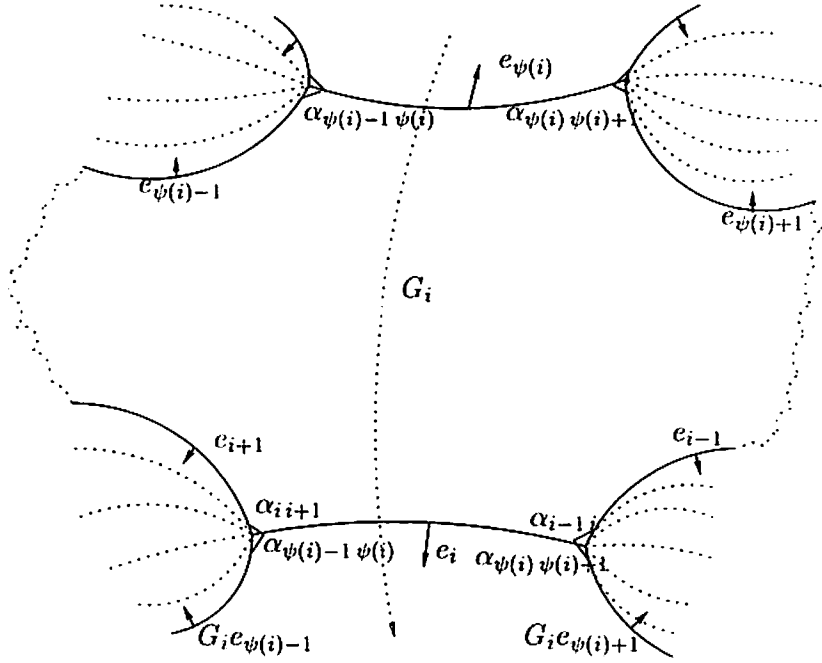


Figure 4.3: Four-legged picture

taking  $a_{\psi(i)} = -a_i$ . So, we have  $E$  "four-legged" pictures and corresponding equations to consider.

Notice, also, that the coefficients involved into equation (i) correspond to the central edge (actually pair of edges containing this edge) and the four adjacent angles. The vectors  $e_{i-1}, e_{i+1}, e_{\psi(i)-1}, e_{\psi(i)+1}$  point outwards and the vector  $e_i$  downwards in this picture. Let's also denote the vertex of the polygon  $P$  between the sides  $e_i$  and  $e_{i+1}$ , considered as a vector in Minkowsky space, by  $v_{i+1}$ . (This vector, of course, belongs to the hyperboloid.) We are going to abuse the notation by using  $v_{i+1}$  to denote both the vertex and its vector. Similarly we will use  $e_i$  to denote both the

side and its outward pointing normal unit vector in the de Sitter Sphere. Also, keep in mind that  $\{v_{i+1}\}_{i=1}^{2E}$  is the set of vertices of polygon  $P$  in  $\mathbb{H}^2$ , rather than the set of vertices on the surface, which will be identified with the orbits of vertices  $\{v_{i+1}\}$  under the group  $G$  action. Notation for the latter will be given later, as we need it.

Fix  $i$ . Since  $v_{i+1}$  is orthogonal in Minkowsky metric to the adjacent edge vectors  $e_i, e_{i+1}, G_i e_{\psi(i)+1}$ , if we now take the inner product of both sides of the equation (i) with  $v_{i+1}$ , we get

$$b_{i-1} \langle v_{i+1}, e_{i-1} \rangle - b_{\psi(i)+1} \langle v_{i+1}, G_i e_{\psi(i)+1} \rangle = 0$$

It is a famous result (mentioned in preliminaries) that  $\sinh$  of the hyperbolic distance between a point and a straight line on the hyperbolic plane is equal to the scalar product of the central vector of this point and a unit normal vector of this line pointing into the half-plane containing this point. Therefore,

$$-b_{i-1} \sinh \text{dist}(v_{i+1}, e_{i-1}^\perp) + b_{\psi(i)+1} \sinh \text{dist}(v_{i+1}, (G_i e_{\psi(i)+1})^\perp) = 0$$

where  $e_i^\perp$  denotes the straight line in  $\mathbb{H}^2$  dual to the vector  $e_i$ . Now, by hyperbolic right-angle triangle trigonometry (Fig. 4.4), denoting the length of the edge dual to  $e_i$  by  $l_i$ , that is,  $l_i = \text{dist}(v_{i-1}, v_{i+1})$ , we have

$$\begin{aligned} \sinh \text{dist}(v_{i+1}, e_{i-1}^\perp) &= \sinh l_i \sin \alpha_{i-1} \\ \sinh \text{dist}(v_{i+1}, G_i e_{\psi(i)+1}^\perp) &= \sinh l_i \sin \alpha_{\psi(i)+1} \end{aligned}$$

So, finally,

$$b_{i-1} \sin \alpha_{i-1} = b_{\psi(i)+1} \sin \alpha_{\psi(i)+1} \tag{4.4.1}$$

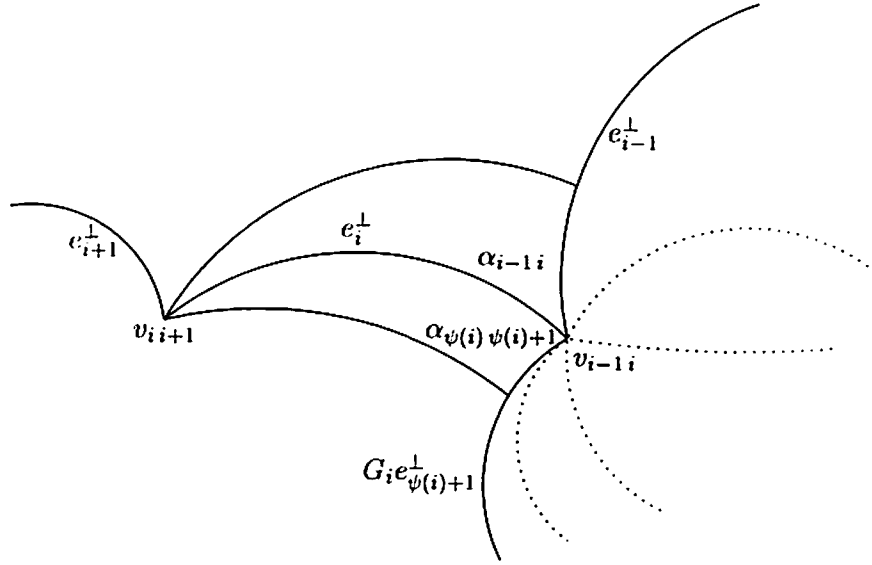


Figure 4.4: Right-angle triangle

#### 4.5 Relations for $b$ -coefficients in the star of a vertex

Now we will consider the star of the vertex  $v_{i-1}$  in hyperbolic plane.(Fig.4.5)

This is, of course, equivalent to looking at the star of the corresponding vertex on the surface, which, as we mentioned, can be identified with the orbit of vertex  $v_{i-1}$  and is its image under the covering map. Denote this vertex on the surface (orbit) by  $V_j$ . It can also be identified with the cycle of vertices of the polygon  $P$  under the side-pairing action of  $\psi$ . In the future we will use either one of these notions depending on the convenience of the interpretation and assuming that their equivalence is understood. If no confusion may arise, we will simply say vertex  $V_j$ .

Since the argument at the end of the previous section can be repeated for any



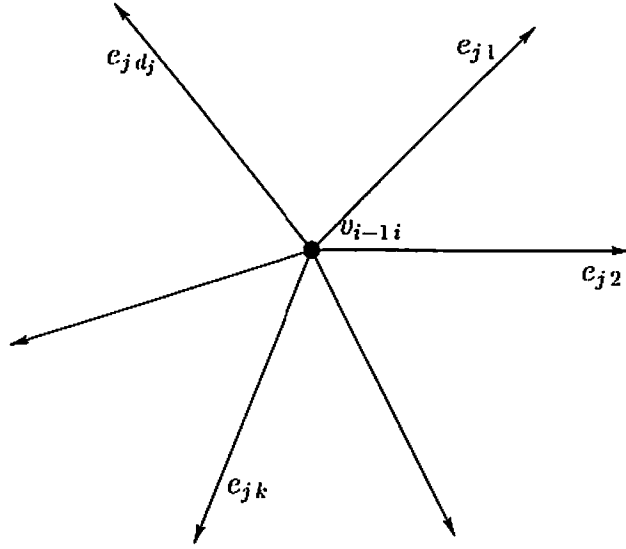


Figure 4.5: Vertex star of  $v_{i-1i} \in V_j$

three consecutive edges in the star of  $v_{i-1i}$  ( $V_j$ ), denoting angles in this star as  $\{\alpha_l^j\}_{l=1}^{d_j}$  moving clockwise around the vertex  $V_j$ , where  $d_j$  is the degree of this vertex, and also denoting corresponding  $b$ -coefficients  $\{b_l^j\}_{l=1}^{d_j}$ , we get

$$b_1^j \sin \alpha_1^j = b_2^j \sin \alpha_2^j = \dots = b_{d_j}^j \sin \alpha_{d_j}^j, \quad (4.5.1)$$

Therefore, coefficients  $b_{m+1}$  corresponding to the angles in this star (or, in the cycle corresponding to  $V_j$ ) are all proportional, and hence there exists one free parameter  $t_j$  for each vertex  $V_j$  such that

$$b_{m+1} = \frac{t_j}{\sin \alpha_{m+1}} \quad (4.5.2)$$

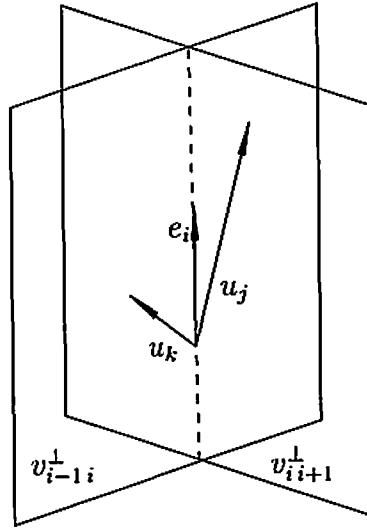


Figure 4.6: Intersecting planes

where angle  $\alpha_{m m+1}$  is in the star of this vertex.

#### 4.6 Solving for the coefficients

Now, substituting 4.5.2 for  $b_{i-1 i}$ ,  $b_{i i+1}$ ,  $b_{\psi(i)-1 \psi(i)}$  and  $b_{\psi(i) \psi(i)+1}$  into the equation (i) and assuming that vertex  $v_{i-1 i}$  is in the cycle  $V_j$  and vertex  $v_{i i+1}$  is in the cycle  $V_k$  (which, of course, may coincide), we obtain

$$\begin{aligned}
 a_i e_i + t_j \left( \frac{1}{\sin \alpha_{i-1 i}} e_{i-1} - \frac{1}{\sin \alpha_{\psi(i), \psi(i)+1}} G_i e_{\psi(i)+1} \right) \\
 + t_k \left( \frac{1}{\sin \alpha_{i i+1}} e_{i+1} - \frac{1}{\sin \alpha_{\psi(i)-1 \psi(i)}} G_i e_{\psi(i)-1} \right) = 0 \quad (4.6.1)
 \end{aligned}$$

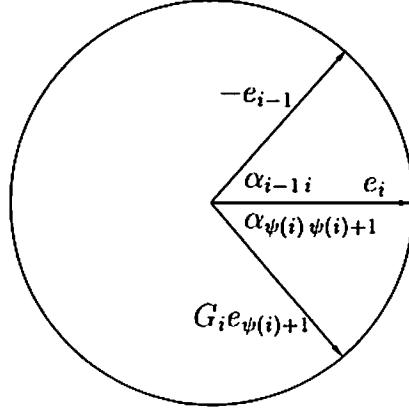


Figure 4.7: Picture in the plane  $v_{i-1 i}^\perp$

Now, notice that if  $t_k \neq 0$  or  $t_j \neq 0$ , the corresponding vectors in parentheses  $u_k$  and  $u_j$  must be colinear to the vector  $e_i$  for the left side of the equation 4.6.1 to be zero, since these two vectors lie in different planes  $v_{i-1 i}^\perp$  and  $v_{i+1 i}^\perp$  and  $e_i$  is in their intersection (Fig. 4.6). In fact, they are. To see this let's look at the plane  $v_{i-1 i}^\perp$  (Fig. 4.7)

The angle between vectors  $-e_{i-1}$  and  $e_i$  is  $\alpha_{i-1 i}$  and the angle between vectors  $G_i e_{\psi(i)+1}$  and  $e_i$  is  $\alpha_{\psi(i), \psi(i)+1}$  and the two angles lie on opposite sides of  $e_i$ , that is to say, they have different orientations. Applying Proposition A.4 of the Appendix A we obtain

$$\frac{1}{\sin \alpha_{i-1 i}} e_{i-1} - \frac{1}{\sin \alpha_{\psi(i), \psi(i)+1}} G_i e_{\psi(i)+1} = -(\cot \alpha_{i-1 i} + \cot \alpha_{\psi(i), \psi(i)+1}) e_i$$

Similarly for the vector corresponding to  $t_k$ . Substituting this into 4.6.1 we have

$$a_i e_i - t_j (\cot \alpha_{i-1 i} + \cot \alpha_{\psi(i) \psi(i)+1}) e_i - t_k (\cot \alpha_{i i+1} + \cot \alpha_{\psi(i)-1 \psi(i)}) e_i = 0$$

or, since  $e_i \neq 0$ ,

$$a_i - t_j (\cot \alpha_{i-1 i} + \cot \alpha_{\psi(i) \psi(i)+1}) - t_k (\cot \alpha_{i i+1} + \cot \alpha_{\psi(i)-1 \psi(i)}) = 0$$

Therefore,

$$a_i = t_j (\cot \alpha_{i-1 i} + \cot \alpha_{\psi(i) \psi(i)+1}) + t_k (\cot \alpha_{i i+1} + \cot \alpha_{\psi(i)-1 \psi(i)})$$

Also, recalling equations (I) we find coefficients  $\Lambda_i$

$$\Lambda_i = -b_{i-1 i} e_{i-1}^* - b_{i i+1} e_{i+1}^* - a_i e_i^* = -\frac{t_j}{\sin \alpha_{i-1 i}} e_{i-1}^* - \frac{t_k}{\sin \alpha_{i i+1}} e_{i+1}^* - a_i e_i^*$$

Thus, we have the following solution for the coefficients:

$$\begin{cases} b_{m m+1} = \frac{t_n}{\sin \alpha_{m m+1}} \\ a_i = t_j (\cot \alpha_{i-1 i} + \cot \alpha_{\psi(i) \psi(i)+1}) + t_k (\cot \alpha_{i i+1} + \cot \alpha_{\psi(i)-1 \psi(i)}) \\ \Lambda_i = -\frac{t_j}{\sin \alpha_{i-1 i}} e_{i-1}^* - \frac{t_k}{\sin \alpha_{i i+1}} e_{i+1}^* - a_i e_i^* \end{cases}$$

where  $v_{m m+1}$  is in the cycle (orbit)  $V_n$ ,  $v_{i-1 i}$  (and therefore  $v_{\psi(i) \psi(i)+1}$ ) is in the cycle (orbit)  $V_j$  and  $v_{i i+1}$  is in the cycle (orbit)  $V_k$ .

Now we can see that there are at most  $V$  free parameters, where  $V$  is the number of vertices on the surface for this tessellation (the number of orbits under the action of the group  $G$ ). Therefore, the rank of the matrix  $M$  of our original system is at least  $6E - V$ , that means that the dimension of the space of solution of system (S) is at most  $V$ .

## 4.7 The Local Vertex Equations

It is not difficult to think of the reason for this result. We have an excess of one equation for each vertex cycle since the sum of angles at each vertex on the surface is  $2\pi$  and this sum does not change as we perturb the polygon. We have implicitly used this fact when multiplied equation (i) by vertices adjacent to the side  $e_i$  as we assumed three of the five vectors dual to the edges in the "four-legged" picture to be orthogonal to the vectors representing these vertices. Hence, for each vertex cycle one of the conditions of constancy of the angles through the deformation became dependent on the rest of them and this sum condition. We will now add one equation for each vertex cycle to account for this last condition. Then we will show that with these new equations the rank of the system becomes precisely  $6E$ , which implies it has only trivial solution. Hence, local rigidity holds.

For the vertex  $V_j$  let  $\{e_{jk}\}_{k=1}^{d_j}$  be the set of adjacent edges (normal vectors pointing clockwise) numbered as we move counterclockwise around the vertex. Let the angles between the edges be correspondingly  $\{\alpha_{jkk+1}\}_{k=1}^{d_j}$ . Then by Lemma A.2 of the Appendix A we have

$$\sum_{k=1}^{d_j} \left( \tan \frac{\alpha_{jk-1k}}{2} + \tan \frac{\alpha_{jkk+1}}{2} \right) e_{jk}(t) = 0$$

Differentiating this equation at 0 one has

$$\sum_{k=1}^{d_j} \left( \tan \frac{\alpha_{jk-1k}}{2} + \tan \frac{\alpha_{jkk+1}}{2} \right) e'_{jk} = 0 \quad (4.7.1)$$

This adds three linear equations for each cycle  $V_j$  (one for each component of the edge vectors  $\{e_{jk}\}_{k=1}^{d_j}$ ), which is two too many (we only expected one from our

earlier heuristic dimension count). We will make one equation out of three by taking their linear combination with some specially chosen coefficients  $N_{j_1}N_{j_2}N_{j_3}$ , specific to each triple of equations. These coefficients form vector  $N_j$  which we will choose later. Then the coefficient of such a combined equation for the cycle  $V_j$  in the linear combination of the equations is  $c_j$ , or equivalently the three separate equations enter the linear combination with coefficients  $c_jN_{j_1}, c_jN_{j_2}, c_jN_{j_3}$ .

Before we can add these equations to our original system  $(S)$ , however, we must take care of the notation since, at the moment, each of the equations 4.7.1 uses a local numeration of the edges in the star of each vertex  $V_j$ . So, we again assume our original numeration  $\{e_i\}_{i=1}^{2E}$  as we move clockwise around polygon  $P$ . To see what equations 4.7.1 will look like in this notation we must take a look at the structural equations of the group  $G$ .

## 4.8 Structural equations for the group $G$ and the Global Vertex Equations

The generators  $\{G_i\}_{i=1}^{2E}$  of the group  $G$  are subject to certain relations (see [9], [31] or [3]), one for each cycle, as well as obvious ones we have already used  $G_{\psi(i)} = G_i^{-1}$ . For cycle  $V_j$  this relation is

$$\prod_{k=1}^{d_j} G_{i_{jk}} = \text{Id} \tag{4.8.1}$$

where numbers  $\{i_{jk}\}_{k=1}^{d_j}$  are given for each cycle in the definition of the group. These equations, of course, can be written in a number of different (and equivalent) ways

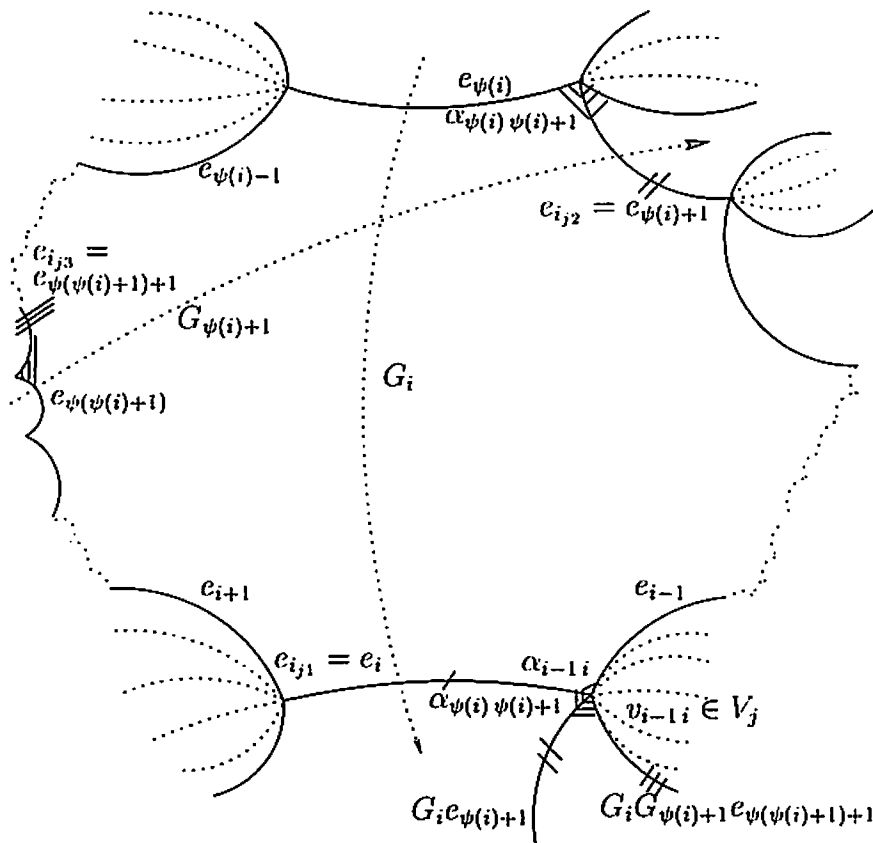


Figure 4.8: Structural Equations for the group  $G$  and involution  $\psi$

depending on which representative in a cycle is chosen and the direction of moving around it (these relations are obtained by moving around cycle representatives, writing down the sequence of group generators producing the translation and observing that after  $d_j$  translations the result is trivial).

Now, we make the necessary choices to fix the equations 4.8.1. For cycle  $V_j$  we choose representative  $v_{i-1,i}$ , preceding in clockwise direction around  $P$  one of the edges

$e_i$  we used before. We also choose the counterclockwise direction moving around this representative. Then sequence  $\{i_{jk}\}_{k=1}^{d_j}$  can be deduced from the action of  $\psi$  on the set  $1, \dots, 2E$  (Fig. 4.8), namely

$$i_{j1} = i, \quad i_{jk} = \psi(i_{j,k-1}) + 1, \quad k = 1, \dots, d_j \quad (4.8.2)$$

Therefore, the edges  $\{e_{jk}\}_{k=1}^{d_j}$  in the local vertex notation we encounter moving counterclockwise around representative  $v_{i-1i}$  are

$$e_{i_{j1}}, G_{i_{j1}} e_{i_{j2}}, G_{i_{j1}} G_{i_{j2}} e_{i_{j3}}, \dots, G_{i_{j1}} \dots G_{i_{j,d_j-1}} e_{i_{j,d_j}}$$

In view of 4.8.1 the next edge is equal to the first one.

We will call  $v_{i-1i}$  the *preferred* representative of the cycle  $V_j$ . It is therefore characterized by the fact that it precedes in the clockwise direction edge  $e_{i_{j1}}$ , which is first in the sequence of edges around the cycle  $V_j$  in counterclockwise direction. In other words, the preferred representative is

$$v_{i_{j1}-1 i_{j1}}$$

Now, we can apply equation 4.7.1 to this sequence of edges. First we have to observe that for each edge  $e_{i_{jk}}$  two angles adjacent to it in the star of the vertex are in fact the angle  $\alpha_{i_{j,k-1} i_{jk}}$  preceding this edge and the angle  $\alpha_{\psi(i_{jk}) \psi(i_{jk})+1}$  following its pair (Fig. 4.8 and Fig. 4.9). Hence,

$$\sum_{k=1}^{d_j} \left( \tan \frac{\alpha_{i_{j,k-1} i_{jk}}}{2} + \tan \frac{\alpha_{\psi(i_{jk}) \psi(i_{jk})+1}}{2} \right) G_{i_{j1}} \dots G_{i_{j,k-1}} e'_{i_{jk}} = 0 \quad (4.8.3)$$



where of course the product of elements in front of  $e_{i,j_1} = e_i$  is vacuous.

To make all of this look a bit more compact we will introduce the following notation:

$$\lambda_i = \tan \frac{\alpha_{i-1} i}{2} + \tan \frac{\alpha_{\psi(i)} \psi(i)+1}{2}$$

and

$$\begin{cases} g^{j1} = \text{Id} \\ g^{jk} = \prod_{l=1}^{k-1} G_{i,l} \end{cases}$$

Notice that this data is defined by the choice of the group  $G$  and polygon  $P$ .

Equation 4.8.3 then becomes

$$\sum_{k=1}^{d_j} \lambda_{i,j,k} g^{jk} e'_{i,j,k} = 0 \quad (4.8.4)$$

## 4.9 Augmented system of Tessellation Equations

Finally, we will add the equations 4.8.4 to the system  $(S)$  - one for each cycle. Hence, the augmented system is

$$\begin{cases} G_i e'_{\psi(i)} + e'_i & = 0 \\ \langle e'_i, e_{i+1} \rangle + \langle e_i, e'_{i+1} \rangle & = 0 \\ \langle e'_i, e_i \rangle & = 0 \\ \sum_{k=1}^{d_j} \lambda_{i,j,k} g^{jk} e'_{i,j,k} & = 0 \end{cases} \quad (\tilde{S})$$

where  $i = 1, \dots, 2E$  and  $j = 1, \dots, V$ .

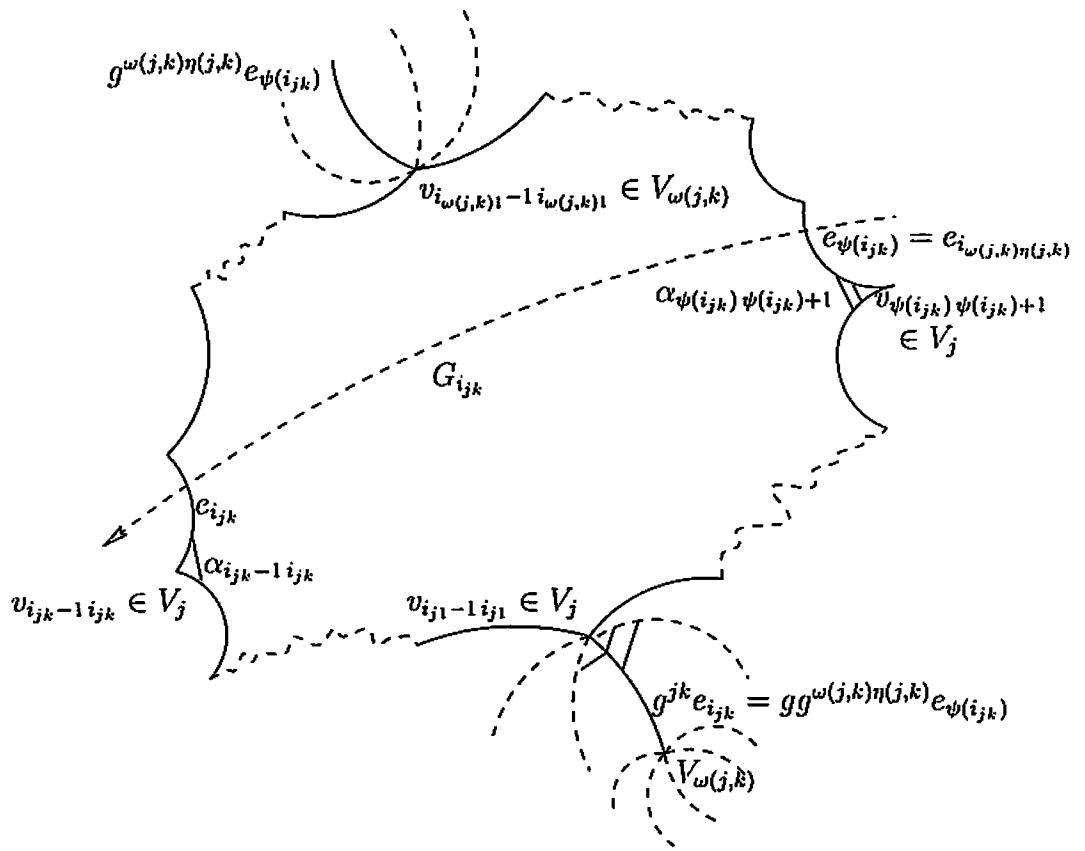


Figure 4.9: Functions  $\omega$  and  $\eta$

Notice now that each edge  $e_i$  is incident to the vertices of the polygon which may or may not belong to the same cycle. In either case, each edge  $e_i$  will enter precisely one equation 4.8.4 since each such equation only involves edges incident to the cycle representatives preceding them when traveling clockwise around the polygon. The equation for the cycle with representative following edge  $e_i$  (whether it is the same cycle or not) will involve its pair  $e_{\psi(i)}$ . If both representatives do belong to the same cycle, both edges will enter the same equation, otherwise not. Before we write matrix of this modified system, we will introduce some more notation.

Let  $V_{\omega(j,k)}$  be the cycle incident to the cycle  $V_j$  through the edge  $e_{i_{jk}}$ . As we explained above, the edge  $e_{\psi(i_{jk})}$  is, of course, incident to this cycle as well and will enter its equation (Fig. 4.9). Let  $\eta(j,k)$  be the position of the edge  $e_{\psi(i_{jk})}$  in the sequence of edges around the chosen representative of this cycle. In other words, we have

$$e_{\psi(i_{jk})} = e_{i_{\omega(j,k)\eta(j,k)}} \quad (4.9.1)$$

or, equivalently,

$$i_{\omega(j,k)\eta(j,k)} = \psi(i_{jk}) \quad (4.9.2)$$

Then, writing out explicitly for the additional equations just the columns for  $e_{i_{jk}}$  and  $e_{\psi(i_{jk})}$  and the only two triples of rows having non-zero entries in them (which

can actually coincide if both representatives belong to the same cycle), we have:

$$\begin{array}{rcccccccc}
\text{Var} & \vdots & e'_{ijk}{}^1 & e'_{ijk}{}^2 & e'_{ijk}{}^3 & \dots & e'_{\psi(i,j,k)}{}^1 & e'_{\psi(i,j,k)}{}^2 & e'_{\psi(i,j,k)}{}^3 \\
c_j N_{j1} & \vdots & \lambda_{ijk} g_{11}^{jk} & \lambda_{ijk} g_{12}^{jk} & \lambda_{ijk} g_{13}^{jk} & \dots & 0 & 0 & 0 \\
c_j N_{j2} & \vdots & \lambda_{ijk} g_{21}^{jk} & \lambda_{ijk} g_{22}^{jk} & \lambda_{ijk} g_{23}^{jk} & \dots & 0 & 0 & 0 \\
c_j N_{j3} & \vdots & \lambda_{ijk} g_{31}^{jk} & \lambda_{ijk} g_{32}^{jk} & \lambda_{ijk} g_{33}^{jk} & \dots & 0 & 0 & 0 \\
\vdots & \vdots & \vdots & \vdots & \vdots & \vdots & \vdots & \vdots & \vdots \\
c_{\omega(j,k)} N_{\omega(j,k)1} & \vdots & 0 & 0 & 0 & \dots & \lambda_{\psi(i,j,k)} g_{11}^{\omega(j,k)\eta(j,k)} & \lambda_{\psi(i,j,k)} g_{12}^{\omega(j,k)\eta(j,k)} & \lambda_{\psi(i,j,k)} g_{13}^{\omega(j,k)\eta(j,k)} \\
c_{\omega(j,k)} N_{\omega(j,k)2} & \vdots & 0 & 0 & 0 & \dots & \lambda_{\psi(i,j,k)} g_{21}^{\omega(j,k)\eta(j,k)} & \lambda_{\psi(i,j,k)} g_{22}^{\omega(j,k)\eta(j,k)} & \lambda_{\psi(i,j,k)} g_{23}^{\omega(j,k)\eta(j,k)} \\
c_{\omega(j,k)} N_{\omega(j,k)3} & \vdots & 0 & 0 & 0 & \dots & \lambda_{\psi(i,j,k)} g_{31}^{\omega(j,k)\eta(j,k)} & \lambda_{\psi(i,j,k)} g_{32}^{\omega(j,k)\eta(j,k)} & \lambda_{\psi(i,j,k)} g_{33}^{\omega(j,k)\eta(j,k)}
\end{array}$$

As we mentioned already, these rows contain other non-zero entries (for all edges incident to these cycles), but the columns do not (for this new addition to the matrix  $\tilde{M}$ ). And these two triples of rows can in fact coincide. This won't, though, affect our argument at all.

## 4.10 Equations for $c$ -coefficients

Now, we repeat the same procedure of eliminating the coefficients as before. The goal is to show that coefficients  $\{c_j\}_{j=1}^V$  are all zero should any of these newly-added equations enter any nontrivial linear combination. That would mean that these new equations are independent and that they are independent from the rest of the equations we had before. This of course will mean that the rank of this new expanded system is precisely  $6E$  leading to the desired result.

As before, for the rows with non-zero entries in the columns corresponding to the

edges  $e'_{i_{jk}}$  and  $e'_{\psi(i_{jk})}$  in our new expanded matrix to be in the linear combination of rows, the following equations , generalizing equations (I), must hold:

$$\left\{ \begin{array}{l} \Lambda_{i_{jk}} + b_{i_{jk}-1} e_{i_{jk}-1}^* + b_{i_{jk}+1} e_{i_{jk}+1}^* + a_{i_{jk}} e_{i_{jk}}^* \\ \quad + c_j \lambda_{i_{jk}} N_j g^{jk} = 0 \\ \Lambda_{i_{jk}} G_{i_{jk}} + b_{\psi(i_{jk})-1} e_{\psi(i_{jk})-1}^* + b_{\psi(i_{jk})+1} e_{\psi(i_{jk})+1}^* \\ \quad + c_{\omega(j,k)} \lambda_{\psi(i_{jk})} N_{\omega(j,k)} g^{\omega(j,k)\eta(j,k)} = 0 \end{array} \right. \quad (\tilde{I})$$

Taking transposes of the equations, as we did before, multiplying by the corresponding coefficients and subtracting one from the other, we have:

$$- \left\{ \begin{array}{l} J \left\{ \begin{array}{l} \Lambda_{i_{jk}} + b_{i_{jk}-1} e_{i_{jk}-1}^* + b_{i_{jk}+1} e_{i_{jk}+1}^* + a_{i_{jk}} e_{i_{jk}}^* \\ + c_j \lambda_{i_{jk}} g^{jkT} N_j = 0 \end{array} \right. \\ G_{i_{jk}} J \left\{ \begin{array}{l} G_{i_{jk}}^T \Lambda_{i_{jk}} + b_{\psi(i_{jk})-1} e_{\psi(i_{jk})-1}^* + b_{\psi(i_{jk})+1} e_{\psi(i_{jk})+1}^* \\ + c_{\omega(j,k)} \lambda_{\psi(i_{jk})} g^{\omega(j,k)\eta(j,k)T} N_{\omega(j,k)} = 0 \end{array} \right. \end{array} \right.$$

and consequently

$$\begin{aligned} & a_{i_{jk}} e_{i_{jk}} + b_{i_{jk}-1} e_{i_{jk}-1} + b_{i_{jk}+1} e_{i_{jk}+1} - \\ & - b_{\psi(i_{jk})-1} \psi(i_{jk}) G_{i_{jk}} e_{\psi(i_{jk})-1} - b_{\psi(i_{jk})+1} \psi(i_{jk}) G_{i_{jk}} e_{\psi(i_{jk})+1} + \\ & + c_j \lambda_{i_{jk}} J g^{jkT} N_j - c_{\omega(j,k)} \lambda_{\psi(i_{jk})} G_{i_{jk}} J g^{\omega(j,k)\eta(j,k)T} N_{\omega(j,k)} = 0 \quad (i_{jk}) \end{aligned}$$

As before, we now take inner product of both sides of this equation with  $v_{i_{jk} i_{jk}+1}$  to get

$$\begin{aligned}
& b_{i_{jk}-1, i_{jk}} \langle v_{i_{jk}, i_{jk}+1}, e_{i_{jk}-1} \rangle \\
& - b_{\psi(i_{jk}), \psi(i_{jk})+1} \langle v_{i_{jk}, i_{jk}+1}, G_{i_{jk}} e_{\psi(i_{jk})+1} \rangle \\
& + \langle v_{i_{jk}, i_{jk}+1}, c_j \lambda_{i_{jk}} J g^{jk T} N_j \rangle \\
& - \langle v_{i_{jk}, i_{jk}+1}, c_{\omega(j,k)} \lambda_{\psi(i_{jk})} G_{i_{jk}} J g^{\omega(j,k)\eta(j,k) T} N_{\omega(j,k)} \rangle = 0
\end{aligned} \tag{4.10.1}$$

First, let's notice that

$$g^{\omega(j,k)\eta(j,k)} = G_{i_{\omega(j,k)1}} \cdots G_{i_{\omega(j,k)\eta(j,k)-1}}$$

and, recalling relation 4.9.2, we therefore have

$$g^{\omega(j,k)\eta(j,k)} G_{\psi(i_{jk})} = g^{\omega(j,k)\eta(j,k)+1}$$

Since also  $G_{i_{jk}} = G_{\psi(i_{jk})}^{-1}$ , and  $g^{jk}$  and  $g^{\omega(j,k)\eta(j,k)}$  are orthogonal transformations for Minkowsky metric, we have

$$J g^{jk T} = (g^{jk})^{-1} J$$

and

$$\begin{aligned}
G_{i_{jk}} J g^{\omega(j,k)\eta(j,k) T} &= G_{\psi(i_{jk})}^{-1} (g^{\omega(j,k)\eta(j,k)})^{-1} J = \\
&= (g^{\omega(j,k)\eta(j,k)} G_{\psi(i_{jk})})^{-1} J = (g^{\omega(j,k)\eta(j,k)+1})^{-1} J \tag{4.10.2}
\end{aligned}$$

Now recalling that

$$\begin{aligned}
\langle v_{i_{jk}, i_{jk}+1}, e_{i_{jk}-1} \rangle &= \sinh \text{dist}(v_{i_{jk}, i_{jk}+1}, e_{i_{jk}-1}^\perp) \\
&= \sinh l_{i_{jk}} \sin \alpha_{i_{jk}-1, i_{jk}} \\
\langle v_{i_{jk}, i_{jk}+1}, G_{i_{jk}} e_{\psi(i_{jk})+1} \rangle &= \sinh \text{dist}(v_{i_{jk}, i_{jk}+1}, G_{i_{jk}} e_{\psi(i_{jk})+1}^\perp) \\
&= \sinh l_{i_{jk}} \sin \alpha_{\psi(i_{jk}), \psi(i_{jk})+1}
\end{aligned}$$

where  $l_{i_j k}$  is the length of the side dual to  $e_{i_j k}$ , and putting all these relations into equation 4.10.1, after some term manipulations one obtains

$$\begin{aligned} c_j \lambda_{i_j k} \langle v_{i_j k} i_{j k+1}, (g^{jk})^{-1} JN_j \rangle - \langle v_{i_j k} i_{j k+1}, c_{\omega(j,k)} \lambda_{\psi(i_j k)} (g^{\omega(j,k) \eta(j,k)+1})^{-1} JN_{\omega(j,k)} \rangle \\ = b_{\psi(i_j k) \psi(i_j k)+1} \sinh l_{i_j k} \sin \alpha_{\psi(i_j k) \psi(i_j k)+1} - b_{i_j k-1 i_j k} \sinh l_{i_j k} \sin \alpha_{i_j k-1 i_j k} \end{aligned}$$

Hence,

$$\begin{aligned} \frac{1}{\sinh l_{i_j k}} \langle v_{i_j k} i_{j k+1}, c_j \lambda_{i_j k} (g^{jk})^{-1} JN_j - c_{\omega(j,k)} \lambda_{\psi(i_j k)} (g^{\omega(j,k) \eta(j,k)+1})^{-1} JN_{\omega(j,k)} \rangle = \\ = b_{\psi(i_j k) \psi(i_j k)+1} \sin \alpha_{\psi(i_j k) \psi(i_j k)+1} - b_{i_j k-1 i_j k} \sin \alpha_{i_j k-1 i_j k} \quad (4.10.3) \end{aligned}$$

The difference between this equation and equation 4.4.1 we had before is that the left side is, *a priori*, no longer zero. Of course, that's what we want to prove by showing that coefficients  $c_j$  are all zeros. We still are going to look at the star of the cycle  $V_j$  represented by the vertex  $v_{i_j k-1 i_j k}$ . Equations 4.10.3 can be obtained for any pair of adjacent angles in this star with a shared edge  $e_{i_j k}$  where  $k$  runs from 1 to  $d_j$ . We will add them all together noticing that each term on the right side will enter precisely two such equations with opposite signs. Therefore, adding equations will yield

$$\sum_{k=1}^{d_j} \frac{1}{\sinh l_{i_j k}} \langle v_{i_j k} i_{j k+1}, c_j \lambda_{i_j k} (g^{jk})^{-1} JN_j - c_{\omega(j,k)} \lambda_{\psi(i_j k)} (g^{\omega(j,k) \eta(j,k)+1})^{-1} JN_{\omega(j,k)} \rangle = 0$$

Since  $g^{jk}$  and  $g^{\omega(j,k) \eta(j,k)+1}$  are in  $SO^+(2, 1)$ , we can write this expression as

$$\sum_{k=1}^{d_j} \frac{1}{\sinh l_{i_j k}} \left( c_j \lambda_{i_j k} \langle g^{jk} v_{i_j k} i_{j k+1}, JN_j \rangle - c_{\omega(j,k)} \lambda_{\psi(i_j k)} \langle g^{\omega(j,k) \eta(j,k)+1} v_{i_j k} i_{j k+1}, JN_{\omega(j,k)} \rangle \right) = 0 \quad (S_j)$$

Chasing around Fig. 4.10 one proves that the vertices  $\{g^{jk} v_{i_j k} i_{j k+1}\}_{k=1}^{d_j}$  form the star of the vertex  $v_{i_j 1-1 i_j 1}$ , the one we chose to be the preferred representative of the cycle  $V_j$  by making it first in the sequence of representatives.

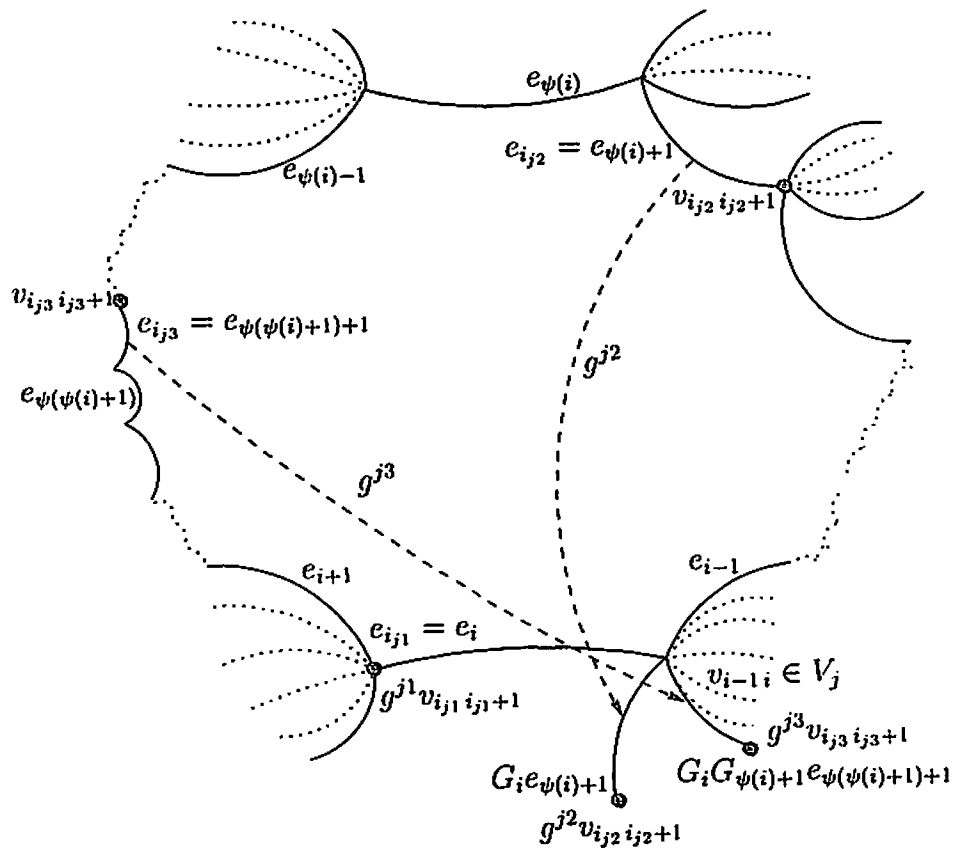


Figure 4.10: Polygon chasing 1



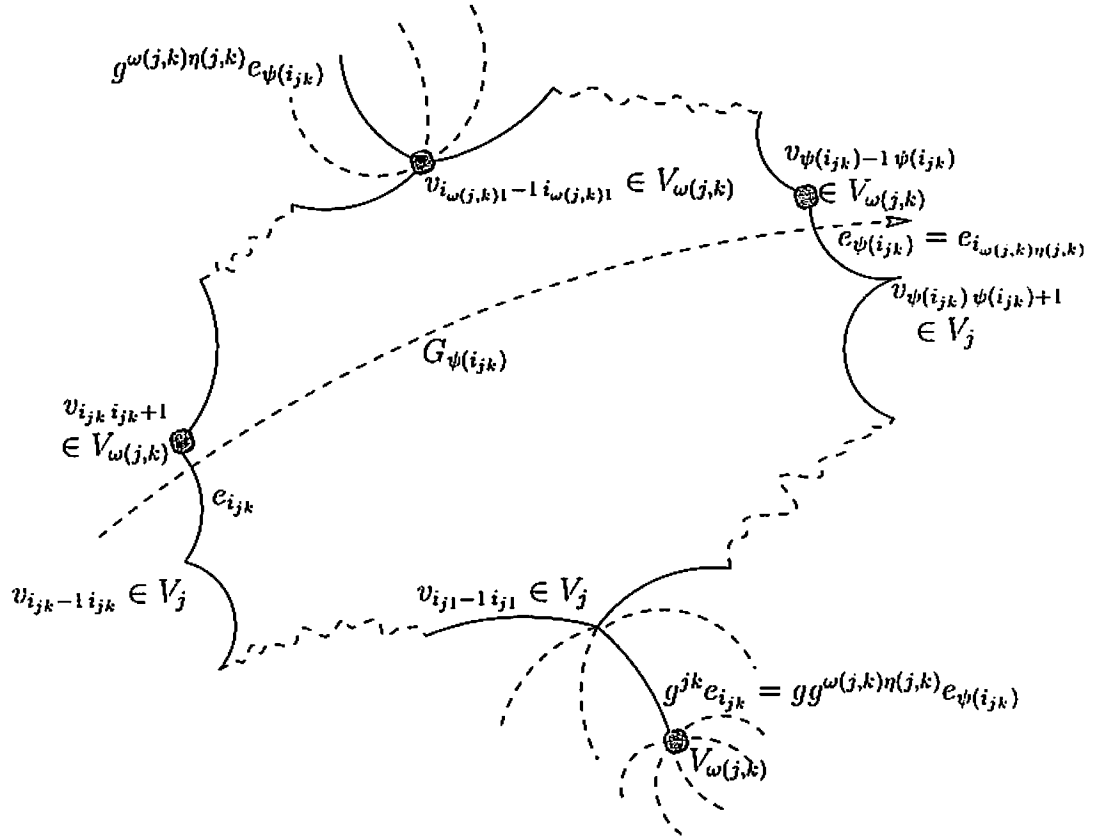


Figure 4.11: Polygon chasing 2

Similarly, from Fig. 4.11 we observe that

$$\begin{aligned}
 g^{\omega(j,k) \eta(j,k)+1} v_{i_{j,k} i_{j,k}+1} &= g^{\omega(j,k) \eta(j,k)} G_{\psi(i_{j,k})} v_{i_{j,k} i_{j,k}+1} = \\
 &= g^{\omega(j,k) \eta(j,k)} v_{\psi(i_{j,k}) \psi(i_{j,k})-1} = v_{i_{\omega(j,k)1}-1 i_{\omega(j,k)1}}
 \end{aligned}$$

which is the preferred representative of the cycle  $V_{\omega(j,k)}$ .

It's time to introduce some more notation.

Let  $\tilde{v}_j$  be the preferred representative  $v_{i_{j1}-1 i_{j1}}$  and let  $\{\tilde{v}_{jk}\}_{k=1}^{d_j}$  be the set of the vertices incident to the preferred one in the induced tessellation of the hyperbolic plane numbered counterclockwise as before. Let  $\{\tilde{e}_{jk}\}_{k=1}^{d_j}$  be the set of edges in the star of  $\tilde{v}_j$  connecting the corresponding vertex to the center of the star. Then  $\lambda_{i_{jk}}$  is the  $\lambda_i$  assigned to the representative of this edge met on the polygon  $P$  after the representative for  $\tilde{v}_{jk}$  in clockwise movement around the polygon.

From the above observations, recalling that the inner product of two timelike unit vectors is the  $-\cosh$  of the hyperbolic distance between the points they represent in  $H^2$ , equation  $S_j$  becomes

$$c_j \sum_{k=1}^{d_j} \lambda_{i_{jk}} \frac{\cosh \text{dist}(\tilde{v}_{jk}, JN_j)}{\sinh \text{dist}(\tilde{v}_{jk}, \tilde{v}_j)} - \sum_{k=1}^{d_j} c_{\omega(j,k)} \lambda_{\psi(i_{jk})} \frac{\cosh \text{dist}(\tilde{v}_{\omega(j,k)}, JN_{\omega(j,k)})}{\sinh \text{dist}(\tilde{v}_{jk}, \tilde{v}_j)} = 0 \quad (\tilde{S}_j)$$

Equations  $\tilde{S}_j$ ,  $j = 1, \dots, V$  form a system of  $V$  homogeneous linear equations for  $V$  unknowns  $\{c_j\}_{j=1}^V$ . We claim that we can choose a set of coefficient vectors  $\{N_j\}_{j=1}^V$ , which so far were quite arbitrary, in such a way, that the rank of this system is precisely  $V$ , forcing all coefficients  $c_j$  to be zero. In fact, we will choose vectors  $\{N_j\}_{j=1}^V$  to be the conjugates  $\{J\tilde{v}_j\}_{j=1}^V$  of the vectors representing the preferred vertices in the Minkowsky space (non-zero time-like vectors which are the preferred representatives of the respective cycles). The equations  $\tilde{S}_j$  then become

$$c_j \sum_{k=1}^{d_j} \lambda_{i_{jk}} \frac{\cosh \text{dist}(\tilde{v}_{jk}, \tilde{v}_j)}{\sinh \text{dist}(\tilde{v}_{jk}, \tilde{v}_j)} - \sum_{k=1}^{d_j} c_{\omega(j,k)} \lambda_{\psi(i_{jk})} \frac{\cosh \text{dist}(\tilde{v}_{\omega(j,k)}, \tilde{v}_{\omega(j,k)})}{\sinh \text{dist}(\tilde{v}_{jk}, \tilde{v}_j)} = 0$$

or, since the distance from a point to itself is 0 and  $\cosh 0 = 1$ ,

$$c_j \sum_{k=1}^{d_j} \lambda_{i_{jk}} \frac{\cosh \text{dist}(\tilde{v}_{jk}, \tilde{v}_j)}{\sinh \text{dist}(\tilde{v}_{jk}, \tilde{v}_j)} - \sum_{k=1}^{d_j} c_{\omega(j,k)} \lambda_{\psi(i_{jk})} \frac{1}{\sinh \text{dist}(\tilde{v}_{jk}, \tilde{v}_j)} = 0 \quad (\tilde{S}_j)$$

Before we consider general case having to write down a big matrix, lets take a look at the special case of one cycle. This, of course, is the famous example of  $4g$ -gons.

#### 4.11 A special case - one cycle

In this case  $V = 1$ , hence  $j = 1$  and  $\omega(1, k) = 1$ . Then  $(\tilde{S}_j)$  becomes

$$c_1 \sum_{k=1}^{d_1} \left( \lambda_{i_{1k}} \frac{\cosh \text{dist}(\tilde{v}_{1k}, \tilde{v}_1)}{\sinh \text{dist}(\tilde{v}_{1k}, \tilde{v}_1)} - \lambda_{\psi(i_{1k})} \frac{1}{\sinh \text{dist}(\tilde{v}_{1k}, \tilde{v}_1)} \right) = 0 \quad (4.11.1)$$

Now we just have to notice that each edge of the polygon is incident to the two different representatives of the same cycle. Therefore, it will appear twice in moving around the vertex - once as itself  $(e_{i_{1k}})$  and once as its pair  $(e_{\psi(i_{1k})})$ . Hence, this last equation can be rewritten as

$$c_1 \sum_{k=1}^{d_1} \left( \lambda_{1k} \frac{\cosh \text{dist}(\tilde{v}_{1k}, \tilde{v}_1)}{\sinh \text{dist}(\tilde{v}_{1k}, \tilde{v}_1)} - \lambda_{1k} \frac{1}{\sinh \text{dist}(\tilde{v}_{1\eta(1,k)}, \tilde{v}_1)} \right) = 0$$

Observing that  $\text{dist}(\tilde{v}_{1k}, \tilde{v}_1) = \text{dist}(\tilde{v}_{1\eta(1,k)}, \tilde{v}_1)$  since both distances are the lengths of the same edge of the tessellation, we have

$$c_1 \sum_{k=1}^{d_1} \frac{\lambda_{1k}}{\sinh \text{dist}(\tilde{v}_{1k}, \tilde{v}_1)} (\cosh \text{dist}(\tilde{v}_{1k}, \tilde{v}_1) - 1) = 0$$

But the expressions in parenthesis are always positive since the vertices are different. Since all  $\lambda_{1k}$  are also positive numbers as are the sinh of the edge lengths, the whole sum is positive which forces  $c_1$  to be zero. Hence, in this case local rigidity is true.

## 4.12 General case - $V$ cycles

To write down the matrix for the system  $\tilde{S}_j$  we need the following notation. Let  $l_{jk} = \text{dist}(\tilde{v}_{jk}, \tilde{v}_j)$ . Let  $(j, i)$  denote an edge from the cycle  $V_j$  to the cycle  $V_i$ . Also let  $l_{(j,i)}$  denote its length and  $\lambda_{(j,i)i}$  be the  $\lambda$  associated with this edge at the vertex  $V_i$ . Then for the  $j^{\text{th}}$  and  $i^{\text{th}}$  rows we have (showing only diagonal and off diagonal elements in the  $i^{\text{th}}$  and  $j^{\text{th}}$  column correspondingly):

$$\begin{array}{ccc}
 & j & i \\
 j & \sum_{k=1}^{d_j} \frac{\lambda_{jk}}{\sinh l_{jk}} \cosh \text{dist}(\tilde{v}_{jk}, \tilde{v}_j) - \sum_{\substack{\text{all} \\ \text{edges} \\ (j,j)}} \frac{\lambda_{(j,j)j}}{\sinh l_{(j,j)}} & - \sum_{\substack{\text{all} \\ \text{edges} \\ (j,i)}} \frac{\lambda_{(j,i)i}}{\sinh l_{(j,i)}} \\
 i & - \sum_{\substack{\text{all} \\ \text{edges} \\ (i,j)}} \frac{\lambda_{(i,j)j}}{\sinh l_{(i,j)}} & \sum_{k=1}^{d_i} \frac{\lambda_{ik_i}}{\sinh l_{ik_i}} \cosh \text{dist}(\tilde{v}_{ik_i}, \tilde{v}_i) - \sum_{\substack{\text{all} \\ \text{edges} \\ (i,i)}} \frac{\lambda_{(i,i)i}}{\sinh l_{(i,i)}}
 \end{array}$$

The same argument as in the case of one cycle now shows that the absolute value of each diagonal entry (which is the entry itself since it is positive) is greater than the sum of the absolute values of the rest of the entries in the same column (which is the sum of the entries taken with a minus sign since they are all negative). Now, a simple lemma of linear algebra, proved as Lemma B.1 in Appendix B shows that the determinant of such a matrix is not equal to zero (in fact it is positive). That concludes the proof of the local rigidity in the general case.

## CHAPTER 5

### ON GLOBAL RIGIDITY

#### 5.1 Global Rigidity in a fixed isotopy class

As before, marked closed surface  $S_g$  with hyperbolic metric on it is fixed along with combinatorial type of the one-cell tessellation with a face angle assignment.

Assume now that there exists infinitely many different (geometric) tessellations  $T_\nu$  of this given combinatorial type and angle assignment on  $S_g$ , where  $\nu$  ranges over some infinite index set. Let  $\{v_i^\nu\}_{i=1}^V$  be the set of vertices of the tessellation  $T_\nu$ . Here  $V$  is the number of vertices of the tessellation on the surface.

Then, since  $S_g$  is compact, each set  $\{v_i^\nu\}$  will have at least one accumulation point  $v_i$  for each  $i = 1, \dots, V$ . Lets consider an infinite sequence  $T_n$  so that sequence of the corresponding vertices converges to the corresponding accumulation point.

Assume now that sequence  $T_n$  contains an infinite subsequence of isotopic tessellations.

Passing to a subsequence, if needed, we obtain a well-defined limiting tessellation  $T$ , which does not necessarily have to be of the same combinatorial type. If it is of the same combinatorial type, then it has same angle assignment and we can construct a smooth isotopy to  $T$  with constant angles. That of course contradicts the local rigidity

proved in the previous chapter. If, on the other hand,  $T$  is of different combinatorial type, we only have to notice that it is obtained by introducing degeneracies into the original type. In fact, the only possible type of degeneracies is allowing collapsed edges, i.e. the lengths of some edges become 0. This can happen whenever the set of the generators identifying the sides of the polygon is not minimal. Nevertheless, we can still consider the sequence of the vectors orthogonal to the sides in the polygon representation of  $T_n$ 's and their limits which are well defined. The argument of the previous chapter now goes through without any changes, again bringing us to a contradiction.

Hence, sequence  $T_n$  does not contain infinitely many isotopic tessellations. This proves the following

**Theorem B (Global Rigidity in a fixed isotopy class).** *Given an isometry class of a marked hyperbolic surface, there exist at most finitely tessellations with the same combinatorial structure, face angles and isotopy class.*

## 5.2 Rigidity and unboundness of the edge lengths

We continue in the setting of the previous section. As we have shown, there are no infinitely many tessellations in the same isotopy class. We would like to show that then there exists an infinite sequence  $T_n, n \in \mathbb{N}$  such that the length of at least one edge becomes unbounded. We will say that such an edge becomes infinitely long, or simply, long.

To this end let's consider open convex neighborhoods  $U_i$  of points  $v_i$  in the surface.

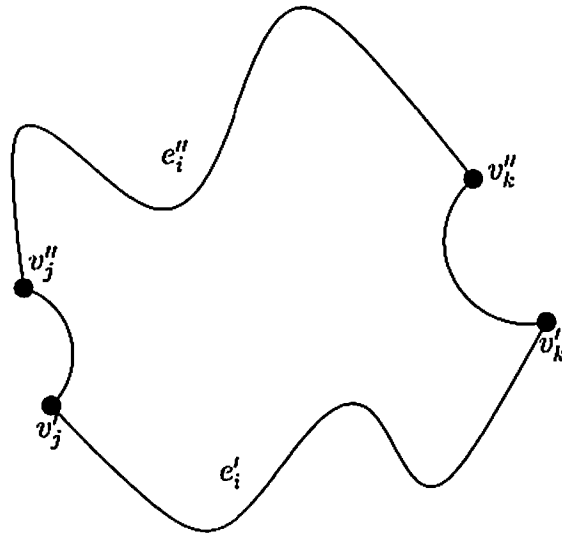


Figure 5.1: Loop

Let's consider an infinite sequence  $T_n$  so that the sequence of the corresponding vertices converges to an accumulation point and so that all these points are inside the corresponding neighborhood  $U_i$ .

If open neighborhoods  $U_i$  are small enough, two tessellations  $T'$  and  $T''$  with vertices in corresponding neighborhoods are isotopic if and only if all loops

$$e_i' \circ v_j' v_j'' \circ e_i'' \circ v_k'' v_k', \quad i = 1, \dots, E$$

are trivial. Here, the edge  $e_i$  is incident to the vertices  $v_j$  and  $v_k$  and  $E$  is the number of edges.

Now, let's pick one tessellation out of the sequence, say  $T_1$ . We claim that we can find an infinite subsequence  $T_l$  of  $T_n$  so that at least one sequence of loops  $e_i^l \circ v_j^l v_j^l \circ$

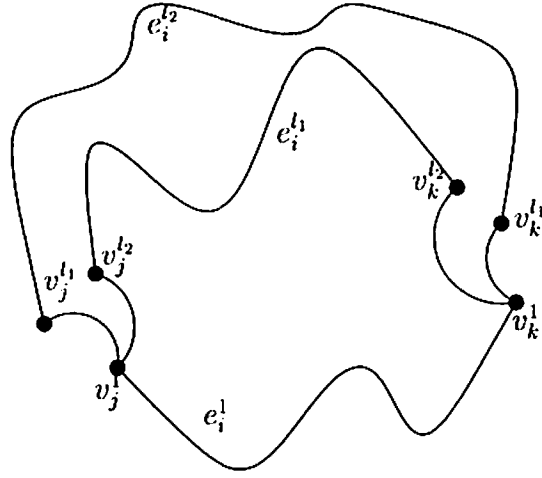


Figure 5.2: Two loops

$e_i^l \circ v_k^l v_k^l$  (for some  $i$ ) will contain representatives of infinitely many different isotopy classes. Otherwise there would be infinitely many tessellations with corresponding loops in the same isotopy class for all edges, and therefore all these tessellations would be isotopic (the corresponding loops for any two such tessellations are trivial) - contradicting our previous argument.

Since now for at least one edge we have an infinite sequence of corresponding loops in different isotopy classes, the set of lengths of these loops must be unbounded. Indeed, each such loop is longer than the (unique) closed geodesic in its isotopy class (which according to Dehn coincides with its homotopy class) and there are finitely many closed geodesics of bounded length on the surface  $S_g$  (see [24], Theorem 3.15.1 or [3], Theorem 10.3.6). Now, the length of the loop  $e_i^l \circ v_j^l v_j^l \circ e_i^l \circ v_k^l v_k^l$  is the sum of the lengths of the edges  $e_i^l$  and  $e_i^l$  and the lengths of the geodesic segments  $v_j^l v_j^l$  and



$v_k^l v_k^l$ . The first edge length is fixed, while the last two lengths are bounded (by the diameters of the neighborhoods). Hence, the edges  $e_i^l$  become infinitely long.

Therefore, the rigidity theorem holds unless there is an infinite sequence of tessellations such that the set of lengths of at least one edge is unbounded. To finish the proof of rigidity one would need to show that this is impossible. The authors fruitless attempts to do this led him to the belief that it is not so. In the next section we therefore present the idea for constructing a possible counterexample.

### 5.3 Example of a potential counterexample

In the previous section we showed that if the global rigidity does not hold, then there exists an infinite sequence of tessellations with lengths of some sides unbounded. We will still concentrate on the one cell case, which means that we have a sequence of fundamental polygons with the sides in certain pairs become long. The hyperbolic version of the Geometric Cauchy Lemma (see lemma 4.4 in [23]) also shows that there is at least one pair of sides of bounded (in fact decreasing) length. The most convenient model for us here is the Poincare disk model. Such a sequence of polygons, then, will have an accumulation polygon (limit) in the compactified hyperbolic plane, which is the compact disk. The vertices of the accumulation polygon are the accumulation points of corresponding vertices as vertices and its edges are the limits of the corresponding sides. However, this polygon need not be proper. Indeed, it is not, since a long side must be incident to at least one ideal vertex. To resolve the Rigidity

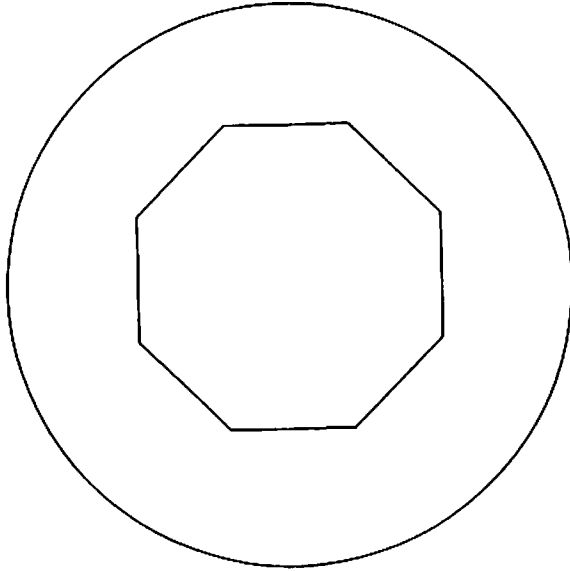


Figure 5.3: Octagon producing  $S_2$  by identifying opposite sides

Conjecture one would need to investigate the types of degeneracies of the fundamental polygons and their limits. Here we will give an example of one possibility, which seems to be, actually, the general case.

Let us assume that the sequence only has one long pair. In particular, we could consider a sequence of octagons producing a surface of genus 2 by identifying their opposite sides (Fig. 5.3). Since the identified endpoints of long sides are bounded distance away from each other in  $\mathbb{H}^2$  and the two sides become arbitrarily long, the two lines containing them become arbitrarily close (Fig 5.4) (for example in the metric on de Sitter sphere parametrizing all oriented lines).

In the limit, obviously, we obtain either one straight line or a configuration on

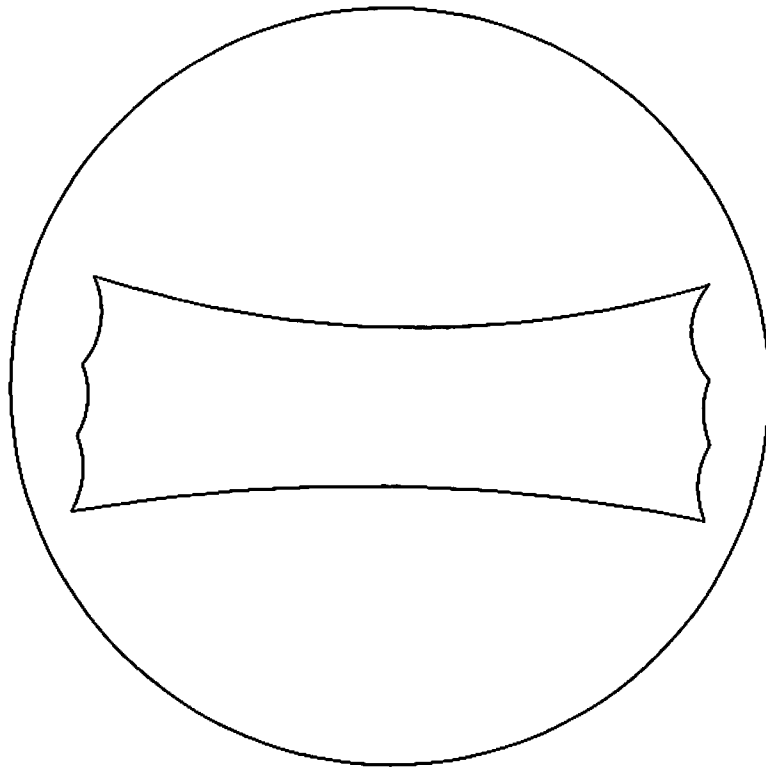


Figure 5.4: Octagon with a pair of long sides

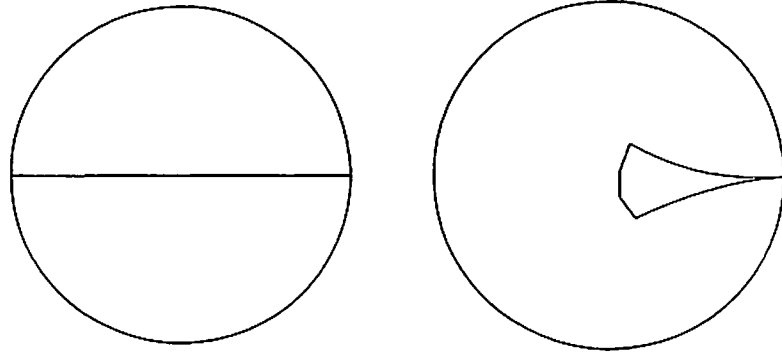


Figure 5.5: Accumulation polygons

Fig 5.5. The two situations simply correspond to different translates of the fundamental polygon in  $\mathbb{H}^2$ , and therefore may be obtained from one another by applying some translations in the group  $G$  to polygons of the sequence on each stage.

We claim that in the first case the straight line is a translation axis of a unique (up to taking the inverse) element of  $G$  which projects under the action of this element to a once traversed closed geodesic which is necessarily simple. In the second case this axis is recovered as the axis of the unique element (up to taking the inverse) in  $G$  having this ideal vertex as one end of its axis (see theorem 4.3.5 or theorem 5.1.2 in [3]) and projecting its axis to a once traversed closed geodesic which is necessarily simple. Moreover, starting at some point in the sequence of polygons, the two long sides are identified by this element.

To see this let us notice that as the sides become longer, there will be a pair of points, one on each of them, realizing the distance between these lines inside the polygon (which we will assume convex for simplicity), and this distance becomes

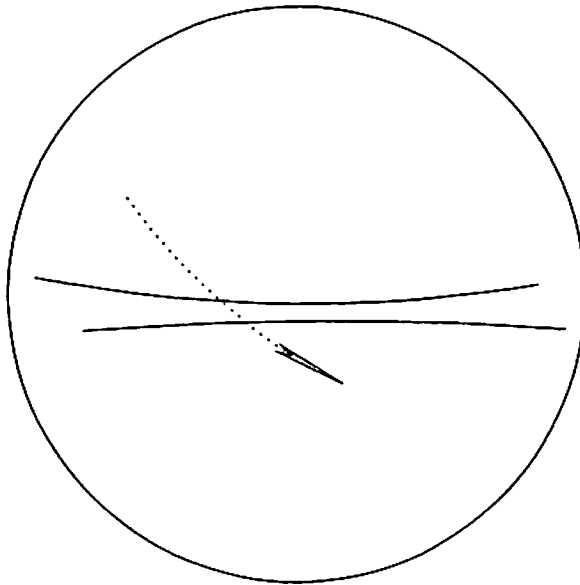


Figure 5.6: Side shift

arbitrarily small. If these point were identified, this would prove the Global Rigidity Theorem as we would have found a nontrivial loop of an arbitrarily small length on the surface which is impossible (since it is compact or in view of finiteness of the number of closed geodesics of bounded length). The problem is that these points do not have to be identified (Fig. 5.6).

Then, however, the image of one of them on the other side and the point on that other side are arbitrarily close and this distance is not bigger then the minimum of the sum of lengths of the two sequences of short sides plus some arbitrarily small  $\epsilon$ . If this distance is becoming arbitrarily small we once again obtain a short loop. If not, then there is a limit distance such that for a subsequence of polygons, two

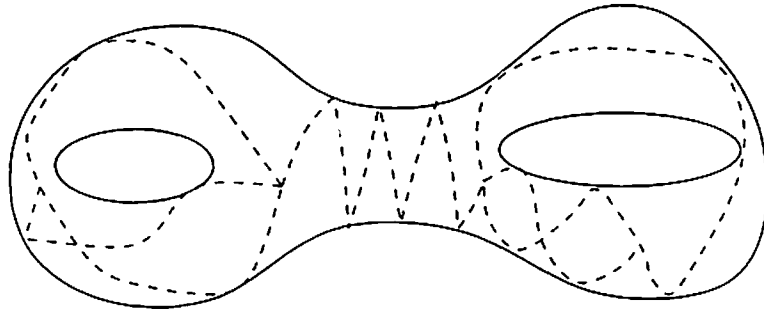


Figure 5.7: Possible tessellation

points on the long side are arbitrarily close on the surface while distance between them along the side approaches the limit. This means that a segment bounded by these two points approaches a closed geodesic, and since there are finitely many closed geodesics of bounded length, we can assume it is the same geodesic by passing to a subsequence. The long edge of the tessellation is then wrapping around this closed geodesic arbitrarily close to it. In particular, this closed geodesic may not have self intersections, i.e., it is simple. In view of discreteness of  $G$ , it is also clear that the pairing element of this pair must stabilize to the translation along the lift of this closed geodesic by its length.

Thus, the conceivable situation is shown on Fig. 5.7. These wraps become arbitrarily tight. In the limit, corresponding to the Fig 5.5 the long edge will break into three pieces - the closed simple geodesic we have constructed and two geodesic wrapping to it infinitely close from different sides (Fig. 5.8).

That then gives an idea for constructing an actual counterexample. We shall

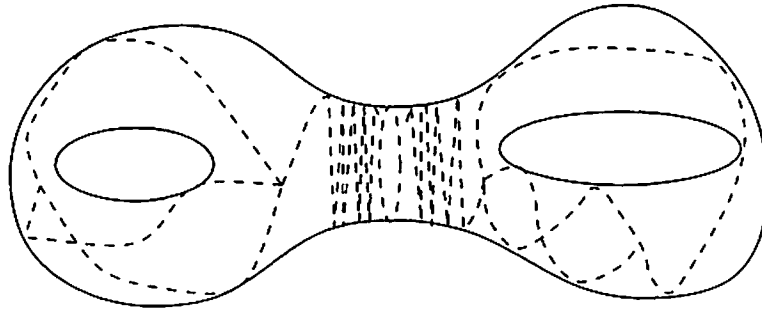


Figure 5.8: Limit of a sequence of tessellations

start with a closed simple geodesic and two geodesics wrapping to it infinitely close. Then moving some distance away from the closed geodesic along the tube we will truncate the two wrapping edges. We can choose this distance in such a way that the two remaining half-infinite segments do not have self-intersections. Now, connect the two truncating points by any simple curve along the tube and construct a graph on the rest of the surface so that it contains these points as vertices and along with the chosen curve represents cutting the surface into a polygon. Now consider a ripped polygon formed by this graph and the two long wrapping segments. Fix all the angles. It seems feasible to slightly perturb the vertices of the ripped polygon to obtain an infinite family of polygons so that all angles are preserved and the two wrapping geodesics coincide.

CHAPTER 6

EQUIVARIANT SPACELIKE CONVEX POLYHEDRA IN  
MINKOWSKY SPACE AND THE LOCAL RIGIDITY  
THEOREM

6.1 Spacelike convex cones

**Definition 6.1.1.** A *spacelike convex cone*  $C$  is the boundary of a convex body  $C_{\text{full}}$  in Minkowsky space obtained as an intersection of half spaces determined by finitely many spacelike planes meeting at a given point in  $\mathbb{R}^{2,1}$ .

Consider the set  $F = \{f\} \subset \mathbb{H}^2$  of the normal inward-pointing unit vectors to the face planes of the cone  $C$ . It is not difficult to see that they form a convex polygon in  $\mathbb{H}^2$ . This polygon will be called a *dual cell* of the cone and could be described as follows. Let  $\tilde{C}$  be the affine translate of  $C_{\text{full}}$  to the origin of  $\mathbb{R}^{2,1}$ . Then

$$F = \{f \in \mathbb{H}^2 : \langle f, c \rangle \geq 0 \forall c \in \tilde{C}\} \tag{6.1.1}$$

Equivalently, then

$$\tilde{C} = \{c \in \mathbb{R} : \langle c, f \rangle \geq 0 \forall f \in F\}$$

The boundary of the cell, of course, corresponds to the equality sign in the above formula. Convexity of the cone is equivalent to the convexity of the dual cell. Indeed,



a segment of a spacelike straight line centrally projects onto a segment of a hyperbolic geodesic with the endpoints projecting to the endpoints. Convexity means that whenever the endpoints of a segment belong to the space the whole segment is in it. Central projection then provides the equivalence of the convexities of the two objects.

Since all faces of the cone  $C$  lie in spacelike planes, their angles at the vertex of the cone are well defined, and therefore the total cone angle  $\alpha(C)$  can be defined as their sum. It is easy to see and is quite a standard result that the angles at the vertices of the dual polygon are supplementary to the angles of the cone faces dual (orthogonal) to these vertices. That is so since the central planes through the edges of the dual polygon are orthogonal to the dual edges of the cone and points of  $\mathbb{H}^2$  are orthogonal to the tangent planes of  $\mathbb{H}^2$  at them. More on this duality will be said later as we consider Gauss Map (also see [23] or [7]).

**Proposition 6.1.2.**

$$\alpha(C) = 2\pi + \text{Area}(F) \tag{6.1.2}$$

*Proof.* Assume that cone  $C$  has  $n$  faces with face angles  $\{\alpha_i\}$  and the corresponding angles of  $F$  are  $\tilde{\alpha}_i$ . Then

$$\alpha(C) = \sum_{i=1}^n \alpha_i = \sum_{i=1}^n (\pi - \tilde{\alpha}_i) = \pi n - \sum_{i=1}^n \tilde{\alpha}_i = \pi n - (\pi(n-2) - \text{Area}(F)) = 2\pi + \text{Area}(F)$$

□

**Corollary 6.1.3.** *The total angles of a spacelike convex cone is not smaller than  $2\pi$  with strict inequality iff the cone is not degenerate, i.e. there exist at least three distinct faces.*

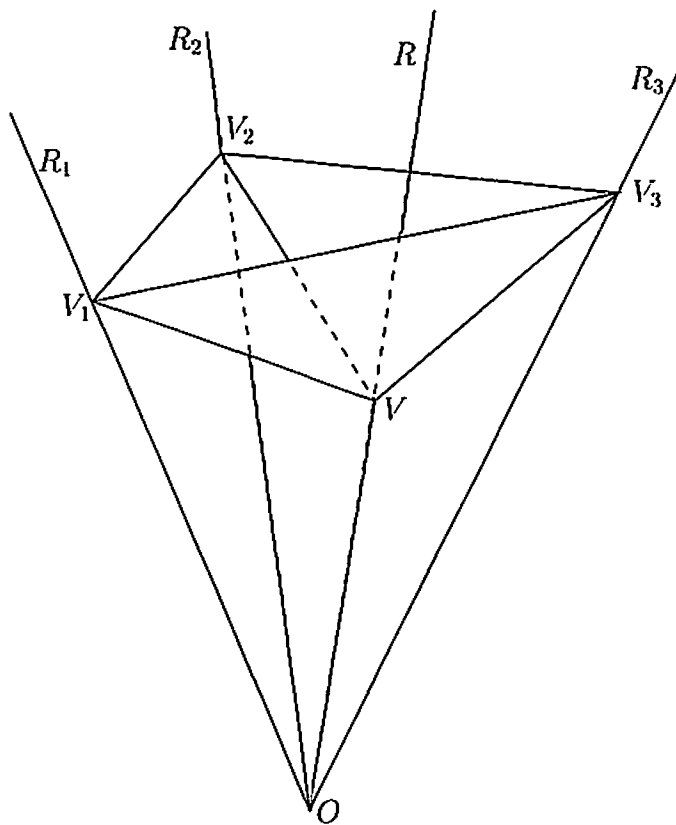


Figure 6.1: Sliding vertices

Let us now consider the following situation, which we will encounter later (Fig 6.1). Assume we have a non-degenerate spacelike convex cone  $C$  with the vertex  $V$  inside the light cone. Assume also that there has been chosen a point  $V_i$  on each edge  $e_i$  of  $C$ . Let us construct central rays  $\{R_i\}$  through the points  $\{V_i\}$  and ray  $R$  through the vertex  $V$  of the cone.

Now, let us slide the vertex  $V$  along the ray  $R$  and denote by  $r$  the absolute value

of the length  $|OV|$ , i.e.  $r = \frac{1}{i} \sqrt{\langle V, V \rangle}$ . Similarly, we will slide points  $\{V_i\}$  along their rays denoting  $r_i = \frac{1}{i} \sqrt{\langle V_i, V_i \rangle}$

**Claim 6.1.4.** *In the above situation the cone angle  $\alpha(C)$  strictly decreases as a function of  $r$  and strictly increases as a function of  $r_i$ . Moreover,*

$$\frac{\partial \alpha(C)}{\partial r} < 0 \tag{6.1.3}$$

$$\frac{\partial \alpha(C)}{\partial r_i} > 0, \forall i \tag{6.1.4}$$

*Proof.* Let us slightly push  $V$  away from the origin of  $\mathbb{R}^{2,1}$ . It is clear that the new (deformed) cone  $C'$  is strictly contained in  $C$  we started with, since the vertex  $V$  moves "inside" the cone. That implies

$$\tilde{C} \subset \tilde{C}'$$

where the inequality is proper. Therefore, in view of 6.1.1, we see that

$$F' \subset F$$

which implies

$$Area(F') < Area(F)$$

and therefore

$$\alpha(C') < \alpha(C)$$

As for the derivative, convexity implies that the derivative of the displacement of any of the dual vertices, being a measure of the corresponding plane rotation,

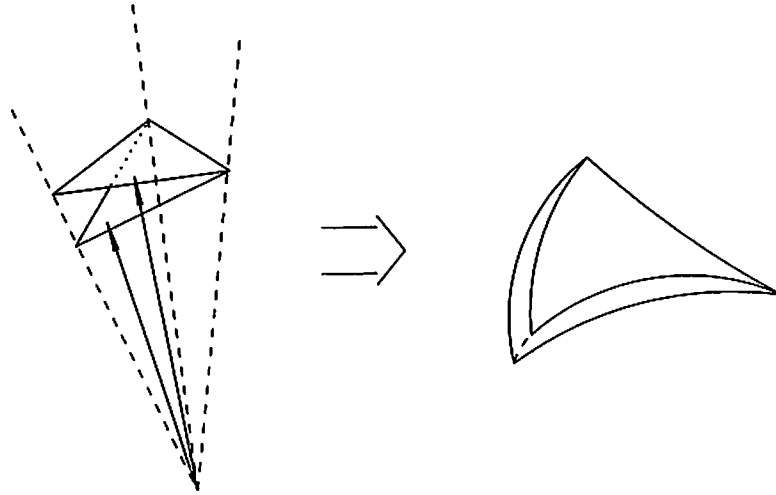


Figure 6.2: Cell area evolving

is not zero with respect to  $r$ .  $\text{Area}(F)$  has non-zero derivative with respect to this displacement (Fig. 6.2). Therefore the chain rule gives the desired result.

The case of moving  $V_i$  is treated similarly. □

## 6.2 Equivariant spacelike convex polyhedra

**Definition 6.2.1.** A connected surface in  $\mathbb{R}^{2,1}$  will be called a *spacelike convex polyhedron* if it is the boundary of a convex body lying entirely inside the light cone and if it can be defined by a locally finite collection of supporting planes, each of which are spacelike.

*Remark 6.2.2.* All supporting planes of a convex spacelike polyhedron are spacelike.

**Definition 6.2.3.** If a spacelike convex polyhedron is equivariant under the action of a Fuschian group  $\Gamma \in SO^+(2,1)$  we will call it *an equivariant spacelike convex polyhedron*, or, simply, a *polyhedron*.

**Proposition 6.2.4.** *An equivariant spacelike convex polyhedron is homeomorphic to  $\mathbb{H}^2$  and its quotient under the action of  $\Gamma$  is homeomorphic to the Riemann surface obtained as the quotient  $\mathbb{H}^2 / \Gamma$ .*

*Proof.* The required homeomorphism is readily provided by the central projection of the polyhedra onto the upper sheet of the hyperboloid in Minkowsky space.

Central projection is clearly equivariant.

It is injective since otherwise there are two points of the polyhedron on the same (timelike) central ray projecting to the same point of the hyperboloid. But in view of connectivity that means that there is a face of the polyhedra containing timelike vector giving a contradiction.

For surjectivity notice that a finite collection of faces will cover the fundamental domain of the group action on  $\mathbb{H}^2$ . Now apply equivariance. □

### 6.3 The Gauss Map in Minkowsky space and the dual tessellation

**Definition 6.3.1.** The *Gauss Map*  $\mathcal{G}$  of a spacelike convex polyhedron  $P$  is a *set-valued function* from  $P$  to the hyperbolic plane  $\mathbb{H}^2$  represented by the upper-sheet of the hyperboloid in Minkowsky space, which assigns to each point  $p$  the set of inward pointing unit normals to supporting planes of  $P$  at  $p$ .

Thus, the whole interior of a face  $f$  is mapped by  $\mathcal{G}$  to a single point - the inward pointing normal unit vector of  $f$ , which is timelike and therefore belongs to  $\mathbb{H}^2$ .

An edge  $e$  of  $P$  is mapped to a geodesic segment  $\mathcal{G}(e)$  on  $\mathbb{H}^2$ , whose length will be called the (*exterior*) *dihedral angle* at  $e$  as it is a measure of the relative position of the two abutting along  $e$  faces.

A vertex  $v$  of  $P$  is mapped by  $\mathcal{G}$  to a hyperbolic polygon  $\mathcal{G}(v)$ , whose sides are the images under  $\mathcal{G}$  of the edges incident to  $v$ , and whose angles are seen to be the angles supplementary to the planar angles of the faces incident to  $v$ . That is,  $\mathcal{G}(e_1)$  and  $\mathcal{G}(e_2)$  meet at the angle  $\pi - \alpha$  whenever  $e_1$  and  $e_2$  meet at an angle  $\alpha$ . This is, of course, exactly the dual cell of the spacelike polyhedral cone at  $v$  discussed in section 6.1. Therefore,  $\mathcal{G}(P)$  is obtained by piecing together the dual cells of the polyhedral cones at the vertices. It is easily seen to be combinatorially the dual of  $P$  while metrically it is  $\mathbb{H}^2$ . This cellulation of  $\mathbb{H}^2$  will be called *the dual tessellation of the convex spacelike polyhedron*. In case of an equivariant convex spacelike polyhedron this gives rise to the tessellation of the surface by convex polygons.

**Proposition 6.3.2.** *All cone angles of the spacelike convex polyhedron are greater than  $2\pi$ .*

*Proof.* An immediate consequence of the corollary 6.1.3. □

## 6.4 The Local Rigidity Theorem

Now, let us consider the Cauchy problem for the equivariant spacelike convex polyhedron. It would make sense to pose a question of rigidity of such a polyhedron

with fixed face angles provided the group  $\Gamma$  is fixed inside  $SO^+(2, 1)$ . That would in particular mean that all such polyhedra have a canonical homeomorphisms onto each other as well as onto a fixed Riemann surface as a conformal structure or a metric of constant curvature  $-1$ . All in total analogy to the Euclidean case where once the origin is fixed there are such canonical homeomorphisms between convex polyhedra and the sphere. The situation is only different from the considered here in view of uniqueness of the conformal structure on the sphere (or equally, uniqueness of metric of constant curvature 1) unlike the higher genus case.

Obviously then, each equivariant spacelike convex polyhedron for fixed group  $\Gamma$  gives rise to its dual tessellation through the Gauss Map and therefore we immediately obtain following

**Theorem 6.4.1 (Local Rigidity Theorem for equivariant spacelike convex polyhedron).** *An equivariant spacelike convex polyhedron cannot be infinitesimally perturbed so as to preserve the face angles and remain equivariant for the same group up to conjugation. Equivalently, the dihedral angles are locally determined by the face angles and the conformal class of the underlying surface.*

*Proof.* This is a direct corollary of Theorem 1. □

To make things look a bit more compact and closer to the Euclidean case, let us call the quotient of the equivariant spacelike convex polyhedron for the group  $\Gamma$  the *convex polyhedron* on the corresponding surface  $S_g$ . Then, we can reformulate the Local Rigidity Theorem as follows:

**Theorem B (Local Rigidity Theorem for convex polyhedra on surfaces of**

genus  $g > 1$ ). A convex polyhedron on a surface  $S_g$  with fixed metric of constant curvature  $-1$  cannot be infinitesimally perturbed so as to preserve the face angles. Equivalently, the dihedral angles are locally determined by the face angles.



CHAPTER 7  
THE CONVEX HULL CONSTRUCTION IN  
MINKOWSKY SPACE AND THE REALIZATION OF  
SINGULAR EUCLIDEAN STRUCTURES OF  
NON-POSITIVE CURVATURE ON CLOSED RIEMANN  
SURFACES BY CONVEX POLYHEDRA

**7.1 The Basic Construction and the Main Theorem**

Fix the conformal structure  $\zeta$  on the surface  $S_g$  of genus  $g > 1$ . In the hyperboloid model of the hyperbolic plane this gives a monomorphism  $\pi_1(S_g) \rightarrow SO^+(2, 1)$ , well-defined up to conjugation by an element of  $SO^+(2, 1)$ . Fix a  $p$ -tuple  $v = (v_1, \dots, v_p)$  of  $p$  points on  $S_g$ . In the hyperboloid model that corresponds to fixing  $p$  points inside of the fundamental region for the  $\pi_1(S_g)$  action on  $\mathbb{H}^2$  or, if you will,  $p$  orbits. Now we can take the convex hull of these points in  $\mathbb{R}^{2,1}$ . That this is well defined and the boundary of it is a spacelike polyhedra (all faces are spacelike) equivariant under the group action on  $\mathbb{R}^{2,1}$  was shown in [1] without restricting to the 2-dimensional case. The chosen points also determine  $p$  central timelike rays passing through them in  $\mathbb{R}^{2,1}$ . The points themselves can be (and will be) considered as imaginary unit

length vectors in  $\mathbb{R}^{2,1}$  along these rays and will be denoted by the same letters (to be precise the letter denotes the entire orbit of vectors). Now we can start moving the points along the corresponding rays in an equivariant manner (it is always assumed that we are moving the entire orbits and will not be mentioned again) allowing the points to leave the hyperboloid. We can do so and still get a well defined convex hull with a spacelike boundary as long as no orbit belongs to the interior of the convex hull of the others. Denote the space of boundaries of all possible convex hulls obtained in this way by  $Pol(\zeta, v_1, \dots, v_p)$ , or, by  $Pol(\zeta, v)$ . For each particular polyhedron  $P$  in  $Pol(\zeta, v)$  let  $\theta(P) = (\theta_1(P), \dots, \theta_p(P))$  be the  $p$ -tuple of the cone angles at the vertices of this polyhedron (all faces are spacelike therefore all angles are well defined). The quotient of the polyhedron  $P$  under the group action is homeomorphic to the surface and therefore provides a piecewise Euclidean structure on it. In this chapter we will show that any set

$$\theta = \left\{ \theta_i : \sum_{i=1}^p \theta_i = 2\pi(p - \chi), \theta_i \geq 2\pi \right\}_{i=1}^p$$

of real numbers satisfying only Gauss-Bonnet relation can be realized as a set of cone angles of some polyhedron in  $Pol(\zeta, v)$ . The inequalities for the angles mean that the piecewise Euclidean metric is non-positively curved since the link of each vertex is greater than  $2\pi$  (see [12]). This condition holds for all spacelike polyhedra (see proposition 6.3.2).

The space  $Pol(\zeta, v)$  can be parametrized by the absolute values  $r_i$  of the lengths of the vectors corresponding to the vertices. Since two sets of these parameters represent the same polyhedron  $P$  in  $Pol(\zeta, v)$  if they are proportional (then two metrics differ

by scaling which, after normalization, say by area, are essentially the same metrics), we can require that

$$\sum_{i=1}^p r_i = 1$$

which shows that  $Pol(\zeta, v)$  is a subset of a standard simplex

$$\Delta_r^{p-1} = r_i \geq 0 : \sum_{i=1}^p r_i = 1$$

in  $\mathbb{R}^p$ . The set of all  $p$ -tuples

$$\left\{ \theta = (\theta_1, \dots, \theta_p) : \sum_{i=1}^p \theta_i = 2\pi(p - \chi), \theta_i \geq 2\pi \right\}$$

of cone angles satisfying the non-positive curvature conditions and the Gauss-Bonnet equation also forms an affine simplex in  $\mathbb{R}^p$  of codimension 1. Denote it  $\Delta_\theta^{p-1}$ . Therefore we have a natural map

$$\theta : Pol(\zeta, v) \rightarrow \Delta_\theta^{p-1}$$

assigning to each polyhedra its set of cone angles.

**Theorem D.** *Map  $\theta : Pol(\zeta, v) \rightarrow \Delta_\theta^{p-1}$  is a homeomorphism.*

## 7.2 Pseudo-Dirichlet regions

Let  $T$  be the dual tessellation of the polyhedron  $P$  obtained by the convex hull construction (this is not really a restriction since every equivariant spacelike convex polyhedron can be obtained in this way). Let us centrally project  $P$  onto  $\mathbb{H}^2$ . That is well defined, since  $P$  is spacelike, and we can consider the graph  $\tilde{P}$ , which is the

image of the 1-skeleton of  $P$  in  $S_g$ . (Everything we have done so far is equivariant.) It is clear that the common edge of the two incident faces of  $P$  is orthogonal (in Minkowsky metric) to the plane spanned by the two corresponding dual vectors. Therefore, dual to this edge geodesic segment of  $T$  (the intersection of this two plane with  $\mathbb{H}^2$ ) is orthogonal to its image in the sense that they lie on the orthogonal geodesics in  $\mathbb{H}^2$  (the two segments do not necessarily need to intersect). Thus, we obtain two mutually orthogonal graphs on  $S_g$ .

We now recall that the dual tessellation is obtained by gluing together dual cells of the vertex cones and therefore a restatement of Proposition 6.1.2 is following.

**Proposition 7.2.1.** *The hyperbolic area  $A(V_i)$  of the cell  $A_i$  of  $T$  dual to the vertex  $v_i$  of polyhedron  $P$  is given by the formula*

$$A(V_i) = \theta_i - 2\pi$$

This in particular gives an easy proof of the Gauss-Bonnet Theorem which can now be reformulated as

**Proposition 7.2.2 (Gauss-Bonnet Theorem).**

$$\sum_{i=1}^p A(V_i) = -2\pi\chi$$

Of course the real Gauss-Bonnet statement is then to show that the quantity on the right is the area of the surface.

It is not difficult to observe that similar polyhedra  $P'$  and  $P''$  (differing by scaling only), representing therefore the same class in  $Pol(\zeta, v)$ , give rise to the same dual

tessellation  $T$ . On the other hand, given a tessellation  $T$ , dual and orthogonal to the given graph  $\tilde{P}$ , we can construct convex hull boundary polyhedron on the rays through vertices of this graph (which therefore is its trace). To this end choose a plane orthogonal to the corresponding vertex of  $T$ . We can now arrange these planes (in an equivariant manner) so that they meet on the rays through vertices of  $P$  according to its pattern. The fact that small loops around each vertex of  $\tilde{P}$  have trivial holonomy (or in a less fancy language, the faces around each ray all meet in one point on it) is ensured by the orthogonality condition of  $\tilde{P}$  and  $T$ .

In [3] the convex hull construction is carried out for compact surfaces with one fixed vertex. In that case sliding vertices (of a single orbit) produces neither a new  $P$  (up to similarity) nor a new  $T$ . It is shown there also that (a single) cell of projection of  $T$  onto  $S_g$  (which we will call  $\hat{T}$ ) is a *Dirichlet* polygon for the chosen point on  $S_g$ , or, in other words, that  $T$  is a *Dirichlet* tessellation of the orbit on  $\mathbb{H}^2$ . This means that the edges of the tessellation are equidistant from the ends of the dual edge of  $\tilde{P}$  (or  $P$  since their vertices actually coincide). Vertices of  $T$  are then equidistant from the vertices of the dual face of  $\tilde{P}$  ( $P$ ).

Hence, the faces of  $P$  are cyclic polygons (a polygon is cyclic if it is inscribable into a circle) with centers at the vertices of  $T$  (this last fact is shown by observing that each face is an intersection of hyperboloid with a spacelike plane which looks like an ellipse but in Minkowsky metric is actually a circle in total analogy to the spherical case). It is interesting to remark that in the generic case when  $\hat{P}$  is actually a triangulation of  $S_g$ , it is exactly the *Delaunay* triangulation of its vertex set (one vertex in this case).

When we originally placed all the vertices on the hyperboloid, everything said above remained true, in other words, we obtain the Dirichlet tessellation with vertices at the centers of the (cyclic) faces of  $P$ . But as soon as we start moving the vertices along the rays, the faces of  $P$  no longer have to be cyclic, therefore the vertices of  $T$  are no longer equidistant from the vertices of the dual cell. So the duality is only understood as orthogonal relation described above. We will call such tessellations  $T$  *pseudo-Dirichlet*. They are characterized by the existence of the dual orthogonal graph  $\tilde{P}$ .

As we move vertices of  $P$  along the rays, the corresponding tessellation  $T$  will evolve, still remaining orthogonal to the original  $\tilde{P}$ . The combinatorial (topological) structure of  $T$  may actually change. The two basic transformations correspond to the two faces of  $P$  with a common edge becoming parallel (therefore lying in the same plane) and to one of the vertices of  $P$  moving onto the boundary of the convex hull of the others (therefore presenting obstruction to the further movement in this direction) so that all faces incident to it become parallel.

In the first case the edge dual to the common edge of the faces collapses as the vertices of  $T$  dual to these two faces move towards each other until they coincide (Fig. 7.1)

In the second case, the dual face of the disappearing vertex of  $P$  collapses to a point as the vertices of  $T$  dual to the faces of  $P$  incident to the disappearing vertex move in to coincide (Fig. 7.2).

Since by passing from polyhedra to the dual pseudo-Dirichlet tessellation the similarity is excluded, all the structural changes of  $P$  can readily be seen in the structural

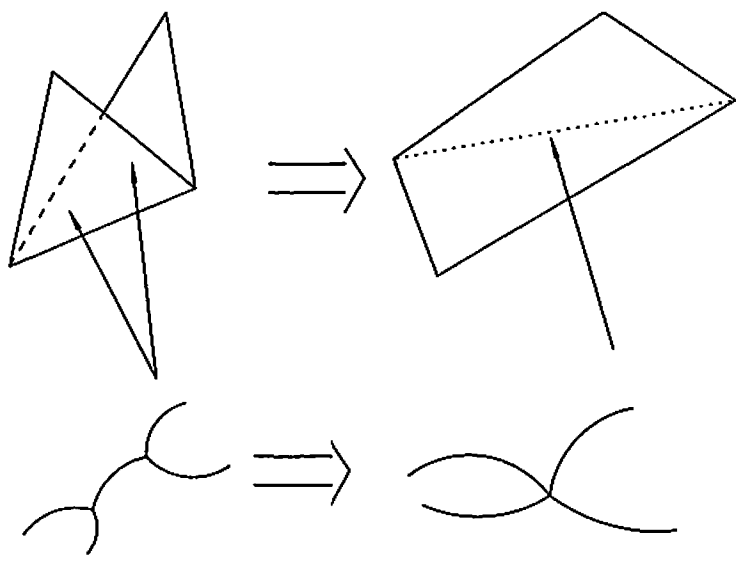


Figure 7.1: Degeneration of an edge of a Pseudo-Dirichlet tessellation

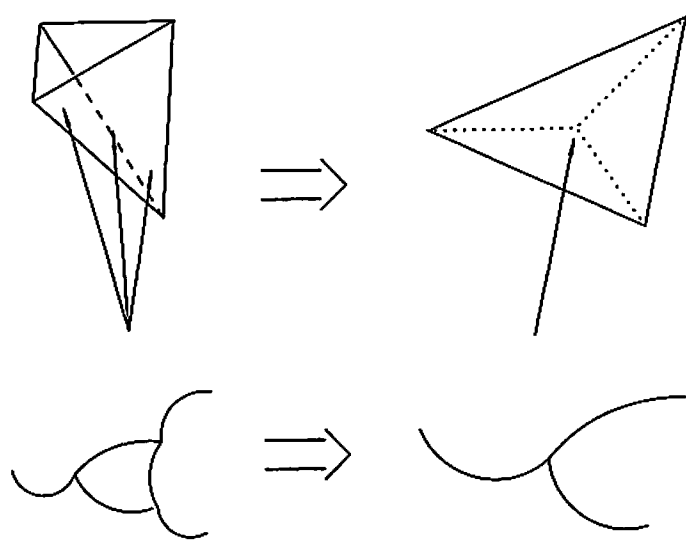


Figure 7.2: Degeneration of a cell of a Pseudo-Dirichlet tessellation

changes of corresponding  $T$ , and, in addition, according to the Proposition 7.2.1 the cone angles of  $P$  can be read of the areas of the cells of  $T$ , we can really substitute the study of polyhedra on the rays by the study of these, so-to-speak "breathing" pseudo-Dirichlet tessellations (a family of pseudo-Dirichlet tessellations) for given fixed graph  $\tilde{P}$ . We will not do it explicitly below, although we have already used this correspondence to prove the results on the derivatives of the cone angles which we will use in the next section.

Notice, that our discussion suggests that the space of the pseudo-Dirichlet tessellations is parametrized by the areas of the cells, which are subject to one simple linear relation - their sum is the total area of the surface  $(-2\pi\chi)$ , which of course is the same Gauss-Bonnet equation for the cone angles we had before. We will show that these areas are indeed local parameters (up to this one relation) which is equivalent to the local injectivity of the map  $\theta$ . This is done in the next section.

### 7.3 Map $\theta$ and its properties

First assume that we are given three timelike vectors  $r_1v_1, r_2v_2, r_3v_3$  where  $v_i$  is a point on the upper sheet of the unit hyperboloid ( $\|v\| = -1$ ) s.t. the triangle formed by these points is spacelike. Then the angle  $\alpha$  at the vertex  $r_3v_3$  is given by the formula

$$\cos a = \frac{\langle r_1v_1 - r_3v_3, r_2v_2 - r_3v_3 \rangle}{\|r_1v_1 - r_3v_3\| \|r_2v_2 - r_3v_3\|} = \frac{-r_3^2 - r_3(r_1l_{13} + r_2l_{23}) + r_1r_2l_{12}}{\sqrt{(r_1^2 + 2r_1r_3l_{13} + r_3^2)(r_2^2 + 2r_2r_3l_{13} + r_3^2)}}$$

where  $l_{ij} = \langle v_i, v_j \rangle = -\cosh(\text{dist}(v_i, v_j))$ ,  $\langle, \rangle$  is the Minkowsky inner product and  $\text{dist}(,)$  is a hyperbolic distance function on the hyperboloid. Now, suppose that  $r_iv_i$



is a vertex of the polyhedra and vertices  $r_{i1}v_{i1}, \dots, r_{ik_i}v_{ik_i}$  ( $k_i$  is the degree of  $r_iv_i$ ) are incident to  $v_i$  in the 1-skeleton induced by the embedding into  $\mathbb{R}^{2,1}$  and are numbered in a cyclic order of their appearance in moving around the vertex  $r_iv_i$  in any direction. Then, if  $a_i^j$  is the angle at the vertex  $r_iv_i$  in the triangle  $r_iv_i, r_{ij}v_{ij}, r_{i,j+1}v_{i,j+1}$  where the indices  $1, \dots, k_i$  are read modulo  $k_i$ , we have

$$\theta(r_i, r_{i1}, \dots, r_{ik_i}) = \sum_{j=1}^{k_i} \alpha_i^j(r_i, r_{ij}, r_{i,j+1}) = \sum_{j=1}^{k_i} \arccos \frac{-r_i^2 - r_i(r_{ij}l_{ij} + r_{i,j+1}l_{i,j+1}) + r_{ij}r_{i,j+1}l_{i,j,j+1}}{\sqrt{(r_{ij}^2 + 2r_i r_{ij} l_{ij} + r_i^2)(r_{i,j+1}^2 + 2r_i r_{i,j+1} l_{i,j+1} + r_i^2)}} \quad (7.3.1)$$

Here  $l_{i,j,j+1} = \langle v_{ij}, v_{i,j+1} \rangle = -\cosh(\text{dist}(v_{ij}, v_{i,j+1}))$  and the distance is measured in the hyperbolic plane. Therefore it may be different from the distance between the images of these vertices in the quotient space. Notice also that the formula may involve representatives of the same orbit.

This function is obviously continuous and differentiable in its domain. Next we will show that it is also locally injective.

**Proposition 7.3.1.** *Moving an orbit of a vertex  $v_i$  away from the origin decreases corresponding cone angle  $\theta_i$  while not increasing other cone angles. Moreover,*

$$\frac{\partial \theta_i}{\partial r_i} < 0, \quad \frac{\partial \theta_j}{\partial r_i} \geq 0, j \neq i$$

and

$$\frac{\partial \theta_i}{\partial r_i} = - \sum_{j \neq i} \frac{\partial \theta_j}{\partial r_i}$$

*Proof.* In case of only one orbit there is nothing to prove, so we assume there are at least two orbits. The inequalities are either direct restatements of the Claim 6.1.4 or,

in case more than one vertex of the cone belong to the same orbit, can be obtained by a slight modification of the same argument. Indeed, a representative of each orbit must be connected by an edge of  $P$  to at least one representative of some other orbit. Otherwise the graph  $\tilde{P}$  would be disconnected, which is not possible. Therefore, after we fix a representative  $v_i$  in its corresponding orbit, moving the orbit away from the origin corresponds to moving  $v_i$  and some (but not all because of the connectedness of the convex hull 1-skeleton) of the vertices in its star, which are in its orbit, or equivalently, moving all the other vertices in its star not contained in its orbit towards the origin. As before, the transformed cone at  $v_i$  is strictly contained in the one we started with, while for other vertices it contains it and the inclusion is not strict. In fact it has to be strict for some orbits in the star of  $v_i$  and is equality for others. The relation for the translated to the origin cones is then reversed and thus, as before, cone angle at  $v_i$  decreases as  $v_i$  moves away from the origin, while cone angles at representatives of other orbits either do not change or increase.

The equation is an immediate consequence of the Gauss-Bonnet relation

$$\sum_{i=1}^p \theta_i = 2\pi(p - \chi)$$

□

*Remark 7.3.2.* In the above proposition the set  $\{r_i\}$  is not normalized.

**Theorem 7.3.3.** *The map  $\theta$  is locally injective.*

*Proof.* The Jacobian matrix of the map  $\theta$  in coordinates  $(r_1, \dots, r_p)$  and  $(\theta_1, \dots, \theta_p)$  has negative entries on diagonal and non-negative entries elsewhere. Moreover, the

sum of entries in each row is zero. Obviously there is at least one linear relation between the columns of the matrix, which is simply that their sum is zero. But that was expected since cone angles are linearly dependent. This is the only linear relation since at least one diagonal minor of dimension  $p - 1$  is non-zero. Indeed, argument, similar to that of the Simple Lemma of Linear Algebra (Lemma B.1 in the Appendix B), with slight modification works here as well. We can choose a column with at least one non-zero off diagonal element. Consider the minor complementary to the diagonal element of that column. Then in at least one row absolute value of the sum of off diagonal elements is strictly smaller than that of the diagonal element itself. Taking this row to be the last in the Gauss Diagonalization process we easily see that the diagonalized matrix will have non-zero diagonal elements.  $\square$

## 7.4 The region $\mathcal{R}$ and its topology

We again assume that the group of isometries and the equivariant system of rays have been fixed. We will call the polyhedron obtained by placing the vertices on the intersection of the rays and the hyperboloid *preferred* and will denote the point corresponding to it in  $Pol(\zeta, v) \subset \Delta_r^{p-1}$  by  $Pr$ . Obviously,

$$Pr = \left( \frac{1}{p}, \dots, \frac{1}{p} \right)$$

As mentioned before, in [8] it is shown that this is a spacelike polyhedron. By the construction every vertex is on the boundary of the convex hull which is equivalent to saying it is not in the convex hull of others. We can now move the vertices slightly along the rays by changing  $r_i$ 's small enough to still get a spacelike polyhedron and

do it until one or more vertices gets into the convex hull of others. The idea of the proof of the main theorem is to show that by this procedure of moving the vertices along the rays away from their positions in *preferred* and changing  $r_i$ 's continuously we can obtain any polyhedron in  $Pol(\zeta, v)$ . Therefore

**Definition 7.4.1.** Let  $\mathcal{R}_0 \subset \Delta_r^{p-1}$  be the union of all half-open straight line segments in  $\Delta_r^{p-1}$  starting at  $Pr$  and extended as long as in the corresponding polyhedra no vertex is in the convex hull of the others.

The end point of each segment (not included in  $\mathcal{R}_0$ ) obviously corresponds to the polyhedron with one or more vertices exactly on the boundary of the convex hull of the others.

**Proposition 7.4.2.** *Definition 7.4.1 is correct, i.e. each straight line segment must end at a point inside  $\Delta_r^{p-1}$ .*

*Proof.* Consider a straight line ray in  $\Delta_r^{p-1}$  starting at  $Pr$ . It has the form

$$\gamma(t) = Pr + tu$$

where  $u = (u_1, \dots, u_p) \neq 0$  is a vector in  $\mathbb{R}^p$  perpendicular to the vector  $n = (1, \dots, 1)$  and  $t > 0$ . Let  $u_k = \min\{u_1, \dots, u_p\}$ . From

$$\sum_{i=1}^p u_i = 0$$

it follows that  $u_k < 0$  and for at least one  $j \neq i$  we must have  $u_j > 0 > u_k$ . Now as we are moving vertices according to this path we can scale  $r_i$ 's so that  $r_k$  stays constant.

That is equivalent to moving along the ray  $\tilde{\gamma}(\tilde{t}) = Pr + \tilde{t}\tilde{u}$ , where

$$\tilde{u} = -u_k \cdot n + u = (u_1 - u_k, \dots, u_p - u_k)$$

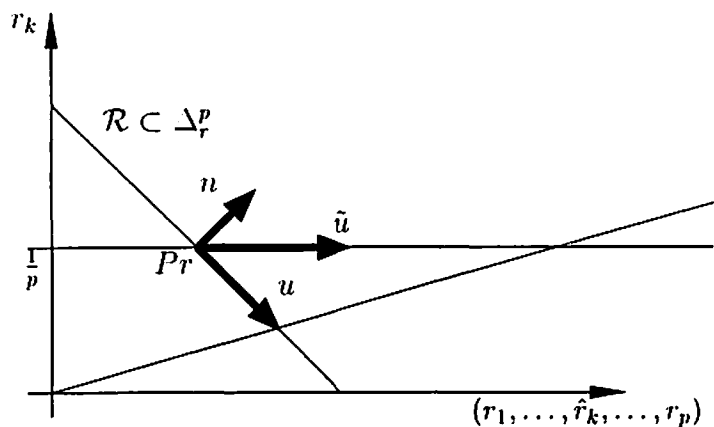


Figure 7.3: To the proof of Proposition 7.4.2

is the vector forming the basis of the 1-dimensional intersection of the 2-plane spanned by  $u$  and  $n$  and codimension-1 affine subspace  $r_k = \frac{1}{p}$  (Fig. 7.3). We see that all components of  $\tilde{u}$  are non-negative and at least one is positive. So in this setting we keep vertex (orbit)  $v_k$  in place and move the rest of the vertices (at least one) away from the origin. Notice that up to similarity we still are getting the same singular Euclidean structures.

First of all we need to make sure that the convex hull remains a spacelike polyhedra, that is none of its faces becomes light or timelike. If one of those possibilities were realized, the plane of such a face would split  $\mathbb{H}^2$  into two non-compact regions of infinite area (a horoball and its complement or two half-planes). One of these areas would have to correspond to the part outside the convex hull. But this is impossible since in either case it contains fundamental domain of the group action and therefore at least one vertex, which should belong to the convex hull.

Now it is obvious that for some finite  $\tilde{t} > 0$  at least one of the moving vertices will hit the boundary of the convex hull of vertex  $v_k$  since any central ray meets (once) this boundary (see [8] and [18]). Geometrically it is obvious that corresponding  $\gamma(t)$  remains inside  $\Delta_r^{p-1}$ . To be more rigorous we need to find connection between  $t$  and  $\tilde{t}$ .

For corresponding  $t$  and  $\tilde{t}$  points  $Pr + tu$  and  $Pr + \tilde{t}u$  are scalar multiples of each other (lie on the same straight line through origin). Therefore

$$\lambda(t)(Pr + tu) = (Pr + \tilde{t}u)$$

For  $k^{\text{th}}$  component that becomes

$$\lambda(t)\left(\frac{1}{p} + tu_k\right) = \left(\frac{1}{p} + \tilde{t} \cdot 0\right)$$

and hence

$$\lambda(t) = \frac{1}{1 + tpu_k}$$

Now for  $j^{\text{th}}$  component we have

$$\frac{1}{1 + tpu_k}(1 + tu_j) = \left(\frac{1}{p} + \tilde{t}(u_j - u_k)\right)$$

which after simple calculation becomes

$$t = \frac{\tilde{t}}{1 - \tilde{t}pu_k}$$

Since  $u_k < 0$  we have

$$t = \frac{1}{\frac{1}{\tilde{t}} - pu_k} \xrightarrow{\tilde{t} \rightarrow +\infty} -\frac{1}{pu_k}$$

and, therefore, for the smallest component

$$(Pr + tu)_k = \frac{1}{p} + tu_k \xrightarrow{\tilde{t} \rightarrow +\infty} \frac{1}{p} - \frac{1}{pu_k} u_k = 0$$

remaining positive for all finite values of  $\tilde{t}$ . □

**Lemma 7.4.3.** *The region  $\mathcal{R}_0$  has the following properties:*

1. *It is star shaped with respect to  $Pr$*
2. *It is open*

*Proof.* The first statement is a direct corollary of the definition of  $\mathcal{R}_0$ . As for openness, it is clear that along with any point  $\mathcal{R}_0$  contains its small open neighborhood, since the vertices can be perturbed slightly without breaking the combinatorics of the convex hull 1-skeleton. □

Let's denote by  $\partial\mathcal{R}$  the set of end points of all segments in the definition of  $\mathcal{R}_0$  and define

$$\mathcal{R} = \mathcal{R}_0 \cup \partial\mathcal{R}$$

We have

$$\mathcal{R} \subset \text{Pol}(\zeta, v)$$

Therefore the map  $\theta$  can be restricted to a map also denoted by  $\theta : \mathcal{R} \rightarrow \Delta_{\theta}^{p-1}$ . We will later show that inclusion above is actually an equality and the map is a homeomorphism. That will then constitute the proof of Theorem D.

Before we do that we will investigate the topology of  $\mathcal{R}$  and show the following

**Proposition 7.4.4.**  *$\mathcal{R}$  is homeomorphic to a closed  $(p-1)$ -dimensional simplex.*

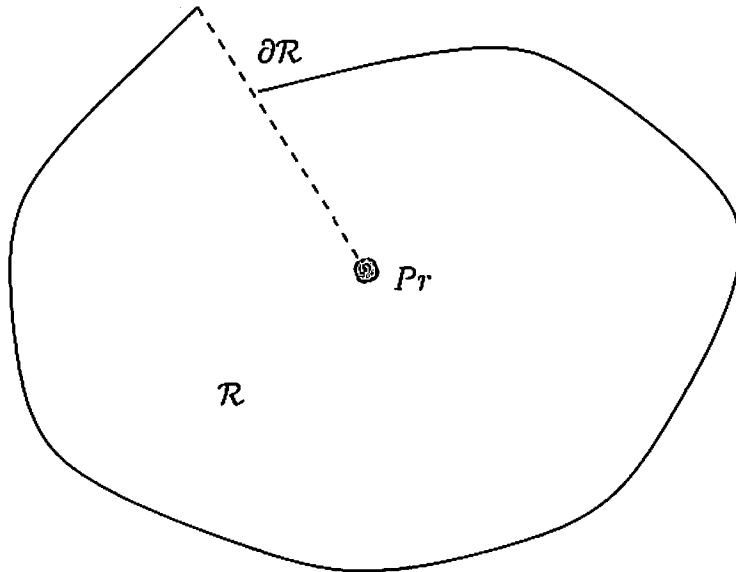


Figure 7.4: Impossible configuration

In view of Lemma 7.4.3 it is enough to show that  $\mathcal{R}$  is a manifold with boundary. Therefore, we need to prove that  $\partial\mathcal{R}$  is the boundary of  $\mathcal{R}$  as a manifold with boundary, i.e. each ending point has neighborhood homeomorphic to  $\mathbb{R}_+^{p-1}$ . Basically, we want to rule out the possibility of configuration of Fig 7.4. This will be done by induction on the number of points in the extreme set of the polyhedra (vertices spanning the convex hull).

Let's consider cases with  $p = 1$  and  $p = 2$  (basis of the induction).

Case  $p = 1$ :

This case has been considered in [18]. We only have one orbit of vertices  $v_1$ . All of the curvature is concentrated in this vertex and the angle  $\theta_1 = 2\pi(1 - \chi)$ . In this



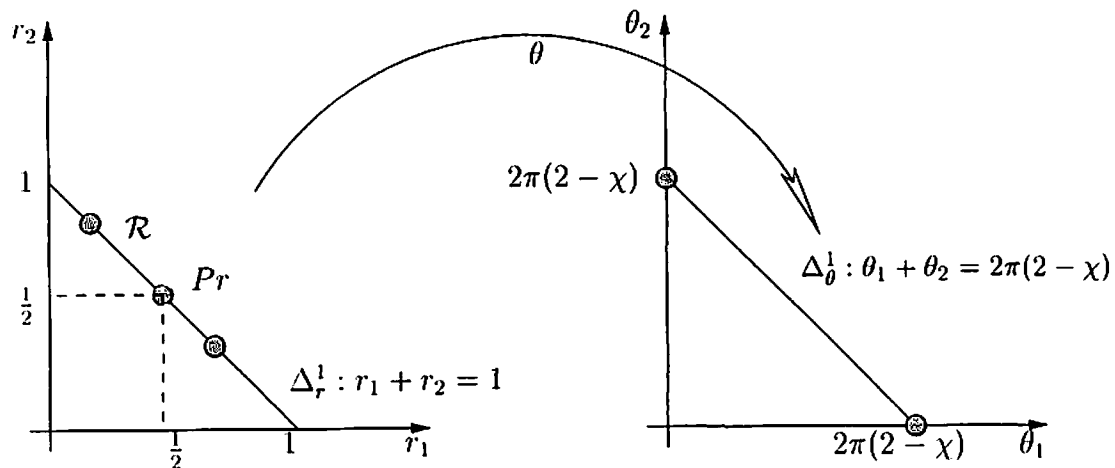


Figure 7.5: Case  $p = 2$

case there only exists one polyhedron since moving the vertex (orbit) along the ray does not change the singular Euclidean metric (up to scaling). In our notation that corresponds to the fact that map  $\theta : \Delta_r^0 \rightarrow \Delta_\theta^0$  is, obviously, a homeomorphism.

Case  $p = 2$ :

In *preferred* we have two orbits of vertices  $v_1$  and  $v_2$  with corresponding angles  $\theta_1$  and  $\theta_2$  connected by the condition  $\theta_1 + \theta_2 = 2\pi(2 - \chi)$ . We can start moving one of them, say  $v_1$ , away from the origin in  $\mathbb{R}^{2,1}$ . During this process  $\theta_1$  will continuously decrease to  $2\pi$  until  $r_1 v_1$  hits the convex hull of  $v_2$ . The angle  $\theta_2$  will increase to  $2\pi(1 - \chi)$ . In this final polyhedron vertex  $v_1$  is no longer singular and all of the curvature is concentrated in  $v_2$ . Moving  $v_1$  in the other direction from its position in *preferred* (towards origin), or, equivalently, moving  $v_2$  away from origin, we change their roles. This geometrically evident process in our notation corresponds to the fact

that the map  $\theta : \mathcal{R} \rightarrow \Delta_\theta^1$  is a homeomorphism (Fig. 7.5), showing at once that  $\mathcal{R}$  is a one-dimensional simplex and is equal to  $Pol(\zeta, v)$  in this case.

As before, let  $\gamma(t) = Pr + tu$  be a straight line ray (for  $t > 0$ ) in  $\Delta_r^{p-1}$  coming out of  $Pr$ . Again we have  $u \perp n = (1, \dots, 1)$ . Let  $\gamma_0 = \gamma(t_0)$  be the endpoint of the segment  $\gamma$ . We may assume that  $t_0 = 1$  so that  $u = \gamma_0 - Pr$ . We would like to show that in the neighborhood of  $\gamma_0$ ,  $\partial\mathcal{R}$  is a continuous hypersurface and that  $u$  is transversal to it at  $\gamma_0$ .

We may assume for the beginning that we are in the most generic case when only one vertex, say  $r_p v_p$  belongs to the convex hull of others at  $\gamma_0$ . In order to derive and investigate the equation of  $\partial\mathcal{R}$  near  $\gamma_0$  we will consider function

$$r_p = \alpha(r_1, \dots, r_{p-1})(v_p)$$

obtained by intersecting central ray  $v_p$  with the convex hull of other vertices. In this representation the  $r_i$ 's are not assumed to satisfy any scaling condition. We may think of  $\alpha(r_1, \dots, r_{p-1})(v_p)$  as the equation of the boundary for the convex hull on the surface as  $v_p$  varies over the fundamental domain. When  $v_p$  is fixed we will omit last parentheses in this formula.

**Proposition 7.4.5.** *The function  $\alpha(r_1, \dots, r_{p-1})$  is positive, homogeneous of degree 1 and*

$$\frac{\partial \alpha}{\partial r_i} \geq 0 \quad \forall i = 1, \dots, p-1$$

*Proof.* We have  $\alpha(\lambda r_1, \dots, \lambda r_{p-1}) = \lambda \alpha(r_1, \dots, r_{p-1})$  since multiplying  $r_1, \dots, r_{p-1}$  by scalar amounts to similarity in  $\mathbb{R}^{2,1}$  hence proving the first statement. The inequalities cannot be proved because of their self-evidency (really, each face of the polyhedra is

a convex hull of its vertices; moving one of them away from the origin will move all points inside the face away from the origin as well and the ray  $v_p$  either intersects this face or does not). The fact that  $\alpha(r_1, \dots, r_{p-1})$  is actually differentiable will be shown later when we obtain a formula for it.  $\square$

Now we can apply induction since we have reduced the number of vertices by one. Then by the hypothesis  $Pol(\zeta, v_1, \dots, v_{p-1})$  is homeomorphic to  $\Delta_r^{p-2}$ . The point  $\gamma_0$  obviously represents a polyhedron in this space. We would like to show that  $Pol(\zeta, v_1, \dots, v_{p-1})$  embeds into  $Pol(\zeta, v_1, \dots, v_p)$  as a submanifold and constitutes part of  $\partial\mathcal{R}$ .

Clearly,  $\alpha(r_1, \dots, r_{p-1})$  defines a map

$$A : Pol(\zeta, v_1, \dots, v_{p-1}) \rightarrow Pol(\zeta, v_1, \dots, v_p) \subset \Delta_r^{p-1}$$

by the following formula:

$$A : (r_1, \dots, r_{p-1}) \mapsto \frac{1}{1 + \alpha(r_1, \dots, r_{p-1})} (r_1, \dots, r_{p-1}, \alpha(r_1, \dots, r_{p-1}))$$

where  $Pol(\zeta, v_1, \dots, v_{p-1})$  is considered as a subset of  $\Delta_r^{p-2}$  by requiring  $\sum_{i=1}^{p-1} r_i = 1$ .

Let  $Proj$  denote the projection of  $\mathbb{R}^p$  onto the codimension-1 subspace  $\mathbb{R}^{p-1}$  of the first  $p - 1$  coordinates along the last coordinate axis :

$$Proj((r_1, \dots, r_{p-1}, r_p)) = (r_1, \dots, r_{p-1})$$

Since

$$\begin{aligned} & \frac{1}{1 + \alpha(r_1, \dots, r_{p-1})} (r_1, \dots, r_{p-1}, \alpha(r_1, \dots, r_{p-1})) = \\ & \left( \frac{r_1}{1 + \alpha(r_1, \dots, r_{p-1})}, \dots, \frac{r_{p-1}}{1 + \alpha(r_1, \dots, r_{p-1})}, \alpha \left( \frac{r_1}{1 + \alpha(r_1, \dots, r_{p-1})}, \dots, \frac{r_{p-1}}{1 + \alpha(r_1, \dots, r_{p-1})} \right) \right) \end{aligned}$$

the image  $\Sigma$  of the map  $A$  in  $\Delta_r^{p-1}$  bijectively projects by  $Proj$  onto the hypersurface  $\tilde{\Sigma}$  defined by the equation

$$\sum_{i=1}^{p-1} r_i + \alpha(r_1, \dots, r_{p-1}) = 1 \quad (7.4.1)$$

in the set

$$\tilde{\Delta}_r^{p-1} = \left\{ (r_1, \dots, r_{p-1}) : \sum_{i=1}^{p-1} r_i \leq 1, r_i \geq 0 \forall i = 1, \dots, p-1 \right\} \subset \mathbb{R}^{p-1} \subset \mathbb{R}^p$$

that is

$$\tilde{\Sigma} = Proj(\Sigma)$$

The image  $\Sigma$  is, therefore, a hypersurface in  $\Delta_r^{p-1}$

$$\Sigma = \left\{ (r_1, \dots, r_{p-1}, \alpha(r_1, \dots, r_{p-1})) : \sum_{i=1}^{p-1} r_i + \alpha(r_1, \dots, r_{p-1}) = 1 \right\}$$

and could be considered as a graph of the function  $\alpha$  restricted to  $\tilde{\Sigma}$  (Fig. 7.6).

**Proposition 7.4.6.**  $\tilde{\Sigma}$  is locally a submanifold of  $\tilde{\Delta}_r^{p-1}$ .

*Proof.* Since  $\tilde{\Sigma}$  is given by the equation  $S = 0$ , where

$$S = \sum_{i=1}^{p-1} r_i + \alpha(r_1, \dots, r_{p-1}) - 1$$

one needs to show that the gradient  $\nabla S \neq 0$ . We have

$$N = \nabla S = \left( 1 + \frac{\partial \alpha}{\partial r_1}, \dots, 1 + \frac{\partial \alpha}{\partial r_{p-1}} \right) \neq 0$$

since  $\frac{\partial \alpha}{\partial r_i} \geq 0$  for all  $i = 1, \dots, p-1$  by Proposition 7.4.5 proving the assertion of the lemma.  $\square$

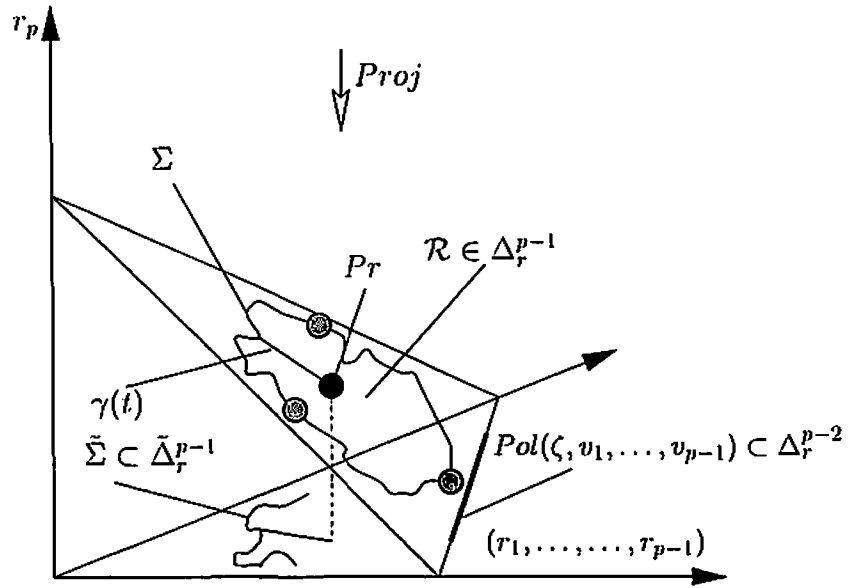


Figure 7.6: Hypersurfaces  $\Sigma$  and  $\tilde{\Sigma}$

**Proposition 7.4.7.** *The ray  $\gamma(t)$  is transversal to  $\Sigma$  at  $\gamma_0 = \gamma(1)$  ( in  $\Delta_r^{p-1}$  ).*

*Proof.* It is clearly enough to show that  $Proj(u)$  is transversal to  $\tilde{\Sigma} = Proj(\Sigma)$  where  $u = \gamma_0 - Pr$ . We have  $\gamma_0 = (r_1, \dots, r_{p-1}, r_p)$  and therefore

$$u = \left( r_1 - \frac{1}{p}, \dots, r_{p-1} - \frac{1}{p}, r_p - \frac{1}{p} \right)$$

Hence

$$\begin{aligned} \langle N, Proj(u) \rangle &= \sum_{i=1}^{p-1} \left( 1 + \frac{\partial \alpha}{\partial r_i} \right) \left( r_i - \frac{1}{p} \right) = \\ &= \sum_{i=1}^{p-1} \left( r_i + r_i \frac{\partial \alpha}{\partial r_i} - \frac{1}{p} - \frac{1}{p} \frac{\partial \alpha}{\partial r_i} \right) = \\ &= \sum_{i=1}^{p-1} r_i + \sum_{i=1}^{p-1} r_i \frac{\partial \alpha}{\partial r_i} - \frac{p-1}{p} - \frac{1}{p} \sum_{i=1}^{p-1} \frac{\partial \alpha}{\partial r_i} \end{aligned}$$

By Euler's Theorem for homogeneous functions we have

$$\sum_{i=1}^{p-1} r_i \frac{\partial \alpha}{\partial r_i} = 1 \cdot \alpha(r_1, \dots, r_{p-1})$$

Substituting  $1 - \frac{1}{p}$  instead of  $\frac{p-1}{p}$  we get

$$\langle N, Proj(u) \rangle = \sum_{i=1}^{p-1} r_i + \alpha(r_1, \dots, r_{p-1}) - 1 + \frac{1}{p} - \frac{1}{p} \sum_{i=1}^{p-1} \frac{\partial \alpha}{\partial r_i}$$

Finally, using equation 7.4.1 of the surface  $\tilde{\Sigma}$ , one obtains

$$\langle N, Proj(u) \rangle = \frac{1}{p} \left( 1 - \sum_{i=1}^{p-1} \frac{\partial \alpha}{\partial r_i} \right)$$

To show that ray  $\gamma(t)$  is transversal to  $\partial \mathcal{R}$  at  $\gamma_0$  we need to show that

$$\langle N, Proj(u) \rangle \neq 0$$

Therefore, to finish the proof one needs to prove inequality

$$\sum_{i=1}^{p-1} \frac{\partial \alpha}{\partial r_i} \neq 1 \tag{7.4.2}$$

This will be done in section 7.7 after a deeper analysis of function  $\alpha(r_1, \dots, r_{p-1})$ .  $\square$

Now we can complete the proof of the Proposition 7.4.4.

*Proof of Proposition 7.4.4.* First of all let's notice that the assumption made about just one vertex entering the convex hull of others is easy to get rid of. If  $k$  vertices simultaneously enter the convex hull of the others, then the corresponding ray from  $Pr$  will intersect  $\partial\mathcal{R}$  in the intersection of the boundary hypersurfaces of these vertices. The fact that the ray is transversal to each of them and they homeomorphically project onto their corresponding coordinate hyperplanes guarantees that this intersection is actually a submanifold itself. Therefore, the boundary  $\partial\mathcal{R}$  is composed of the simplices  $\partial\mathcal{R}(v') \cong \text{Pol}(\zeta, v')$ , for all proper subsets of  $v' \subset v = \{v_1, \dots, v_k\}$ , pieced together in such a way that  $\partial\mathcal{R}(v'')$  is a (topological) face of  $\partial\mathcal{R}(v')$  iff  $v'' \subset v'$ . That presents a simplicial cellulation of the boundary of  $\partial\mathcal{R}$ . Since  $\mathcal{R}$  is starshaped, has a continuous boundary and is of full dimension, it is topologically a simplex.  $\square$

## 7.5 Proof of the Main Theorem

We are now in the position to prove the Main Theorem, as the following

**Theorem D.** *The map  $\theta : \mathcal{R} \rightarrow \Delta_{\theta}^{p-1}$  is a homeomorphism.*

**Proposition 7.5.1.**

$$\mathcal{R} = \text{Pol}(\zeta, v)$$

*Proof.* Let us assume the contrary, i.e., there exists polyhedron  $P'$  represented by  $r = (r_1, \dots, r_p)$ , which is not in  $\mathcal{R}$ . Consider a straight line segment from  $Pr$  to  $r$ . According to Proposition 7.4.3 it will cross the boundary  $\partial\mathcal{R}$  at some point  $\tilde{r}$ . That

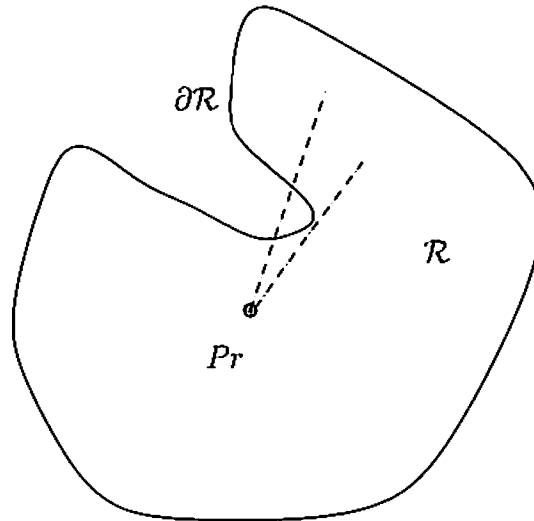


Figure 7.7: Impossible shape

point represents the first time one or more vertices of  $P$  are in the convex hull of the others, in fact on its boundary, moving along this line segment away from  $P_r$ . Moving further along this line will actually push these vertices into the interior of the convex hull. It is clear that on the way to  $P'$  there would be a point when all these vertices return to the convex hull boundary. That means that a piece of  $\partial\mathcal{R}$  is intersected by the ray twice (Fig. 7.7).

By the mean value theorem there is a ray tangent to this piece of  $\partial\mathcal{R}$  giving contradiction with transversality.  $\square$

*Proof of Theorem D.* We will again proceed by induction on the number of singular (cone) points  $n$ .



The cases of  $n = 1$  and  $n = 2$  have already been considered earlier in this section. The induction step will be a generalization of the argument of the second case.

Assume that theorem holds for all  $k < n$ . As shown in Proposition 7.4.4 above, we have a simplicial cellulation of the boundary of  $\partial\mathcal{R}$ . By assumption, the map  $\theta$  is a homeomorphism on each cell and is, clearly, consistent on the cell intersections. Therefore, we obtain that  $\theta$  is a continuous, injective map of a ball into a ball such that the restriction to the boundary of the source is a homeomorphism onto the boundary of the target. Since the sphere is not a retract of a ball, it follows then that  $t$  is necessarily onto, hence, a homeomorphism. This completes the proof of Theorem D.  $\square$

We still have to show that the map  $\alpha$  is differentiable and that its derivatives satisfy inequality C.1. This is done in the next two sections.

## 7.6 Barycentric representation of the function $\alpha$

We will first obtain an analytic formula for  $\alpha(r_1, \dots, r_{p-1})$  to see that it is differentiable and in the appendix C we will find its derivatives by a synthetic argument in a more general setting.

Assume that we have a nondegenerate spacelike triangle formed by three vertices  $r_1v_1, r_2v_2$  and  $r_3v_3$  and let ray  $v$  intersect this triangle at point  $rv$ . Then there are well defined barycentric coordinates  $\alpha_1, \alpha_2$  and  $\alpha_3$  of  $rv$  with respect to this triangle, i.e.

$$rv = \sum_{i=1}^3 \alpha_i \cdot r_i v_i \tag{7.6.1}$$

where  $r = \alpha(r_1, r_2, r_3)$ . Therefore we obtain

$$r^2 = -\langle rv, rv \rangle = -\left\langle \sum_{i=1}^3 \alpha_i \cdot r_i v_i, \sum_{i=1}^3 \alpha_i \cdot r_i v_i \right\rangle = -\sum_{i=1}^3 \sum_{j=1}^3 \alpha_i \alpha_j r_i r_j \langle v_i, v_j \rangle$$

As before we have  $l_{ij} = -\langle v_i, v_j \rangle = \cosh(\text{dist}(v_i, v_j))$  and hence

$$r^2 = -\sum_{i=1}^3 \sum_{j=1}^3 \alpha_i \alpha_j r_i r_j l_{ij} = \sum_{i=1}^3 \alpha_i^2 r_i^2 + 2 \sum_{1 \leq i < j \leq 3} \alpha_i \alpha_j r_i r_j l_{ij}$$

In the generic case the ray  $v_p$  intersects the convex hull boundary inside of a triangle face (perhaps on its border). Then this barycentric representation for  $\alpha(r_1, \dots, r_{p-1})$  is well-defined and unique and is preserved under small perturbations of the boundary.

Therefore we have

$$\alpha(r_1, \dots, r_{p-1}) = \sqrt{\sum_{i=1}^3 \alpha_i^2 r_i^2 + 2 \sum_{1 \leq i < j \leq 3} \alpha_i \alpha_j r_i r_j l_{i,j}}$$

where  $1 \leq l_k \leq p-1$ . This shows that function  $\alpha(r_1, \dots, r_{p-1})$  is continuously differentiable in its domain.

In the special case when the ray hits the boundary inside of a face other than triangle we only need to notice that under small perturbation the face either is not destroyed or is destroyed by breaking into faces with fewer vertices. In either case, the we can choose a triangle containing the intersection of the ray with the convex hull boundary during the perturbation, thus reducing to the case considered above.

Calculating derivatives of  $\alpha(r_1, \dots, r_{p-1})$  from this formula though does not look very attractive. Therefore we will do this geometrically in appendix C.

## 7.7 Proof of transversality in proposition 7.4.7

To apply Theorem C.2 of Appendix C to our situation we can notice that we only need the norm to be defined for vectors  $\Delta - \{0\}$  and their scalar multiples, where  $\Delta$  is  $span(A_1, \dots, A_n)$  or close to it subspace  $span(A'_1, A_2, \dots, A_n)$ . It, obviously, holds in  $\mathbb{R}^{2,1}$  for timelike  $A_1, A_2, A_3$  forming a spacelike triangle with  $|V| = \frac{1}{i} \cdot \sqrt{\langle V, V \rangle}$  for  $V$  timelike and  $|V| = \sqrt{\langle V, V \rangle}$  for  $V$  spacelike. If points  $A_1, A_2, A_3$  are slightly perturbed along their rays  $span(A_1, A_2, A_3)$  remains spacelike.

To prove necessary inequality

$$\sum_{i=1}^{p-1} \frac{\partial \alpha}{\partial r_i} \neq 1 \quad (7.7.1)$$

let's first assume the generic case of ray  $v_p$  intersecting the convex hull boundary inside of the triangle with vertices so that we have representation 7.6.1 for  $\alpha$ . Then by Theorem C.2 inequality 7.7.1 becomes

$$\sum_{l=1}^3 \frac{\alpha(r_{i_1}, r_{i_2}, r_{i_3})}{r_{i_l}} \cdot \alpha_{i_l} \neq 1$$

Notice that according to the second part of Theorem C.2 we obtain the same formula even if two or all three of these vertices belong to the same orbit and therefore corresponding  $r_i$ 's are equal.

In fact we will prove more, namely

$$\sum_{l=1}^3 \frac{\alpha(r_{i_1}, r_{i_2}, r_{i_3})}{r_{i_l}} \cdot \alpha_{i_l} > 1 \quad (7.7.2)$$

To prove this inequality let us fix points  $r_{i_1} v_{i_1}, r_{i_2} v_{i_2}, r_{i_3} v_{i_3}$  (i.e., fix  $r_{i_1}, r_{i_2}, r_{i_3}$ ) and consider the function

$$\tilde{\alpha}(v_p) = \alpha(r_{i_1}, r_{i_2}, r_{i_3})(v_p)$$

as a function of a ray  $v_p \in H^2$ . Then

$$\bar{\alpha}(v_p) = \text{dist}(0, v_p \cap \text{span}(r_{i_1}v_{i_1}, r_{i_2}v_{i_2}, r_{i_3}v_{i_3}))$$

where  $\text{dist}(0, V) = |V| = \frac{1}{i} \cdot \sqrt{\langle V, V \rangle}$  for a timelike  $V \in R^{2,1}$ , so it can be considered as function  $d(x)$  on the 2-plane  $\text{span}(r_{i_1}v_{i_1}, r_{i_2}v_{i_2}, r_{i_3}v_{i_3})$ :

$$d(x) = \bar{\alpha}(i \cdot \frac{x}{|x|})$$

Now, since in barycentric coordinates we have

$$r_p v_p = \sum_{i=1}^3 \alpha_{i_i} \cdot r_{i_i} v_{i_i}$$

and  $r_i = d(r_i v_i) = \text{dist}(0, r_i v_i)$ , we may rewrite 7.7.2 as

$$\sum_{i=1}^3 \alpha_{i_i} \cdot \frac{1}{d(r_{i_i} v_{i_i})} > \frac{1}{d(\sum_{i=1}^3 \alpha_{i_i} \cdot r_{i_i} v_{i_i})}$$

This inequality manifests the convexity of function

$$f(X) = \frac{1}{d(X)}$$

on the intersection of any spacelike affine plane with the interior of the light cone which is shown in Appendix D.

## Appendix A

### ONE SIMPLE LEMMA OF EUCLIDEAN PLANIMETRY

**Definition A.1.** A unit star of degree  $n$  in a Euclidean plane is a collection of  $n$  unit vectors with a common base.

**Lemma A.2.** Let unit vectors  $\mathbf{a}_1, \dots, \mathbf{a}_n$  form a unit star in a Euclidean plane. Also, let the angles  $\alpha_{i i+1}$  be correspondingly the

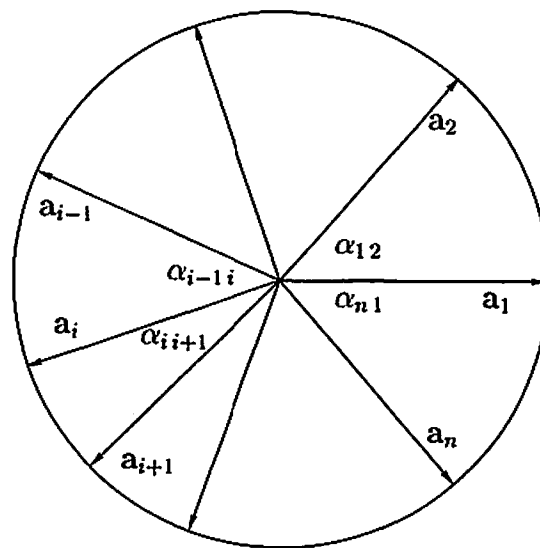


Figure A.1: Unit star

angles between vectors  $\mathbf{a}_i$  and  $\mathbf{a}_{i+1}$ , where  $i$  is an integer module  $n$ . Then the following relation holds:

$$\sum_{i=1}^n \left( \tan \frac{\alpha_{i-1i}}{2} + \tan \frac{\alpha_{ii+1}}{2} \right) \mathbf{a}_i = 0 \quad (\text{A.1})$$

*Remark A.3.* In case of a symmetric star (with all angles equal) the statement of the lemma reduces to the famous relation  $\sum_{i=1}^n \mathbf{a}_i = 0$ .

To prove the lemma we will need the following

**Proposition A.4.** *Let unit vectors  $\mathbf{a}, \mathbf{b}$  and  $\mathbf{c}$  form a unit star of degree 3 and let angle  $\alpha$  be the angle between  $\mathbf{a}$  and  $\mathbf{c}$  not containing  $\mathbf{b}$  and, likewise, let angle  $\beta$  be the angle between  $\mathbf{b}$  and  $\mathbf{c}$  not containing  $\mathbf{a}$ . Then*

$$(\cot \alpha + \cot \beta) \mathbf{c} = \frac{1}{\sin \alpha} \mathbf{a} + \frac{1}{\sin \beta} \mathbf{b} \quad (\text{A.2})$$

*Remark A.5.* For our purposes all angles in the unit stars are not zero. But this Lemma still holds even if there are zero angles. The statement of the proposition A.4 has to be adjusted multiplying by sines of both angles. Then it holds just as well. In this more general form it is  $\sin(\alpha + \beta)\mathbf{c} = \sin \alpha \mathbf{b} + \sin \beta \mathbf{a}$ .

*Proof.* Let  $A, B$  and  $C$  be numbers such that  $C\mathbf{c} = A\mathbf{a} + B\mathbf{b}$  (assuming both angles are non-zero). Multiplying this equation scalarly by  $\mathbf{c}$  and by  $\mathbf{c}^\perp$  (the unit vector orthogonal to  $\mathbf{c}$  and making the positively oriented basis  $\langle \mathbf{c}, \mathbf{c}^\perp \rangle$ ) we obtain:

$$C = A(\mathbf{a}, \mathbf{c}) + B(\mathbf{b}, \mathbf{c})$$

$$0 = A(\mathbf{a}, \mathbf{c}^\perp) + B(\mathbf{b}, \mathbf{c}^\perp)$$

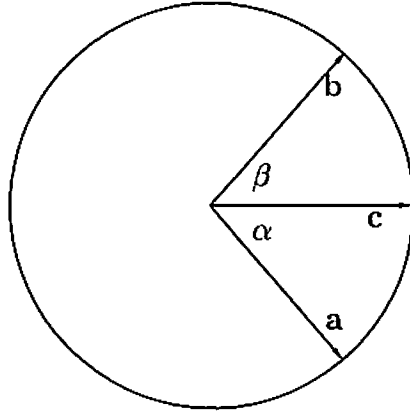


Figure A.2: Unit star of degree 3

Now, assuming without loss of generality that moving counterclockwise from vector  $c$  we meet vector  $b$  before vector  $a$ , we have  $(b, c^\perp) = \cos(\frac{\pi}{2} - \beta) = \sin \beta$  and  $(a, c^\perp) = \cos(\frac{\pi}{2} + \alpha) = -\sin \alpha$ , and therefore we can take  $A = \frac{1}{\sin \alpha}$  and  $B = \frac{1}{\sin \beta}$ . Then, since  $(a, c) = \cos \alpha$  and  $(b, c) = \cos \beta$ , we get the desired equality.  $\square$

*Proof of A.2.* From the previous proposition we have

$$(\cot \alpha_{i-1i} + \cot \alpha_{ii+1}) \mathbf{a}_i = \frac{1}{\sin \alpha_{i-1i}} \mathbf{a}_{i-1} + \frac{1}{\sin \alpha_{ii+1}} \mathbf{a}_{i+1}$$

Adding these equations for all  $i = 1, \dots, n$  we have

$$\sum_{i=1}^n (\cot \alpha_{i-1i} + \cot \alpha_{ii+1}) \mathbf{a}_i = \sum_{i=1}^n \left( \frac{1}{\sin \alpha_{i-1i}} \mathbf{a}_{i-1} + \frac{1}{\sin \alpha_{ii+1}} \mathbf{a}_{i+1} \right)$$

and regrouping terms of the second sum

$$\sum_{i=1}^n (\cot \alpha_{i-1i} + \cot \alpha_{ii+1}) \mathbf{a}_i = \sum_{i=1}^n \left( \frac{1}{\sin \alpha_{i-1i}} + \frac{1}{\sin \alpha_{ii+1}} \right) \mathbf{a}_i$$

The stated result now follows from the wellknown identity

$$\tan \frac{\alpha}{2} = \frac{1 - \cos \alpha}{\sin \alpha}$$

□



## Appendix B

### ONE SIMPLE LEMMA OF LINEAR ALGEBRA

**Lemma B.1.** *Let  $M$  be a real square  $n \times n$  matrix. If absolute value of each diagonal element is (strictly) greater than the sum of absolute values of all other elements of the same column, then matrix  $M$  is non-degenerate.*

*Proof.* Apply the Gauss diagonalization process. Then each diagonal element of the diagonalized matrix is obtained by adding to the corresponding diagonal element of  $M$  the elements of the same column in  $M$  above this diagonal element multiplied by the coefficients in absolute value strictly smaller than 1. Therefore all diagonal elements of the diagonalized matrix are non zero. □

## Appendix C

### DIFFERENTIATION OF A DISTANCE FUNCTION IN BARYCENTRIC REPRESENTATION IN NORMED AFFINE SPACES

In affine normed space  $\mathbb{R}^n$  let's consider affinely independent points  $O, A_1, \dots, A_n$ . In other words, if we think of  $\mathbb{R}^n$  as a linear space with origin  $O$  then vectors  $OA_1, \dots, OA_n$  are linearly independent. The points  $A_1, \dots, A_n$  define a nondegenerate (closed)  $n-1$ -dimensional simplex  $\Delta$ . Therefore they induce well defined barycentric coordinates on the affine space  $span(A_1, \dots, A_n)$ . By construction, of course,  $O \notin span(A_1, \dots, A_n)$ .

Let  $B$  be any point in  $span(A_1, \dots, A_n)$ . Then it has barycentric coordinates  $(\alpha_1(B), \dots, \alpha_n(B))$ , with all  $\alpha_i(B) \geq 0$ . Fix the central rays (taking  $O$  to be the center) through  $A_1, \dots, A_n$  and  $B$  and let  $r_i(A_i) = |OA_i|$  where  $|OX|$  denotes the norm of the vector  $OX$ . If we allow points  $A_1, \dots, A_n$  to slide along the corresponding rays and let  $B$  be the intersection of the corresponding (fixed earlier) ray with  $span(A_1, \dots, A_n)$  we may write  $|OB| = \alpha_B(|OA_1|, \dots, |OA_n|)$  or  $|OB| = \alpha_B(r_1, \dots, r_n)$ . We could obtain a formula for this function similar to that of the section 7.7 (actually it is exactly

same formula except that we should use  $n$  instead of 3 in the upper limit of the summation). But we are interested in the derivatives of  $\alpha_B(r_1, \dots, r_n)$  which are much easier and more elegantly obtained by a geometric argument.

**Definition C.1.** We will call function  $\alpha_B(r_1, \dots, r_n)$  the distance function of a point  $B$  with respect to origin  $O$  and simplex  $\Delta = A_1 \dots A_n$ .

**Theorem C.2.** When  $B \in \Delta$  (all  $\alpha_i(B) \geq 0$ ) the function  $\alpha_B(r_1, \dots, r_n)$  is continuously differentiable and

$$\frac{\partial \alpha_B(r_1, \dots, r_n)}{\partial r_i} = \frac{\alpha_B(r_1, \dots, r_n)}{r_i} \cdot \alpha_i(B), \quad \forall i = 1, \dots, n \quad (\text{C.1})$$

Moreover, if for some indices  $i_1, \dots, i_k$  the variables  $r_{i_1}, \dots, r_{i_k}$  are all held  $= r$ , then

$$\frac{\partial \alpha_B(r, r_1, \dots, \hat{r}_{i_1}, \dots, \hat{r}_{i_k}, \dots, r_n)}{\partial r} = \sum_{i=1}^k \frac{\alpha_B(r_1, \dots, r_n)}{r_{i_i}} \cdot \alpha_{i_i}(B) \quad (\text{C.2})$$

*Proof.* Let us find  $\frac{\partial \alpha_B(r_1, \dots, r_n)}{\partial r_i}$ . To this end let  $A'_i$  be a point on the ray  $OA_i$  different from  $A_i$  (Fig. C.1). Let  $C$  be the intersection point of the 2-plane  $\text{span}(A'_i, A_i, B)$  and  $(n-2)$ -space  $\text{span}(A_1, \dots, \hat{A}_i, \dots, A_n)$  where  $\hat{A}_i$  means that  $A_i$  is missing. Obviously  $B \in A_i C$  (the straight line  $\text{span}(A_i, C)$ ). Let

$$B' = OB \cap A'_i C \in \text{span}(A_1, \dots, A'_i, \dots, A_n)$$

Clearly, if  $|OA'_i| = r'_i$ , then  $|OB'| = \alpha_B(r_1, \dots, r'_i, \dots, r_n)$ . Therefore we have

$$\begin{aligned} \frac{\partial \alpha_B(r_1, \dots, r_n)}{\partial r_i} &= \lim_{r'_i \rightarrow r_i} \frac{\alpha_B(r_1, \dots, r'_i, \dots, r_n) - \alpha_B(r_1, \dots, r_n)}{r'_i - r_i} = \\ &= \lim_{A'_i \rightarrow A_i} \frac{|OB'| - |OB|}{|OA'_i| - |OA_i|} = \lim_{A'_i \rightarrow A_i} \frac{|BB'|}{|A_i A'_i|} \quad (\text{C.3}) \end{aligned}$$

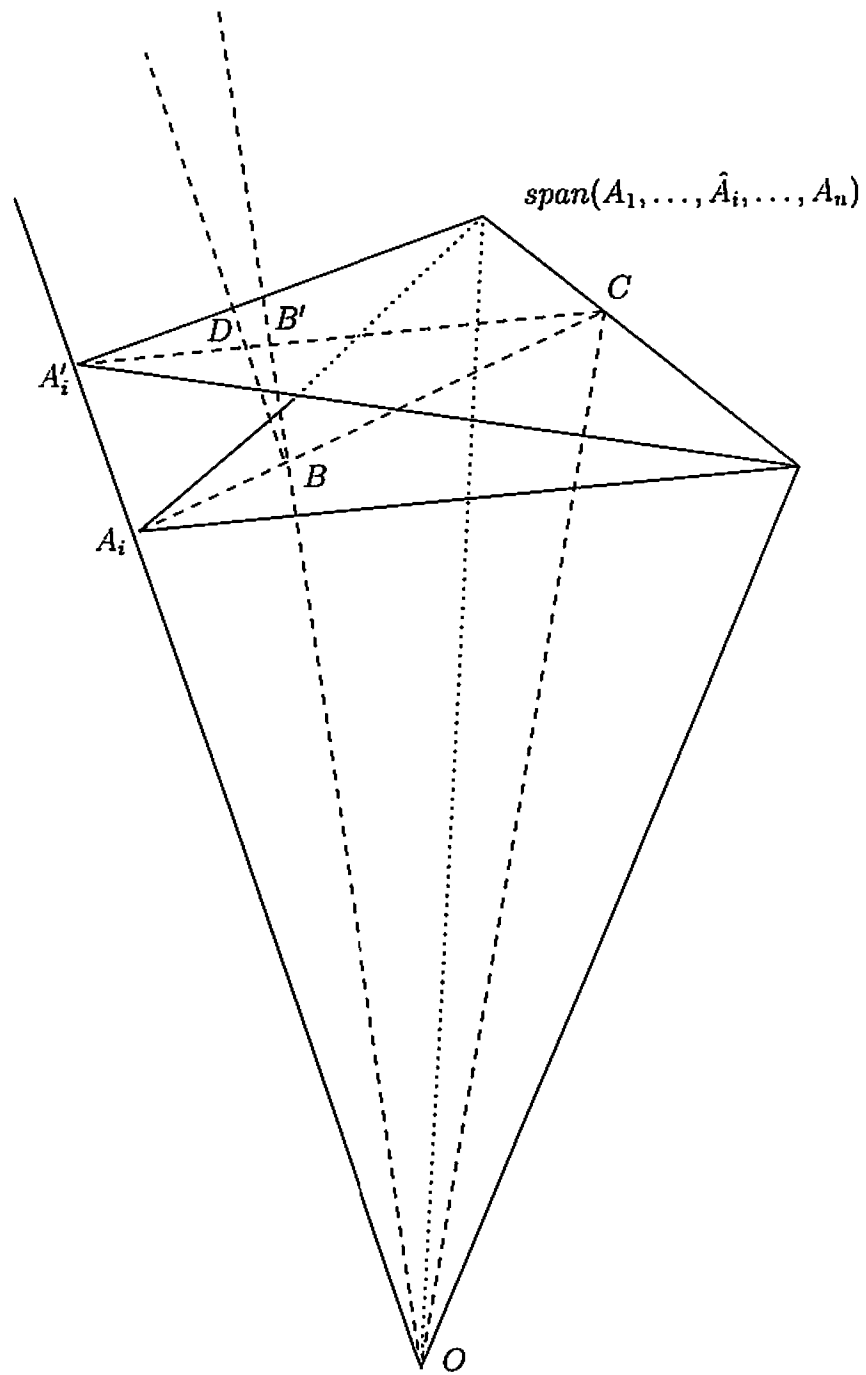


Figure C.1: Differentiating the distance function  
113

Now, let's construct a straight line through  $B$  parallel to  $OA_i$  and let  $D$  be its intersection with  $A'_iC$ . Then we may write

$$\frac{|BB'|}{|A_iA'_i|} = \frac{|BB'|}{|BD|} \cdot \frac{|BD|}{|A_iA'_i|}$$

Let's notice that as  $A'_i$  approaches  $A_i$ ,  $\triangle DBB'$  approaches  $\triangle A_iOB$  up to similarity. Hence,

$$\frac{|BB'|}{|BD|} \xrightarrow{A'_i \rightarrow A_i} \frac{|OB|}{|OA_i|} = \frac{\alpha_B(r_1, \dots, r_n)}{r_i}$$

We also have  $\triangle CBD \sim \triangle CA_iA'_i$  and therefore

$$\frac{|BD|}{|A_iA'_i|} = \frac{|CB|}{|CA_i|} = \alpha_i$$

by definition of barycentric coordinates. Combining last three equalities with equation C.3 one obtains C.1.

Equation C.2 is simply a differentiation of the composite function

$$\alpha_B(r_1, \dots, r_{i_1}, \dots, r_{i_k}, \dots, r_n)$$

with respect to  $r$ , where  $\frac{\partial r_{i_l}}{\partial r} = 1$ , for  $l = 1, \dots, k$ . But we will provide a direct geometric proof in this case as well. It is quite similar to the one above. We only need to change the construction a little bit.

We are assuming that  $|OA_{i_1}| = \dots = |OA_{i_k}|$  and that the points  $A'_{i_1}, \dots, A'_{i_k}$  are such that

$$|OA'_{i_1}| - |OA_{i_1}| = \dots = |OA'_{i_k}| - |OA_{i_k}| = r' - r$$

As before, let

$$B' = OB \cap \text{span}(A_1, \dots, A'_{i_1}, \dots, A'_{i_k}, \dots, A_n)$$

If  $k = n$  (i.e., if all points  $A_i$  are equidistant from  $O$ ) then from similar triangles  $\triangle A'_i OB'$  and  $A_i OB$  we have  $\frac{|BB'|}{|A_i A'_i|} = \frac{|OB|}{|OA_i|}$ . Therefore, recalling that the sum of barycentric coordinates is 1,

$$\begin{aligned} \frac{\partial \alpha_B(r)}{\partial r} &= \lim_{r' \rightarrow r} \frac{\alpha_B(r') - \alpha_B(r)}{r' - r} = \\ &= \lim_{A'_i \rightarrow A_i, \forall i} \frac{|OB'| - |OB|}{|OA'_i| - |OA_i|} = \lim_{A'_i \rightarrow A_i, \forall i} \frac{|BB'| |A_i A'_i| |OB|}{|OA_i|} = \\ &= \frac{\alpha_B(r)}{r} = \frac{\alpha_B(r)}{r} \cdot \sum_{i=1}^n \alpha_i(B) = \sum_{i=1}^n \frac{\alpha_B(r_1, \dots, r_n)}{r_{i_n}} \cdot \alpha_i(B) \quad (\text{C.4}) \end{aligned}$$

If  $k < n$ , then let  $\{j_1, \dots, j_{n-k}\} = \{1, \dots, n\} \setminus \{i_1, \dots, i_k\}$  and consider three new points:

$$C = \sum_{l=1}^{n-k} \alpha_{j_l}(B) \cdot A_{j_l} \quad (\text{C.5})$$

$$E = \sum_{l=1}^k \alpha_{i_l}(B) \cdot A_{i_l} \quad (\text{C.6})$$

$$E' = \sum_{l=1}^k \alpha_{i_l}(B) \cdot A'_{i_l} \quad (\text{C.7})$$

Notice that  $C$  is the same point we had in the special case we considered in the beginning. In that case we also had  $E' = A'_i$  and  $E = A_i$ .

As before let  $D \in \text{span}(A_1, \dots, A'_{i_1}, \dots, A'_{i_k}, \dots, A_n)$  be such that  $BD$  is parallel to  $EE'$ . Now to get C.2 we have a sequence of equalities:

$$\begin{aligned} \frac{|BB'|}{|A_{i_l} A'_{i_l}|} &= \frac{|BB'|}{|EE'|} \cdot \frac{|EE'|}{|A_{i_l} A'_{i_l}|} = \frac{|BB'|}{|BD|} \cdot \frac{|BD|}{|EE'|} \cdot \frac{|OE|}{|OA_{i_l}|} = \\ &= \frac{|BB'|}{|BD|} \cdot \frac{|CD|}{|CE|} \cdot \frac{|OE|}{|OA_{i_l}|} = \frac{|BB'|}{|BD|} \cdot \frac{|OE|}{|OA_{i_l}|} \cdot \sum_{l=1}^k \alpha_{i_l}(B) \quad (\text{C.8}) \end{aligned}$$

obtained from similar triangles  $\Delta A_i OE \sim \Delta A'_i OE'$  and  $\Delta BOE \sim \Delta B' OE'$ . As before, the triangle  $\Delta B' BD$  approaches  $\Delta BOE$  up to similarity as  $A'_i \rightarrow A_i$  (that is to say  $r' \rightarrow r$ ), and hence,

$$\frac{|BB'|}{|BD|} \rightarrow \frac{|OB|}{|OE|}$$

, as  $A'_i \rightarrow A_i$ . Finally one gets

$$\begin{aligned} \frac{\partial \alpha_B(r, r_{j_1}, \dots, r_{j_{n-k}})}{\partial r} &= \lim_{r'_i \rightarrow r_i} \frac{\alpha_B(r', r_{j_1}, \dots, r_{j_{n-k}}) - \alpha_B(r, r_{j_1}, \dots, r_{j_{n-k}})}{r' - r} = \\ &= \lim_{A'_i \rightarrow A_i} \frac{|OB'| - |OB|}{|OA'_i| - |OA_i|} = \lim_{A'_i \rightarrow A_i} \frac{|BB'|}{|A_i A'_i|} = \\ &= \frac{|OB|}{|OE|} \cdot \frac{|OE|}{|OA_i|} \cdot \sum_{l=1}^k \alpha_{i_l}(B) = \frac{\alpha_B(r, r_{j_1}, \dots, r_{j_{n-k}})}{r} \cdot \sum_{l=1}^k \alpha_{i_l}(B) = \\ &= \sum_{l=1}^k \frac{\alpha_B(r_1, \dots, r_n)}{r_{i_l}} \cdot \alpha_{i_l}(B) \quad (\text{C.9}) \end{aligned}$$

□

*Remark C.3.* A slight generalization of this argument with some special cases shows that Theorem C.2 holds for any  $B \in \text{span}(A_1, \dots, A_n)$ , not just for  $B \in \Delta$ . But we do not need it here.

## Appendix D

### CONVEXITY OF THE INVERSE DISTANCE FUNCTION ON A SPACELIKE AFFINE PLANE

Let  $d(V) = |V| = \sqrt{-\langle V, V \rangle}$ .

Let  $\pi$  be a spacelike affine plane in  $\mathbb{R}^{2,1}$  and let  $C$  be its intersection with  $\pi^\perp$ . Then  $C$  is timelike. Let  $c = d(C)$ . For  $X \in \pi$  let

$$x = \text{dist}(C, X) = |X - C| = \sqrt{\langle X - C, X - C \rangle}$$

which is the radius in the polar coordinate system on  $\pi$  with center at  $C$ . Then for  $d(X)$  we have

$$d(X) = \begin{cases} \sqrt{c^2 - x^2}, & X \text{ is timelike } (x < c) \\ 0, & X \text{ is lightlike } (x = c) \\ \sqrt{x^2 - c^2}, & X \text{ is spacelike } (x > c) \end{cases}$$

Now, consider the inverse distance function

$$f(X) = \frac{1}{d(x)}$$

We have

$$f(X) = \begin{cases} \frac{1}{\sqrt{c^2 - x^2}}, & X \text{ is timelike } (x < c) \\ \infty, & X \text{ is lightlike } (x = c) \\ \frac{1}{\sqrt{x^2 - c^2}}, & X \text{ is spacelike } (x > c) \end{cases}$$



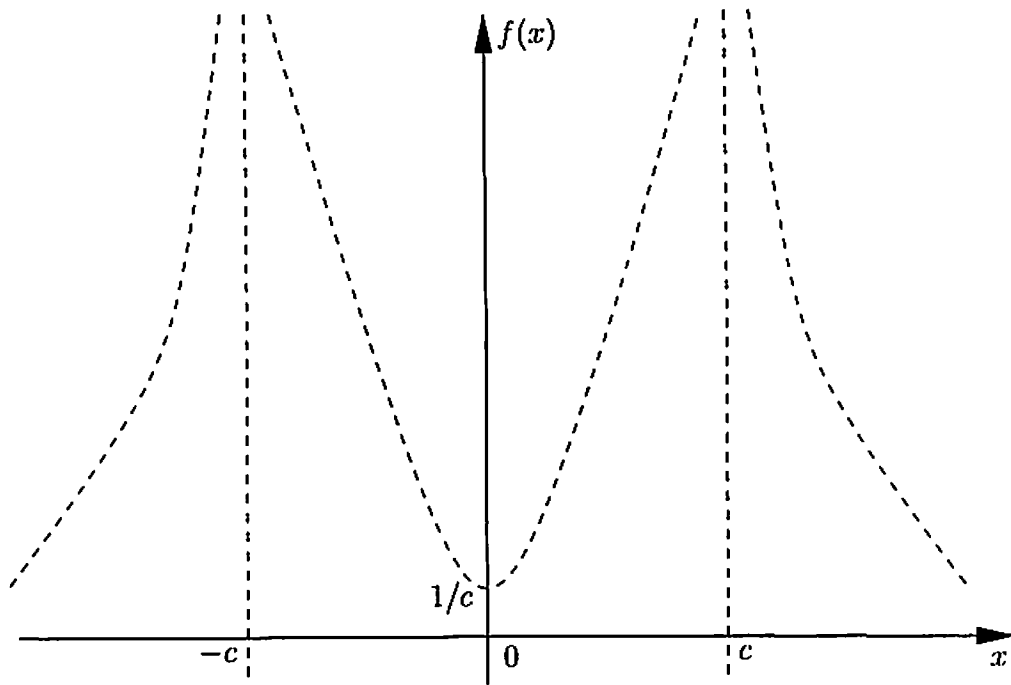


Figure D.1: Graph of function  $f(x)$

The graph of this function is shown on Fig. D.1. By abuse of notation we will write  $f(x)$  instead of  $f(X)$  since function  $f$  only depends on  $x = |X - C|$ . For  $f(x)$  we have

$$f''(x) = \begin{cases} \frac{2x^2 + c^2}{(c^2 - x^2)^{\frac{5}{2}}}, & X \text{ is timelike } (x < c) \\ \frac{2x^2 + c^2}{(x^2 - c^2)^{\frac{5}{2}}}, & X \text{ is spacelike } (x > c) \end{cases}$$

Therefore, for any vector  $X$ , which is not lightlike,  $f''(x) > 0$ , i.e.  $f$  is locally convex on its domain (since it is symmetric with respect to  $C$ ) and, as seen from the

grath, it is globally convex on the timelike part of  $\pi$ . In particular, this means that

$$f\left(\sum_{i=1}^n \alpha_i x_i\right) < \sum_{i=1}^n f(\alpha_i x_i)$$

where  $x_i \in \pi, \alpha_i \geq 0 \forall i = 1, \dots, n$  and  $\sum_{i=1}^n \alpha_i = 1$ .

## Appendix E

# CLOSED MINIMAL NETWORKS AND FOMENKO'S CONJECTURE

**Definition E.1.** A *closed minimal network* on a surface with metric is a graph on the surface such that no infinitesimal perturbation can decrease its total length.

Up to isometry there are precisely 10 possible closed minimal networks on the round two-dimensional sphere (see [13]) and infinitely many on the flat torus, which were classified in [12]. This motivated a natural conjecture, offered to the author as a problem by Professor A.T.Fomenko.

**Conjecture (Fomenko's Conjecture).** *There are finitely many different closed minimal networks on the given closed surface with fixed metric of constant negative curvature.*

It was later realized by the author that finiteness of the number of different closed minimal networks on the sphere is just a special case of the *Cauchy Rigidity Theorem*. And in a similar way *Fomenko's Conjecture* would follow from the generalized *Rigidity Theorem* for tessellations on the surfaces of genus  $g > 1$  with fixed metric of constant negative curvature along with some other facts about the restrictions on the possible topology of such networks. Since it is no longer believed that *Rigidity*

*Theorem* actually holds in general, author suggests that the answer to the Fomenko's Conjecture is negative. In fact a counterexample for minimal networks may be constructed in the same way as for a one-cell tessellation with one long side (section 5.3). Based on the minimizing property of the networks, it is probably even easier to complete the construction. Nevertheless, we will still give an account of the subject as it provides an example of homotopy uniqueness and general motivation for the whole investigation.

The most comprehensive (to date) account of the subject in much more general setting as well as in a number of particular cases is given in the monograph "Minimal Networks: The Steiner Problem and Its Generalizations" by A.O.Ivanov and A.A.Tuzhilin [13]. Here we will introduce necessary notions and state the facts that we need for our purposes.

It turns out that in order to find the networks of (locally) minimal total length it is necessary to allow the perturbations changing the topology of the network. The most classical example is provided by the splitting of the vertex of degree 4 of the network spanning the four vertices of the rectangle into two vertices of degree three (Fig. E.1). Here the rectangle vertices are considered to be fixed, forming the boundary of the network, while the fifth vertex is "mobile". The surface networks we are going to consider are closed, meaning they have empty boundary (no fixed vertices). Since closed surfaces are not contractible (unlike Euclidean space), non-empty boundary is not a necessary condition for the network to be nontrivial (a point).

Example above is nevertheless is most representative of the perturbations changing the topology of a network.

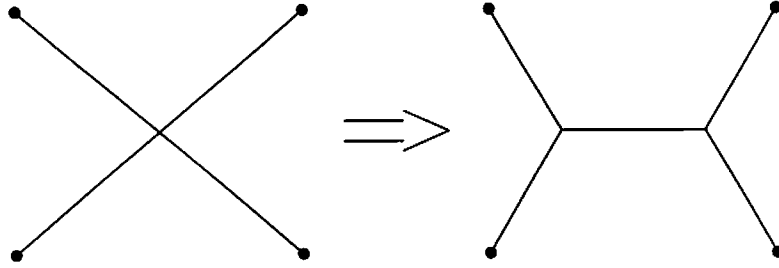


Figure E.1: Variation splitting the vertex and reducing total length

It is shown then (see [13]) that a minimal network has to be a tessellation with all vertices of degree 3 and all angles equal to  $2\pi/3$ . Indeed, the fact that the edges are geodesic segments is quite famous. It follows from the formula for the First Variation of the Length of a smooth curve segment on the manifold:

$$\left. \frac{dl}{dt} \right|_{t=0} = \langle E_1, N_1 \rangle + \langle E_2, N_2 \rangle - \int_{\gamma} \langle E, (\nabla_{\dot{\gamma}} \dot{\gamma})^{\perp} \rangle$$

Here  $\gamma(x)$  is the curve segment,  $\dot{\gamma}(x)$  is its velocity vector,  $E(x) = \left. \frac{d\gamma_t(x)}{dt} \right|_{t=0}$  is the vector field along  $\gamma$  of the one-parameter variation  $\gamma_t$ ,  $l(t)$  is the length of the curve segment  $\gamma_t$ ,  $E_1$  and  $E_2$  are the values of  $E$  at the ends of the segment and  $N_1$  and  $N_2$  are the tangent vectors of the curve coming into the end points (Fig. E.2). If the segment is a local minimum for the length function, then the derivative of the length must be zero:

$$\left. \frac{dl}{dt} \right|_{t=0} = 0$$

Since there is no restriction on the variation, it can be chosen so that the end points

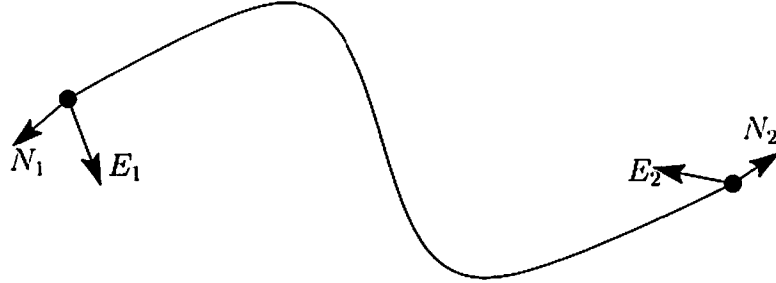


Figure E.2: Variation of a curve

are fixed. Therefore the first two terms disappear and the integral term being equal to zero for any variation yields an equation of a geodesic  $\nabla_{\dot{\gamma}}\dot{\gamma} = 0$ .

Thus the curve segment minimizing length must be geodesic and, therefore, so must be the edges of the minimal network. Taking this into account, the First Variation formula for a (geodesic) curve segment takes form

$$\left. \frac{dl}{dt} \right|_{t=0} = \langle E_1, N_1 \rangle + \langle E_2, N_2 \rangle$$

For the network with vertices  $\{V_i\}$  we therefore obtain

$$\left. \frac{dl}{dt} \right|_{t=0} = \sum_i \langle E_i, N_i \rangle$$

for the variation not destroying the network topology. Here  $N_i$  denotes the sum of the unit tangent vectors of the edges coming into the vertex  $V_i$  (Fig. E.3). This will only be zero for all such variations if and only if for all vertices we have

$$N_i = 0 \tag{E.1}$$

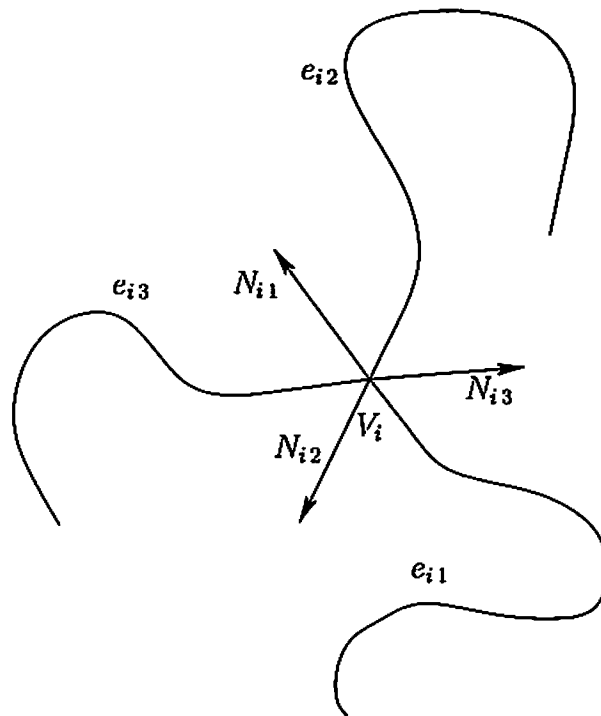


Figure E.3: Edge velocity vectors coming into the vertex

Now, let us make a little digression to the classical Fermat Problem of finding a point on the Euclidean plane such that the sum of distances from it to the given three points is minimal (Fig. E.4).

The solution is then given by the Torricelli point (usually, though, called the Steiner point, as, according to V.I.Arnold, "attribution in mathematics is done by the last") if all angles of the triangle are less than  $120^\circ$  and the vertex of the angle greater than  $120^\circ$  otherwise.

It is then easy to show that the variation splitting the vertex in the figure E.5 minimizes the length if the angle at this vertex is less than  $120^\circ$ .

This holds now for any Riemannian manifold by passing from tangent space to a small neighborhood of such vertex via the exponential map. Since all angles at the vertex of a closed network on any manifold (of any dimension) are no less than  $120^\circ$  in the only case when the degree of the vertex is 3 and the tangent unit vectors of the edges coming into the vertex are coplanar (if not surface) and form a symmetric unit star (also forced by the equation E.1), in all other cases there will exist an infinitesimal variation, possibly breaking the topology of the network, minimizing the total length.

Therefore, as mentioned in the introduction, we could equivalently define closed minimal networks to be the tessellations of the surface with all vertices of degree 3 and all angles equal to  $2\pi/3$ .

At the moment we know that minimal networks are the critical points of the length function. We will show that in presence of negative curvature they are in fact strict local minima. To this end, we will calculate the second variation for the (geodesic) networks. It is clear that any minimal network close enough to the given



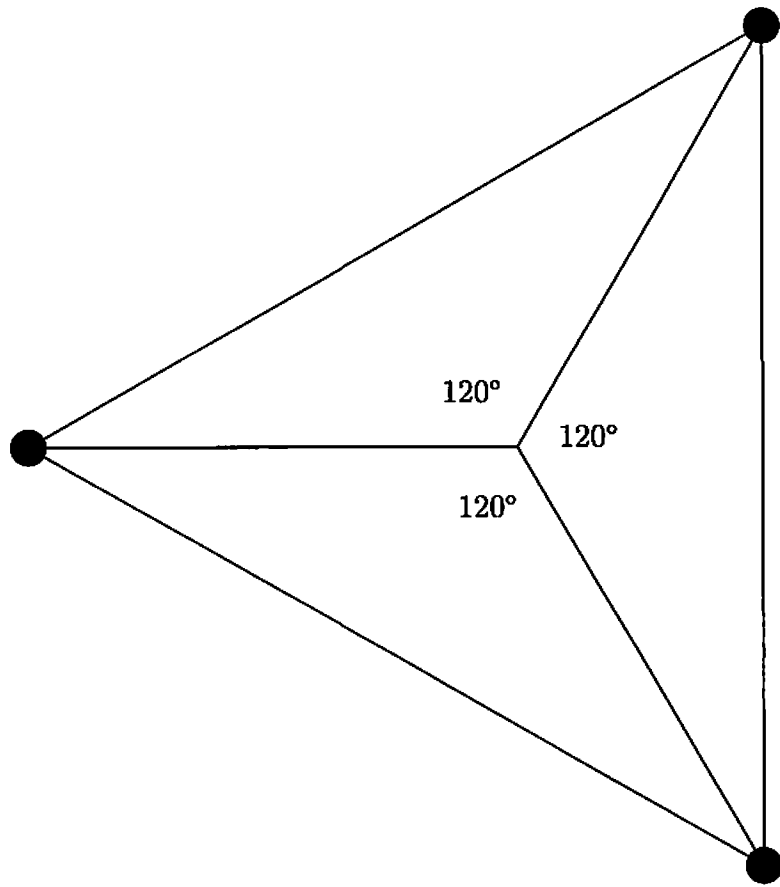


Figure E.4: Steiner-Torricelli point

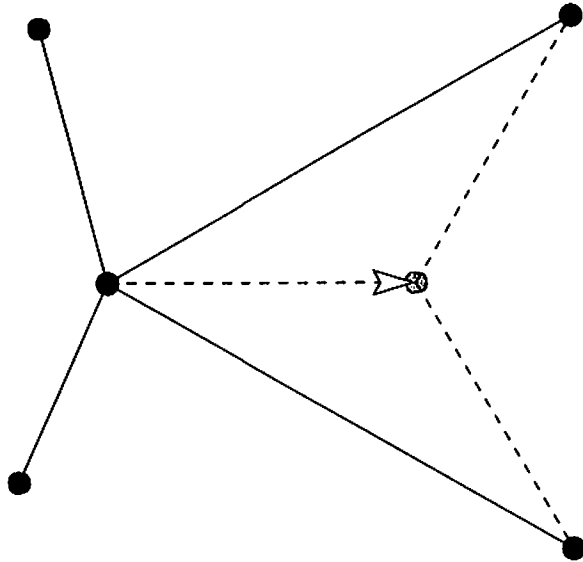


Figure E.5: Variation splitting the vertex and reducing total length

one must have the same topology. Therefore we can restrict ourselves to the variation preserving the topology of the network.

We will need to use the following formula due to Singh for the second variation of the length of the geodesic segment.

$$\left. \frac{d^2 l}{dt^2} \right|_{t=0} = \langle \nabla_Y Y, X \rangle \Big|_a^b + \int_a^b \left( \langle \nabla_X \tilde{Y}, \nabla_X \tilde{Y} \rangle - \langle R(Y, X)X, Y \rangle \right) ds \quad (\text{E.2})$$

Here  $Y(s)$  is the variation vector field of the family of curves  $\gamma_t(s)$  for  $t = 0$ ,  $X(s)$  is the velocity field of the geodesic curve  $\gamma_0(s) = \gamma(s)$  with its natural parameter,  $\tilde{Y}$  is the orthogonal component  $\tilde{Y} = Y - \langle Y, X \rangle X$  and  $R$  is the curvature tensor of the manifold. As before,  $l(t)$  is the length of the curve  $\gamma_t(s)$  for  $t \in [0, 1]$ .

To get the second variation for the length of the minimal network, we add expressions in E.2 over all edges:

$$\begin{aligned}
\left. \frac{d^2 l}{dt^2} \right|_{t=0} &= \\
&= \sum_{i=1}^E \left( \langle \nabla_Y Y_i, X_i \rangle|_{a_i}^{b_i} + \epsilon t_{a_i}^{b_i} \left( \langle \nabla_{X_i} \tilde{Y}_i, \nabla_{X_i} \tilde{Y}_i \rangle - \langle R(Y_i, X_i) X_i, Y_i \rangle \right) ds \right) = \\
&= \sum_{i=1}^E \left( \int_{a_i}^{b_i} \left( \langle \nabla_{X_i} \tilde{Y}_i, \nabla_{X_i} \tilde{Y}_i \rangle - \langle R(Y_i, X_i) X_i, Y_i \rangle \right) ds \right) + \sum_{j=1}^V \langle \nabla_Y Y|_{v_j}, N_j \rangle \quad (\text{E.3})
\end{aligned}$$

Here  $E$  is the number of edges,  $V$  is the number of vertices of the network,  $N_j$  is the sum of the tangent unit vectors of the edges coming into the vertex  $v_j$ ,  $Y$  is the variation of the network.

Now, all terms in the second sum vanish since for the minimal network equations E.1 are satisfied for all vertices. The first term of all integrals is non-negative, while the second term is equal to the product of the Gauss curvature (for surfaces), which is  $-1$  and the length of the vector  $Y$ , and, hence, is non-negative as well. If the deformation is nontrivial, then, since  $|Y|$  is continuous, and, therefore, is non-zero in some neighborhood, the second variation is strictly positive. We have proved the following

**Proposition E.2.** *Minimal networks on closed surfaces (manifolds) of negative curvature are stable, i.e. they are the strict local minima of the length function.*

*Remark E.3.* It is obviously not true on the sphere, where rotation produces a minimal network arbitrarily close to any given one.

Now, since the length function is *strictly convex* in the presence of the negative curvature (see [27]), it can only have one strict minimum. Thus

**Proposition E.4.** *There exists at most one minimal network in each homotopy class.*

*Remark E.5.* Hence the conjecture of the uniqueness of tessellations in the homotopy class is true in case of the minimal networks.

The discussion so far was an alternative way to show local (in fact a bit more, homotopy) rigidity of the minimal networks. This argument was suggested to the author by A.Tuzhilin and A.Ivanov, although the details have never been (to the author's knowledge ) worked out and published.

We will show now, that due to some simple geometric restrictions there exist only finitely many different possible topologies of the minimal networks on the surfaces of the given genus  $g > 1$ . These restrictions are given in [13], but we will present them here for completeness. It is clear then that Fomenko's conjecture is equivalent to the Rigidity Conjecture for minimal networks.

**Lemma E.6.** *All faces of the minimal network on the surface of constant negative curvature must be at least 7-gons.*

*Proof.* Indeed, let a hyperbolic  $n$ -gon be such a face. The, since it is a face of a minimal network, all interior angles are equal to  $2\pi/3$ . Therefore for the area of the polygon we have:

$$\text{Area} = \pi(n - 2) - 2\pi n/3 = (n - 6)\pi/3$$

Since it must be positive,  $n \geq 7$

□

Now, let  $k_i$  be the number of  $i$ -gonal faces of the minimal network  $\Gamma$ . Denote by  $N$  the greatest number of sides of faces from  $\Gamma$ . Then the *Gauss – Bonnet* formula for the area of the surface  $S_g$  (or *Euler* formula with a bit more hustle) gives

$$\sum_{i=7}^N k_i(i-6)\pi/3 = 4\pi(g-1)$$

and we get

**Lemma E.7.** *Numbers  $k_i$  for the closed minimal network on  $S_g$  satisfy the relation*

$$\sum_{i=7}^{\infty} k_i(i-6) = 12(g-1)$$

That immediately implies that a face of such a network cannot have more than  $12g - 6$  edges, thus proving the following

**Corollary E.8.** *There exist finitely many different topological types of closed minimal networks on a given surface  $S_g$ .*

## BIBLIOGRAPHY

- [1] W.Abikof *The real analitic theory of Teichmuller space* Springer-Verlag, 1980
- [2] A.D.Aleksandrov, *Vypuklye mnogogranniki* (Convex Polyhedra), GITTL. 1951. In Russian.
- [3] A.Beardon *The Geometry of Discrete Group*, Springer-Verlag, 1983
- [4] B. Bowditch, *Singular Euclidean structures on surfaces*, Journal of the London Mathematical Society, 44, 1991.
- [5] M.Bridson and A.Haefliger, *Metric spaces of Non-positive Curvature*, Springer-Verlag, 1999
- [6] A.Casson and S.Bleiler *Automorphisms of surfaces after Nielsen and Thurston* ,
- [7] R.Charney and M.Davis, *The polar dual of a convex polyhedral set in hyperbolic space*, Michigan Math. Journal 42, 479-510, 1995.
- [8] R.Charney, M.Davis and G.Moussong, *Nonpositively curved, piecewise Euclidean structures on hyperbolic manifold*, Michigan Math J. 44 (1997), 201-208
- [9] B.A.Dubrovin, A.T.Fomenko, P.S.Novikov, *Modern Geometry: methods and applications* , (in Russian), 2nd ed. (Moscow, Nauka, 1986). English translation: Part 1, GTM 93, 1984; Part 2, GTM 104, 1985; Part 3, GTM 104, 1990 (New York, Springer-Verlag)
- [10] A.L.Edmonds, J.H.Ewing, R.S.Kulkarni *Regular tessellations of surfaces and  $(p, q, 2)$ -triangle groups*, Ann.Math., Ser.2, 1982, v.116, N1, 113-132
- [11] A.O.Ivanov, I.V.Iskhakov, A.A.Tuzhilin *Minimal networks spanning regular  $n$ -gons: linear tilings realization*, (in Russian), Vestnik Moscov.Univers.Ser.1, Mat.-Mech., 6, 1993, 77-80
- [12] A.O.Ivanov, I.V.Ptitsina, A.A.Tuzhilin *Classification of closed minimal networks on flat two-dimensional tori*, (in Russian), Matem.Sbornik, 183 (12) (1992) 3-44

- [13] A.O.Ivanov and A.A.Tuzhilin *Minimal Networks: The Steiner Problem and Its Generalizations*, CRS Press, 1994
- [14] J.Jost, *Compact Riemann surfaces*, Springer-Verlag, 1997
- [15] O.Lehto, *Univalent functions and Teichmüller spaces*, Springer-Verlag, 1987
- [16] W.Magnus, *Noneuclidean tessellations and their groups*, Academic Press, 1974
- [17] J.Montesinos, *Classical tessellations and Three-Manifolds*, Springer-Verlag, 1987
- [18] M.Näätänen and R.C.Penner, *The convex hull construction for compact surfaces and the Dirichlet polygon*, Bull. London Math. Soc. 23 (1991), 568-574.
- [19] V.Nikulin and I.Shapharevich, *Geometriya i gruppy*, Nauka, 1983 (in Russian, English translation exists by Springer-Verlag, *Geometry and Groups*)
- [20] A.V.Pogorelov, *Extrinsic geometry of convex surfaces*, Technical report, Israel Program for Scientific Translation. 1973.
- [21] A.V.Pogorelov, *Geometry*, Mir, 1987
- [22] I.Rivin, *Euclidean structures on simplicial surfaces and hyperbolic volume*, Annals of Math., 143 (1994) 553-580
- [23] I.Rivin and C.Hodgson, *A characterization of compact convex polyhedra in hyperbolic 3-space*, Inventiones mathematicae, 1993
- [24] M.Seppälä, T.Sorvali *Geometry of Riemann Surfaces and Teichmüller Spaces*, North-Holland, 1992
- [25] J.-M. Schlenker, *Surfaces convex dans des espaces lorentziens courbure constante*, Comm. in Analysis and Geometry, 4 (1996) 285-331
- [26] G.Springer, *Introduction to Riemann surfaces*, Addison-Wesley, 1957
- [27] W.Thurston, *Geometry and topology of 3-manifolds*, Lecture Notes, 1978.
- [28] W.Thurston, *Shapes of Polyhedra and triangulations of the sphere*, The Epstein Birthday Schrift, Geometry and Topology Monographs, Vol.1, 511-549, International Press, 1998

- [29] *Travaux de Thurston sur les surfaces*, Astérisque 66-67, Société Mathématique de France, 1979
- [30] M. Troyanov, *Les surfaces euclidiennes singularités conique*, L'Enseignement mathématique, 32(1), 1986.
- [31] H. Zieschang, E. Vogt, H.D. Coldewey *Surfaces and planar discontinuous groups*, Springer-Verlag, 1980